AND HY

NO. 10, OCOTOBER 1979

JPRS L/8830

26 December 1979

USSR Report

METEOROLOGY AND HYDROLOGY

No. 10, October 1979

FBIS FOREIGN BROADCAST INFORMATION SERVICE

NOTE

JPRS publications contain information primarily from foreign newspapers, periodicals and books, but also from news agency transmissions and broadcasts. Materials from foreign-language sources are translated; those from English-language sources are transcribed or reprinted, with the original phrasing and other characteristics retained.

Headlines, editorial reports, and material enclosed in brackets [] are supplied by JPRS. Processing indicators such as [Text] or [Excerpt] in the first line of each item, or following the last line of a brief, indicate how the original information was processed. Where no processing indicator is given, the information was summarized or extracted.

Unfamiliar names rendered phonetically or transliterated are enclosed in parentheses. Words or names preceded by a question mark and enclosed in parentheses were not clear in the original but have been supplied as appropriate in context. Other unattributed parenthetical notes within the body of an item originate with the source. Times within items are as given by source.

The contents of this publication in no way represent the policies, views or attitudes of the U.S. Government.

For further information on report content call (703) 351-2938 (economic); 3468 (political, sociological, military); 2726 (life sciences); 2725 (physical sciences).

APPROVED FOR RELEASE: 2007/02/08: CIA-RDP82-00850R000200030047-5

JPRS L/8830

26 December 1979

USSR REPORT

METEOROLOGY AND HYDROLOGY

No. 10, October 1979

Selected articles from the Russian-language journal METEOROLOGIYA I GIDROLOGIYA, Moscow.

CONTENTS PAGE

CONTENTS (continued) Page

CONTENTS (Continued)

PUBLICATION DATA

English title	:	METEOROLOGY AND HYDROLOGY No 10, Oct 79
Russian title	:	METEOROLOGIYA I GIDROLOGIYA
Author (s)	:	
Editor (s)	:	Ye. I. Tolstikov
Publishing House	:	GIDROMETEOIZDAT
Place of Publication	:	Moscow
Date of Publication	:	1979
Signed to press	:	20 Sep 79
Copies	:	3870
COPYRIGHT	:	"Meteorologiya i gidrologiya," 1979

UDC 551.511.3(215-17)

NUMERICAL EXPERIMENT TO CONSIDER OROGRAPHY AND FRICTION IN MODELS OF ATMOSPHERIC DYNAMICS

Moscow METEOROLOGIYA I GIDROLOGIYA in Russian No 10, Oct 1979 pp 5-13

[Article by Professor N. G. Gcdev, Doctor of Physical and Mathematical Sciences V. V. Penenko, and Candidate of Physical and Mathematical Sciences N. N. Obraztsov, Bulgarian Geophysical Institute, Computer Center of the Siberian Department of the USSR Academy of Sciences, submitted for publication 8 January 1979]

Abstract: The technique and results are stated of a numerical experiment to study the effect of orography on atmospheric processes. The experiment was conducted based on the model of atmospheric dynamics for the Northern Hemisphere.

[Text] The orographic and thermal heterogeneities of the earth's surface have a significant effect on the structure of atmospheric processes of different scales.

The purpose of this work is to analyze and experimentally study certain methods for considering friction and orography in numerical models and their effect on atmospheric processes. An examination of these questions is based on the following hypothesis. It is assumed that the effect of friction and orography on atmospheric dynamics are mutually dependent. By this is meant that the turbulent structure of the atmosphere depends on the irregularities in the earth's surface of different scales, while the effect of orography in turn, depends on the turbulence of the atmosphere. Such an interrelationship, in our opinion, generates certain effects that have significant importance for atmospheric processes. The results of numerical experiments confirm the correctness of such an assumption.

1. The initial point in works that cover the effect of orography on atmospheric dynamics is the condition that air does not pass through the earth's surface, as well as the assignment of a link between certain parameters of the atmosphere and orography. These conditions are formulated differently depending on whether the atmosphere is viewed as an ideal or turbulent liquid.

If the atmosphere is viewed as an ideal liquid, then, as is known, the condition for non-passage through the earth's surface is provided by the expression

$$w_{op} = u\frac{\partial z_0}{\partial x} + v\frac{\partial z_0}{\partial y} \quad \text{with } z = z_0(x, y), \tag{1}$$

where $z_0(x,y)$--function describing the relief of the earth,
u, v, w--components of velocity vector $\vec{V}$ in direction of axes x, y, z;
$\frac{\partial z_0}{\partial x}$ and $\frac{\partial z_0}{\partial y}$ --components of gradient vector ∇z_0. With the help of (1) adopted as the boundary condition for w with $z=z_0(x,y)$, the effect of orography on the atmospheric processes is taken into consideration in this case.

In the systems of coordinates x,y,p or x,y,σ(p and $\sigma=p/p_s$--vertical coordinates, p--pressure, p_s--pressure on earth's surface) which are obtained from the system of coordinates x,y,z--identical transformations, the condition (1) must preserve its physical sense, since in these transformations no new physical hypotheses are involved.

If the earth's atmosphere is assumed to be turbulent, then in order to take into consideration the effect of orography on the atmospheric processes, usually the following is done. It is assumed that the effect of friction and orography are independent of each other, and they are considered based on the following two very widespread systems that are equivalent among themselves.

a) with the help of (1) the orographic component of the vertical wind velocity is defined. Then, considering that the earth's atmosphere is turbulent, while the earth's surface is smooth, the component of vertical velocity w_{typ} is computed that is governed only by turbulence. The turbulent component of vertical velocity w_{typ} is computed from the system of equations for a uniform planetary boundary layer (PBL). Further it is considered that the sum of these two components [3]

$$\overline{w} = w_{op} + w_{typ} \quad \text{with } z = h \tag{2}$$

is sufficient in order to take into account the joint effect of friction and orography on the atmospheric processes. Here h--upper boundary of PBL.

b) the orography is taken into consideration by a special selection of the coordinate system, while on the lower boundary of the atmosphere in some way the friction force $\vec{F}=\vec{F}(z)$ is assigned which is already independent of orography. In physical content this scheme is equivalent to condition (2).

Scheme (2) is based on the assumptions that the friction force does not depend on orography, while the effect of orography on the state of the atmosphere does not depend on turbulence. In the real atmosphere these hypotheses, as observations demonstrate, are not true. Here one can add also that the turbulent structure of the atmosphere strongly depends not only on the horizontal

orographic heterogeneities, but also on the thermal.

2. Now we will examine the quasi-Ekman planetary boundary layer (QEPBL) above the horizontal nonuniform surface. We will use such a definition for the boundary layer in which the coefficient of vertical turbulent exchange ν depends only on x and y; this relationship is taken into account through orography

$$\nu = \nu(z_0(x, y)). \tag{3}$$

Further with the help of this simple model we will examine the effect of orography and friction of the atmospheric processes. We note that all our discussions refer to processes of synoptic scale. For such processes orography must be perceived in a certain averaged sense.

Assume that the linear model of PBL is described by the system of equations

$$\frac{\partial}{\partial z}\nu(z, z_0(x, y))\frac{\partial u}{\partial z} + fv = fv_g, \tag{4}$$

$$\frac{\partial}{\partial z}\nu(z, z_0(x, y))\frac{\partial v}{\partial z} - fu = -fu_g, \tag{5}$$

$$\frac{\partial u}{\partial x} + \frac{\partial v}{\partial y} + \frac{\partial w}{\partial z} = 0. \tag{6}$$

under the conditions

$$u = v = w = 0 \quad \text{with} \quad z = z_0(x, y) \quad \text{and} \quad u \to u_g, v \to v_g \text{ with } z \to h.$$

Here u_g and v_g--components of geostrophic wind,
f--Coriolis parameter.

By comprising according to equation (4) and (5) the eddy equation, excluding $\left(\frac{\partial u}{\partial x} + \frac{\partial v}{\partial y}\right)$ with the help of (6), and by integrating for z from z_0 to h, we obtain for the vertical velocity w (x,y,z) the equation

$$fw(x, y, z) + \nu(z, z_0)\frac{\partial}{\partial z}\left(\frac{\partial v}{\partial x} - \frac{\partial u}{\partial y}\right)\Big|_{z_0}^{h} +$$

$$+ \frac{\partial \nu}{\partial z_0}\frac{\partial}{\partial z}\left(v\frac{\partial z_0}{\partial x} - u\frac{\partial z_0}{\partial y}\right)\Big|_{z_0}^{h} = 0. \tag{7}$$

In the boundary layer $\nu\frac{\partial u}{\partial z}$ and $\nu\frac{\partial v}{\partial z}$ are reduced with altitude, and therefore it is possible, based on (7) to write an approximate formula to define w(h) on the upper boundary of the PBL

$$w(h) = \frac{\nu(z, z_0)}{f}\frac{\partial}{\partial z}\left(\frac{\partial v}{\partial x} - \frac{\partial u}{\partial y}\right)\Big|_{z=z_0} + \frac{1}{f}\frac{\partial \nu(z, z_0)}{\partial z} \times$$

$$\times \frac{\partial}{\partial z}\left(v\frac{\partial z_0}{\partial x} - u\frac{\partial z_0}{\partial y}\right)\Big|_{z=z_0}. \tag{8}$$

The horizontal components of the velocity vector are found from equations (4) and (5) on the conditions

$$u = v = 0 \quad \text{with } z = z_0(x, y) \text{ and } u \to u_g,\ v \to v_g \text{ with } z \to h.$$

Assuming $M = u + iv, M_g = u_g + iv_g$, , where $i = \sqrt{-1}$ we obtain

$$\frac{d}{dz}\,\nu(z, z_0(x, y))\frac{dM}{dz} - ifM = -iM_g(x, y). \tag{9}$$

The solution of this equation with the adopted boundary conditions, as is known, looks like

$$M = M_g(P_0 + iQ_0), \tag{10}$$

where P_0 and Q_0--real functions that depend on z and $z_0(x,y)$, i.e., $P_0 = P_0(z, z_0(x, y))$ and $Q_0 = Q_0(z, z_0(x, y))$

For u and v from (10) the equalities follow

$$\begin{aligned} u &= u_g P_0 - v_g Q_0, \\ v &= u_g Q_0 + v_g P_0. \end{aligned} \tag{11}$$

After replacing u and v in (8) through (11) we obtain

$$w(h) = \bar{a}(\nabla z_0, \vec{v}_g) + \bar{b}[\nabla z_0, \vec{v}_g] + \bar{c}\Omega_g, \tag{12}$$

where

$$\bar{a} = \left(\frac{\nu}{f}\frac{\partial^2 Q_0}{\partial z\,\partial z_0} + \frac{1}{f}\frac{\partial \nu}{\partial z_0}\frac{\partial Q_0}{\partial z}\right)_{z=z_0} = \frac{1}{f}\left(\frac{\partial}{\partial z_0}\,\nu\frac{\partial Q_0}{\partial z}\right)_{z=z_0},$$

$$\bar{b} = \left(\frac{\nu}{f}\frac{\partial^2 P_0}{\partial z\,\partial z_0} + \frac{1}{f}\frac{\partial \nu}{\partial z_0}\frac{\partial P_0}{\partial z}\right)_{z=z_0} = \frac{1}{f}\left(\frac{\partial}{\partial z_0}\,\nu\frac{\partial P_0}{\partial z}\right)_{z=z_0},$$

$$\bar{c} = \left(\frac{\nu}{f}\frac{\partial P_0}{\partial z}\right)_{z=z_0}, \quad \Omega_g = \frac{\partial v_g}{\partial x} - \frac{\partial u_g}{\partial y},$$

$$(\nabla z_0, \vec{v}_g) = \left(u_g\frac{\partial z_0}{\partial x} + v_g\frac{\partial z_0}{\partial y}\right); \quad [\nabla z, \vec{v}_g] = \left(v_g\frac{\partial z_0}{\partial x} - u_g\frac{\partial z_0}{\partial y}\right). \tag{13}$$

We will examine formula (12) for two particular cases.

a) assume ν=const (Ekman boundary layer). In this case the solution to (9) with the adopted boundary conditions is provided for by the expression

$$M_0 = M_g\left(1 - e^{-(1+i)\sqrt{\frac{f}{2\nu}}(z - z_0)}\right). \tag{14}$$

It is apparent that

$$P_0 = 1 - e^{-\sqrt{\frac{f}{2\nu}}(z-z_0)} \cos \sqrt{\frac{f}{2\nu}}(z-z_0);$$

$$Q_0 = e^{-\sqrt{\frac{f}{2\nu}}(z-z_0)} \sin \sqrt{\frac{f}{2\nu}}(z-z_0).$$

Consequently,

$$\left(\frac{\partial P_0}{\partial z}\right)_{z=z_0} = \sqrt{\frac{f}{2\nu}}; \quad \left(\frac{\partial^2 Q_0}{\partial z\, \partial z_0}\right)_{z=z_0} = \frac{f}{\nu}; \quad \left(\frac{\partial^2 P_0}{\partial z_0\, \partial z}\right)_{z=z_0} = 0; \quad \frac{\partial \nu}{\partial z_0} = 0$$

and

$$\bar{a}(z_0) = 1; \quad \bar{b}(z_0) = 0; \quad \bar{c}(z_0) = \sqrt{\frac{\nu}{2f}}.$$

For the vertical velocity w(h) from (12) we obtain

$$w_0(h) = u_g \frac{dz_0}{dx} + v_g \frac{\partial z_0}{\partial y} + \sqrt{\frac{\nu}{2f}}\, \Omega_g \equiv w_{op} + w_{typ}, \qquad (15)$$

i.e., the expression analogous to (2). Expressions (15) and (2) are equivalent in their physical content, and this means that the models in which (2) is adopted as the lower boundary condition describe the interaction of the atmosphere with the earth's surface within the framework of the physical content of the linear system (4-7) with the condition ν=const.

Expression (15) differs from (12) by the fact that it does not contain term $\bar{b}[\nabla z_0, \vec{v}_g]$, and the coefficients $\bar{a}$ and $\bar{c}$ in it are constant. The first means that with linear flow-around of terrestrial obstacles the dynamic effects are not described (since in this case $[\nabla z_0, \vec{v}_g] = v_g \frac{\partial z_0}{\partial x} - u_g \frac{\partial z_0}{\partial y} = 0$), and the second--that the effects of orography and friction are independent between themselves. In normal practice it is acknowledged that the component w_{typ} depends on orography, and measures are taken to correct it by means of introducing a coefficient that depends on orography, $\bar{w}_{typ} = Cd(z_0)\sqrt{\frac{\nu}{2f}}\,\Omega_g$. The feedback, i.e., the dependence w_{op} on friction, is not taken into consideration.

b) we assume that $\nu = \nu(z_0(x, y))$. The solution in this case also will have the form analogous to (14),

$$M_0 = M_g\left(1 - e^{-\sqrt{\frac{f}{2\nu}}(1+i)(z-z_0)}\right) = M_g'(P_0 + iQ_0) = M_g \eta_0. \qquad (16)$$

The difference in (16) from (14) consists of the fact that in (16) through the coefficient ν the dependence on x and y is parametrically considered.

For the coefficients $\bar{a}$, $\bar{b}$, $\bar{c}$ we obtain

$$\bar{a} = 1 + \frac{d\bar{c}}{dz_0}; \quad \bar{b} = \frac{d\bar{c}}{dz}; \quad \bar{c} = \sqrt{\frac{\nu}{2f}}.$$

Thus for the vertical component of the velocity vector we have

$$w_0(h) = \left(1 + \frac{d\bar{c}}{dz_0}\right)(\nabla z_0, \vec{v}_g) + \frac{d\bar{c}}{dz}[\nabla z_0, \vec{v}_g] + \bar{c}\Omega_g. \qquad (17)$$

Expression (17) describes the effect of orography on dynamics in a turbulent atmosphere, as well as the effect of friction in the presence of large-scale orography. It takes into consideration in an explicit form individual factors of the studied process, that are more pithy in their physical sense than (2).

We note that if $\frac{d\bar{c}}{dz_0} > 0$, then with an increase in the altitude of orography its effect rises (with other conditions equal). But the relative increase in this effect $\Delta y = \frac{d\bar{c}}{dz_0} \Big/ \bar{c}$ is reduced with an increase in ν, since

$$\Delta y = \frac{d\bar{c}}{dz_0} \Big/ \bar{c} = \frac{1}{2} \frac{1}{\nu} \frac{\partial \nu}{\partial z_0}.$$

A unique "smoothing" of the orographic effect on the atmospheric dynamics is obtained. Friction increases the weight of small obstacles and does not "permit" the effect of the large to grow excessively, i.e., in this case a natural procedure for the smoothing of orography is obtained that takes into consideration the scales of heterogeneity in the earth's surface.

3. We will now evaluate the role of orography within the framework of the nonlinear model of the PBL. Our goal will be to "isolate" and approximately evaluate certain effects of large-scale orographic effect. In this case instead of (9) we will have

$$\frac{\partial}{\partial t} \nu(z_0(x, y)) \frac{\partial M}{\partial z} - ifM = -ifM_g + u \frac{\partial M}{\partial x} + v \frac{\partial M}{\partial y} + w \frac{\partial M}{\partial z} \equiv F. \qquad (18)$$

We will compute the right side F of equation (18) approximately, by using for this purpose the solution to the linear equation (9) which we will designate through $M = u_0 + iv_0$. As a result we obtain

$$F = -ifM_g + u_0 \frac{\partial M_0}{\partial x} + v_0 \frac{\partial M_0}{\partial y} + w_0 \frac{\partial M_0}{\partial z}. \qquad (19)$$

By expressing u_0, v_0, and w_0 through (16), (17), and by considering for simplicity that M_g=const, we rewrite (19) in the form

$$F = -ifM_g + M_g[P_0(\nabla z_0, \vec{v}_g) - Q[\nabla z_0, \vec{v}_g]]\frac{\partial \tau_0}{\partial z_0} + w_0\frac{\partial \tau_0}{\partial z} =$$

$$= \beta^{(0)} M_g + 2M_g(\beta^{(1)}\alpha^{(1)} + \beta^{(2)}\alpha^{(2)})\frac{\partial \tau_0}{\partial z}; \qquad (19')$$

where $\beta^{(0)}=-if$; $\alpha^{(0)}=1$;

$$\beta^{(1)} = -(z - z_0) + \frac{1}{2a}(P_0 + Q_0); \quad \alpha^{(1)} = (\nabla z_0, \vec{v}_g);$$

$$\beta^{(2)} = \frac{1}{2a}(P_0 - Q_0); \quad \alpha^{(2)} = [\nabla z_0, \vec{v}_g].$$

In order to solve equation (18) with the assigned right side (19) and boundary conditions $M\to 0$ with $z\to z_0$ and $M\to M_g$ with $z\to\infty$ we obtain the following expression

$$M = M_g[1 - e^{-a(1+i)(z-z_0)}] + M_g[\alpha^{(1)}(P^{(1)} + iQ^{(1)}) + \alpha^{(2)}(P^{(2)} +$$

$$+ iQ^{(2)})] = M_0 + M_1, \qquad (20)$$

where

$$P^{(s)} + iQ^{(s)} = \frac{i(1+i)}{2a\gamma}\left\{\varphi_1\int_{z_0}^{z}\varphi_2\beta^{(s)}\,dz - \varphi_2\int_{z_0}^{z}\varphi_1\beta^{(s)}\,dz - \right.$$

$$\left. - \left[\varphi_1 - \varphi_2\frac{\varphi_1(z_0)}{\varphi_2(z_0)}\right]\int_{z_0}^{\infty}\varphi_2\beta^{(s)}\,dz, \right. \qquad (21)$$

$$(s = 1, 2), \quad \varphi_1 = e^{a(1+i)z}; \quad \varphi_2 = e^{-a(1+i)z}.$$

Formula (20) has an iterative nature with iterations with respect to nonlinearity. In practice it is sufficient to limit oneself to the first approximation. The structure of (20) indicates that the first term of the right side yields a solution that corresponds to the linear model of the PBL, while the second is a correction for it as a consequence of the nonlinear terms. Consequently, for the vertical component of velocity also we will have the presentation $w=w_0+w_1$, where w_1 is a correction for w_0 from (17) due to the nonlinear terms, i.e.

$$w(h) = w_0(h) + \frac{\gamma}{f}\sum_{s=1}^{2}\left\{(\nabla\alpha^{(s)}, v_g)\frac{\partial Q^{(s)}}{\partial z} + [\nabla\alpha^{(s)}, \vec{v}_g]\frac{\partial P^{(s)}}{\partial z}\right\}_{z=z_0}, \qquad (22)$$

where

$$\left(\frac{\partial P^{(s)}}{\partial z}+i\,\frac{\partial Q^{(s)}}{\partial z}\right)_{z=z_0}\equiv-\frac{1}{\nu(z_0)}\int_{z_0}^{\infty}\beta^{(s)}\,e^{-\alpha(1+i)(z-z_0)}\,dz.$$

By making the necessary transformation we present the expression for w(h) in the following form:

$$w(h)=\overline{a}(\nabla z_0,\vec{v}_g)+\overline{b}[\nabla z_0,\vec{v}_g]-\overline{A}\nabla^2 z_0\,(u_g^2+v_g^2)-$$
$$-\overline{B}\left(u_g^2\frac{\partial^2 z_0}{\partial x^2}+v_g^2\frac{\partial^2 z_0}{\partial y^2}\right)-\overline{C}\,(u_g^2-v_g^2)\,\frac{\partial^2 z_0}{\partial x\,\partial y}+$$
$$+\overline{D}u_g v_g\left[10\frac{\partial^2 z_0}{\partial x\,\partial y}+3\left(\frac{\partial^2 z_0}{\partial y^2}-\frac{\partial^2 z_0}{\partial x^2}\right)\right]+R, \qquad (23)$$

where

$$\overline{A}=\frac{1}{120}\frac{1}{\sqrt{f^3\nu}}\frac{\partial\nu}{\partial z_0};\quad \overline{B}=\overline{C}=\frac{5}{2}\overline{A};\quad \overline{D}=\overline{A},$$

R--sum of small components which in the future we will ignore.

The physical sense of the terms of this expression are examined in [4]. We note that if $\frac{\partial\nu}{\partial z_0}=0$, i.e., if we assume that the coefficient for turbulence does not depend on orography, then all the coefficients $\overline{A}=\overline{B}=\overline{C}=\overline{D}=0$. And this means that the numerical models in which ν does not depend on orography cannot take into consideration all the effects that are linked with the forms of the earth's surface.

Expression (23) describes certain new physical aspects of the effect of orography and friction on the dynamics of atmospheric processes. These, in turn, are effects that are linked with the shape of the relief and the linear flow-around of obstacles [1,4].

A convenience of the approach stated here is the possibility of "breakdown" into individual components of the effect of orography and friction on atmospheric dynamics. This makes it possible to understand better the essence of the studied phenomenon, and to develop a technique for its correct consideration in numerical models. The analytical solution to the equations (9) and (18) is possible only in a particular case, when the coefficient of turbulence does not depend on altitude. Otherwise the numerical method is used to transform the operator in the left part of (19) and (18).

4. With the help of the described technique a series of numerical experiments was made to predict the fields of meteorological elements above the Northern Hemisphere. For the numerical experiments a model of weather forecasting was used with respect to complete equations in the quasistatic approximation on a spherical earth. The finite-difference approximation was

constructed on the basis of the variation principle and the method of splitting. A detailed description of this model is given in publication [3]. The algorithm for considering orography and friction is included in the numerical model of one of the stages of splitting. The computations were made on a regular grid in a spherical system of coordinates with spacing $\Delta\psi=10^\circ, \Delta\theta=5^\circ$ and with seven levels with respect to vertical ($p=1000, 850, 700, \ldots, p$--pressure, ψ--longitude, θ--supplement to latitude, $0\leqslant\psi\leqslant2\pi$, $0\leqslant\theta\leqslant\pi/2$). The calculations were made:

a) without consideration for the effect of the earth's relief;
b) with regard only for flow-around (i.e., the terms $(\nabla z_0, \vec{v}_g)$ and $[\nabla z_0, \vec{v}_g]$);
c) with regard only for the Laplacian from orography;
d) with regard for flow-around and the Laplacian from orography.

For illustration we present a brief description of the results of diurnal forecasts of the geopotential field for the period 1-5 December 1964.

The baric field above the Northern Hemisphere from 1 through 5 December 1964 was characterized by three main formations. The pole and the regions adjacent to it were occupied by a slowly changing depression. From it to the south along the meridians 20°e.l. and 160°w.l. a region of low pressure was lowered which reached roughly the 30th parallel. Two well-formed anticyclones were located on two sides of this depression.

Figure 1a presents the actual geopotential field at the level 100 mbar for 2 December 1964. A forecast of the baric field from 1 through 2 December 1964 (Figure 1b) without consideration for the effect of the relief unsatisfactorily reflected the main characteristics of the processes that were occurring. The region of low pressure was separated by three independent cyclones, whereby their centers were not located in their places. The same can be noted also for one of the anticyclones. Forecasting only with regard for flow-around did not result in a noticeable improvement in the forecasting of the baric field (Figure 1c). Figure 1d shows the same forecast, with regard only for the Laplacian. It is apparent that the majority of the mentioned shortcomings are eliminated. Figure 1e shows a forecast with regard for the influence of the components in (23) that describe the process of flow-around and the Laplacian from orography. In this case one can also notice a certain improvement as compared to forecast obtained without orography. A comparison of Figure 1b-e demonstrates that consideration of orography results in a more correct description of the processes that are occurring.

Analysis of the results of numerical experiments makes it possible to draw certain conclusions.

1. Inclusion of orography in the numerical plan leads to noticeable changes in their computation results. They can be divided into two groups. The first group includes changes associated with consideration of the Laplacian from the function z_0. As was already noted, the sign of these changes above the given definite point depends only on the sign of the Laplacian and on the wind velocity. In the computations there was a clear tendency towards formation of baric centers of a certain sign. Above the regions characterized by negative values of the Laplacian (for example, Greenland, the Himalayas

and others) an intensification of the anticyclonic formations is noticeable. This trend in our experiments was exaggerated. Above the concave regions (for example, the region of the Mediterranean Sea), where $\Delta^2 z>0$, a trend was noted towards cyclogenesis. The second group of changes is associated with the effect of flow-around of heterogeneities of the earth's surface. The conducted experiments demonstrate that these changes are sensitive to variations in wind direction.

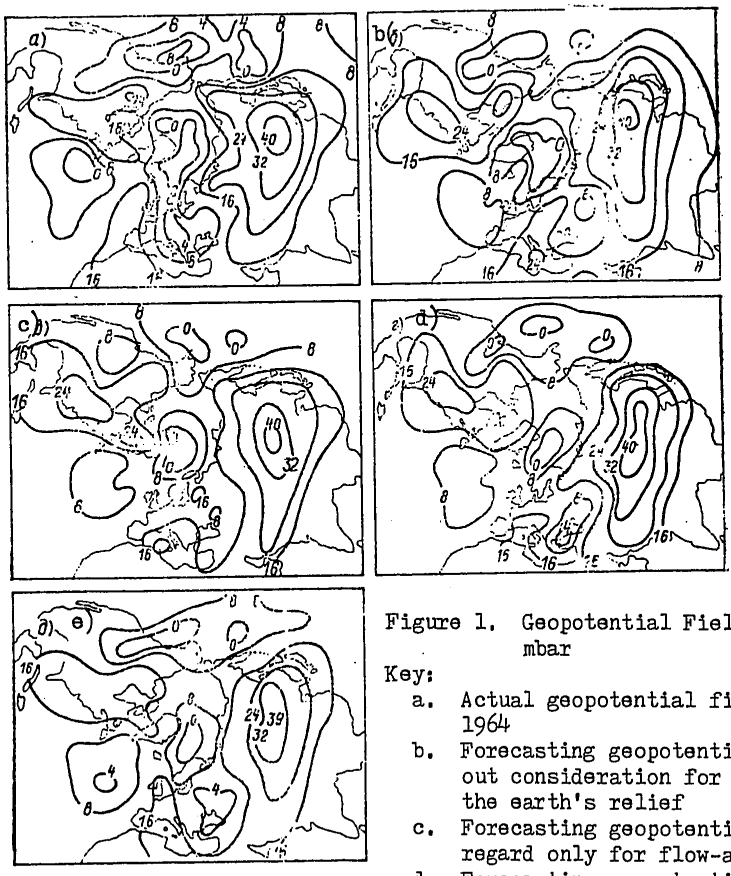

Figure 1. Geopotential Field at Level 1000 mbar

Key:

a. Actual geopotential field for 2 December 1964
b. Forecasting geopotential field without consideration for the effect of the earth's relief
c. Forecasting geopotential field with regard only for flow-around
d. Forecasting geopotential field with regard only for Laplacian
e. Forecasting geopotential field with regard for flow-around and Laplacian

2. Consideration for the effect of the shape of the relief (the term $\nabla^2 z_0 (u^2_g + v^2_g)$ in (23)) also leads to an improvement in the results. One of the reasons consists of the fact that the phenomenon described by this expression plays a considerable role in the formation of atmospheric processes.

3. An improvement in the forecast to which consideration of expression $\nabla^2 z_0 (u^2_g + v^2_g)$ leads, is manifest mainly above the mountain regions. This circumstance is important and intensifies the effectiveness of the consideration in the model of processes of flow-around.

4. The correctness of the consideration of the effect of mountain obstacles on the atmospheric dynamics depends on the method of describing the real mountains by the models. The model of mountain obstacles must be constructed such that it preserves those properties of the real mountains which are most closely linked to the atmospheric dynamics.

BIBLIOGRAPHY

1. Godev, N. G. "Effect of Orography and Near-Ground Friction on Change in Atmospheric Pressure," BOLGARSKOYE GEOFIZICHESKOYE OPISANIYE, Sofia, vol 1, No 2, 1975.

2. Monin, A. A.; and Gavrilin, B. L. "Gidrodinamicheskiy prognoz pogody" [Hydrodynamic Weather Forecast], Leningrad, Gidrometeoizdat, 1977.

3. Penenko, V. V.; and Obraztsov, N. N. "Numerical Model of Atmospheric Dynamics on Spherical Earth," METEOROLOGIYA I GIDROLOGIYA, No 1, 1979.

4. Godev, N. "A Method of Determining Optimum Scales for Averaging the Earth's Topography in Quantitative Study of Atmospheric Cyclo-and Anti-Cyclogenesis," BOUNDARY LAYER METEOROLOGY, vol 12, 1977.

UDC 551.(510.522:551.2)

ADVANCED MODEL OF ATMOSPHERIC PLANETARY BOUNDARY LAYER

Moscow METEOROLOGIYA I GIDROLOGIYA in Russian No 10, Oct 1979 pp 14-22

[Article by Candidates of Physical and Mathematical Sciences A. G. Tarnopol'skiy and V. A. Shnaydman, State Oceanographic Institute, Odessa Hydrometeorological Institute, submitted for publication 27 December 1978]

Abstract: Various methods are discussed for closing the system of equations for the atmospheric planetary boundary layer. An advanced model of the planetary boundary layer is proposed in which closure is implemented with the help of an equation for the rate of turbulent energy dissipation. Results of numerical experiments conducted in order to select the optimum set of numerical values of the empirical constants are presented. Examples are given of the computation of turbulence characteristics according to the new model.

[Text] Currently in the problem of numerical methods of weather forecasting a lot of attention is focused on parametrization of the planetary boundary layer (PBL) of the atmosphere. In addition to methods based on computation of the near-ground streams of impulse, heat and moisture, quantitative characteristics of the vertical PBL structure are widely used for parametrization. The transition to nonadiabatic models of hydrodynamic forecasting required knowledge of differential characteristics of the boundary layer in the horizontal plane, for example, the field vorticity of the vector of tangential friction stress, which governed an increase in the requirements of the computation accuracy of the PBL parameters. All of this demanded a further perfection in the models of the boundary layer, and in particular, the use of physically more substantiated hypotheses for closure of the PBL equation system.

It is known that to close the PBL equation system within the framework of so-called "K-theory" motion equations are used, the balance of kinetic turbulent energy and a number of semi-empirical correlations. In the first place, they include hypotheses for the characteristic size of eddies which can be conventionally separated into two groups:

1) the characteristic eddy size is expressed through the characteristics of vertical profiles of meteorological elements;
2) based on the correlations for the second moments of hydrodynamic field a differential equation is written for the characteristic eddy size.

Analysis of the empirical expressions of the first group is given in the monographs [3, 8, 23] and we will not dwell on them. We will only indicate that this approach was a necessary stage for the further development of the PBL theory.

An important step on the path of transition from studies of the first group to the second was generalization of the Karman hypothesis for the characteristic eddy size [3, 6]. Based on the Karman and Kolmogorov hypothesis a differential equation of the first order was obtained for the characteristic eddy size, and from it--a differential equation for the turbulence coefficient

$$\frac{dk}{dz} - \frac{k}{b}\frac{db}{dz} - \alpha_\varepsilon^{1/4} \varkappa \sqrt{b} = 0, \qquad (1)$$

where z--vertical coordinate;
k--turbulence coefficient;
b--mean energy of turbulent pulsations relative to a unit of mass;
$\varkappa$=0.38--Karman constant;
α_ε--constant.

The advantage of equation (1) consists of the fact that it makes it possible to determine the turbulence coefficient with respect to external PBL parameters (velocity of geostrophic wind G_g, drop in potential temperature $\delta\Theta$, Coriolis parameters $2\omega_z$ and irregularity z_0). Introduction of this equation does not increase the number of empirical closure constants. However that fact that the turbulence coefficient is unambiguously expressed through turbulence intensity is insufficiently substantiated and can be viewed only as the first approximation in the problem on PBL parametrization.

One can consider it more substantiated to construct a differential equation for the characteristic eddy size based on equations of turbulent motion proposed by Kolmogorov [8]. A survey of the technique for construction and a description of the actual equations for the characteristic eddy size are given in [17, 20, 22]. For closure of the PBL equation system an equation is used for the product of the characteristic eddy size for turbulence intensity in which the terms of advection, diffusion, production and dissipation that are "standard" for the balance equations figure. The practical use of this equation is significantly complicated due to the presence of constants which, according to the data of different authors [17-19] can significantly differ. Therefore a decrease in the number of constants as a consequence of selecting the corresponding equations for closure of the system is a reasonable perfection of the model.

In addition to the use of an equation for the characteristic eddy size the equation for the dissipation rate of kinetic turbulent energy into heat has

become widespread in the works of hydrodynamic profile [2, 15, 25]. In recent years alone this equation has begun to be used in problems of atmospheric and ocean physics [1, 4, 5, 7, 25, 26].

For the convenience of a comparative analysis we reduce the equations used for closure of the system to one view. We will examine the stationary barotropic case where the unknown functions depend only on the vertical coordinate:

$$k\left[\left(\frac{du}{dz}\right)^2+\left(\frac{dv}{dz}\right)^2-\alpha_\theta\frac{g}{\overline{T}}\frac{d\Theta}{dz}\right]+\alpha_b\frac{d}{dz}k\frac{db}{dz}-\varepsilon=0, \tag{2}$$

$$\alpha_{1l}kl\left[\left(\frac{du}{dz}\right)^2+\left(\frac{dv}{dz}\right)^2\right]-\alpha_{\theta l}kl\frac{g}{\overline{T}}\frac{d\Theta}{dz}+\alpha_{2l}\frac{dl}{dz}\left(kb\frac{dl}{dz}\right)+$$
$$+\alpha_{3l}\frac{d}{dz}\left(kl\frac{db}{dz}\right)-\alpha_{4l}b^{3/2}=0, \tag{3}$$

$$\alpha_{1\varepsilon}k\frac{\varepsilon}{b}\left[\left(\frac{du}{dz}\right)^2+\left(\frac{dv}{dz}\right)^2\right]-\alpha_{\theta\varepsilon}k\frac{\varepsilon}{b}\frac{g}{\overline{T}}\frac{d\Theta}{dz}+\alpha_{2\varepsilon}\frac{d}{dz}k\frac{d\varepsilon}{dz}-$$
$$-\alpha_{3\varepsilon}\frac{\varepsilon^2}{b}=0, \tag{4}$$

$$k=\alpha_k l\sqrt{b}, \tag{5}$$

$$k=\alpha_\varepsilon b^2/\varepsilon. \tag{6}$$

Here u and v--horizontal components of wind velocities;
$\overline{T}$--mean temperature in the PBL limits;
Θ--potential temperature;
g--acceleration of free fall;
l--characteristic curve of turbulent pulsation;
ε--dissipation rate of turbulent eddy energy;

α_θ, α_b, $\alpha_{\theta l}$, α_{1l}, α_{2l}, α_{3l}, α_{4l}, $\alpha_{\theta\varepsilon}$, $\alpha_{1\varepsilon}$, $\alpha_{2\varepsilon}$, $\alpha_{3\varepsilon}$, α_k --empirical constants.

It is natural that either equations (2), (3), (5) and (6)*, or equations (2), (4) and (6) are used for closure. It seems to us more expedient to use equations (2), (4) and (6) since in this case the number of constants is reduced. This selection is preferable also because in deriving the equation for the balance of kinetic turbulent energy (2) and the dissipation balance (4) equations are used for pulsations in the flow rate found by means of subtracting from the Navier-Stokes equation the Reynolds equation, and the identical-empirical correlations between the second and third moments. Therefore we used the equation system (2), (4), (6), for quantitative estimates of the PBL parameters. Here the task emerged of selecting the numerical values of constants from a fairly broad range of quantities obtained by different authors [4, 5, 14, 16-19, 21, 24, 25]:

$$\alpha_b=0{,}50\div1{,}00;\ \alpha_\theta=\alpha_{\theta\varepsilon}=1{,}0\div1{,}35;\ \alpha_{1\varepsilon}=1{,}35\div1{,}55;\ \alpha_{2\varepsilon}=1{,}00\div1{,}25;$$
$$\alpha_{3\varepsilon}=1{,}80\div2{,}00;\ \alpha_\varepsilon=0{,}04\div0{,}10.$$

*Equation (6) is used to compute dissipation.

This selection was made by comparing the observational data and results obtained from solving the universal system of PBL equations.

In order to obtain a universal system of PBL equations we write the quantities that figure in the equations of balance and dissipation in a dimensionless form:

$$b_n = \alpha_\varepsilon^{1/2}\, b/v_*^2, \quad \eta_n = k\,\frac{du}{dz}\Big|v_*^2, \quad \sigma_n = k\,\frac{dv}{dz}\Big|v_*^2,$$

$$\varepsilon_n = \frac{\varkappa^2}{2\,\omega_z v_*^2}\,\varepsilon, \quad z_n = \frac{2\,\omega_z}{\varkappa\, v_*}\,z, \quad k_n = \frac{2\,\omega_z}{\varkappa^2 v_*^2}\,k.$$

Then equations (2), (4) and (6) can be rewritten as follows (here for $d\theta/dz$ the approximation is adopted proposed in [6]):

$$\frac{\eta_n^2+\sigma_n^2}{k_n} - \mu + \beta\frac{d}{dz_n}k_n\frac{db_n}{dz_n} - \varepsilon_n = 0, \tag{7}$$

$$\frac{\eta_n^2+\sigma_n^2}{k_n} - A_3\mu + A_1\frac{k_n}{b_n}\frac{d}{dz_n}k_n\frac{d\varepsilon_n}{dz_n} - A_2\varepsilon_n = 0, \tag{8}$$

$$k_n = b_n^2/\varepsilon_n, \tag{9}$$

$$\mu = \frac{k_n}{z_n}\left(\mu_0 + \frac{\nu z_n^2}{H_n}\right),$$

$$\mu_0 = -\frac{\varkappa^2 g P_0}{2\,\omega_z \rho c_p \overline{T}\, v_*^2}, \quad \nu = \alpha_\theta\,\frac{\varkappa^4(\gamma_a-\gamma_H)}{(2\,\omega_z)^2}\,\frac{g}{\overline{T}},$$

$$\beta = \alpha_b\,\frac{\varkappa^2}{\sqrt{\alpha_\varepsilon}}, \quad A_1 = \frac{\varkappa^2\alpha_{2\varepsilon}}{\alpha_{1\varepsilon}\sqrt{\alpha_\varepsilon}}, \quad A_2 = \frac{\alpha_{3\varepsilon}}{\alpha_{1\varepsilon}}, \quad A_3 = \frac{\alpha_{e_\theta}}{\alpha_\theta\,\alpha_{1\varepsilon}}.$$

Here

μ_0, ν--inner and outer parameters of stratification;
P_0--turbulent stream of heat near underlying surface;
H_n--dimensionless altitude of PBL;
ρ--air density;
c_p--heat capacity of air with constant pressure;
v_*--dynamic velocity;
γ_a and γ_H--dry-adiabatic and actual (in upper part of PBL) vertical temperature gradients.

The constant in the dimensionless equations (7)-(8) are altered in the following limits: β=0.23-0.72; A_1=0.30-0.53; A_2=1.16-1.48; A_3=0.48-1.00.

Before passing to a selection of the constants we will study the asymptotics of equations (7)-(8) with small z_n for which in the equation of balance and dissipation one can ignore the effect of the buoyancy force, and in the equation of balance--also the diffusion term. Since with small z_n $\eta_n \approx 1$, $\sigma_n \approx 0$ and $k_n \approx z_n$, then $\varepsilon_n \approx 1/z_n$. After substituting these values in the dissipation

equation we obtain $A_2=1+A_1$. If one assumes that in the equation for the dissipation rate all the terms are one order, then the range of possible fluctuation in constant values is narrowed: $A_1=0.29-0.48$; $A_2=1.29-1.48$; $A_3=0.64-0.74$. The given range of A_3 is correct only on the condition of quality of α_θ and $\alpha_{\theta_\varepsilon}$ for any stratification.

We made the numerical solution to the system of dimensionless equations of the PBL in which, in addition to equation (7)-(9) equations were used for turbulent tangential stresses

$$\frac{d^2\eta_n}{dz_n^2}+\frac{\sigma_n}{k_n}=0, \quad \frac{d^2\sigma_n}{dz_n^2}-\frac{\eta_n}{k_n}=0 \qquad (10)$$

and boundary conditions:
with $z_n=(\varkappa^2\chi\,\mathrm{Ro})^{-1}$ $\eta_n=1$, $\sigma_n=0$, $b_n=1$,
$\varepsilon_n=\varkappa^2\chi\,\mathrm{Ro}$, $u_n=v_n=0$;
with $z_n\to\infty$ $\eta_n\to 0$, $\sigma_n\to 0$, $b_n\to 0$, $\varepsilon_n\to 0$. (11)

The conditions for the dimensionless velocity components (u_n, v_n) were used to determine the geostrophic friction coefficient, $\chi=v_*/(\varkappa C_g)$ and the angle for the complete rotation of wind in the planetary boundary layer ($-\alpha$). Here $\mathrm{Ro}=C_g/(2\omega_z z_0)$--Rossby number.

The numerical experiments to select the optimal values for the constants were made according to observational data on the high-altitude meteorological tower of the Institute of Experimental Meteorology (Obninsk), where regular observations were made of the vertical distribution of meteorological elements up to altitude 300 m above the underlying surface. We had at our disposal statistically substantiated data only for the stratification close to the neutral in the lower part of the PBL ($\mu_0=0-5$) and fairly stable in its upper part ($\nu=200-300$) with different values for the flow rate at level 301 m. The calculations were made for six gradations of wind velocity at level 301 m: 0-5.0; 5.1-10.0; 10.1-15.0; 15.1-20.0; 20.1-25.0; over 25 m/s. For each gradation and fixed set of constants differences were found between the calculated and the measured wind velocity on nine levels of measurements in the layer 8-301 m, and the root-mean-square deviation in the entire layer σ_s.

The calculation results demonstrated that for the given range of oscillations in the constant values the amounts σ_s are fairly close to each other. There was also an insignificant difference between the parameters of the dynamic and thermal interaction of the underlying surface and the atmosphere, the vertical profiles of the wind velocity components, temperature, coefficient and intensity of turbulence, and the components of the vector of tangential friction stress. For illustration table 1 presents the values of the altitude PBL H, the maximum turbulence coefficient k_m, v_* α, σ_s for two sets of constants: $\beta=0.41$; $A_1=0.31$; $A_2=1.31$; $A_3=0.70$ (upper line) and $\beta=0.36$; $A_1=0.48$; $A_2=1.48$; $A_3=0.70$. In the last three lines for the mean values $\mu_0=2$, $\nu=245$, $\lg\mathrm{Ro}=5.88$, $C_g=14.0$ m/s the average characteristics of the PBL are placed for all six gradations in velocity for the indicated two sets of

constants, as well as the averaged data obtained according to technique [9, 10], in which the generalized Karman hypothesis is used for closure.

TABLE 1 - QUANTITATIVE CHARACTERISTICS OF PBL AND STANDARD DEVIATIONS FOR TWO SETS OF CONSTANTS

μ_0	ν	lg Ro	C_g м/сек (a)	v_* м/сек (a)	$-\alpha^\circ$	k_m м²/сек (b)	H м	σ_s м/сек (a)
4	175	5,80	7,6	0,30	24	4,4	473	0,45
				0,30	24	4,8	496	0,48
2	225	5,26	11,0	0,49	29	11,6	728	0,49
				0,49	28	12,7	768	0,56
2	235	5,13	15,0	0,69	30	22,4	1029	1,06
				0,69	29	24,3	1076	1,05
4	270	6,79	14,6	0,47	21	9,2	664	1,33
				0,47	21	10,2	700	1,36
2	261	6,13	17,6	0,65	24	19,2	950	1,33
				0,65	23	20,7	968	1,37
3	306	6,19	18,3	0,66	24	18,4	894	2,03
				0,66	24	20,4	966	2,06
3	245	5,88	14,0	0,54	25	14,2	788	1,12
				0,54	25	15,5	829	1,15
				0,59	23	26,0	987	1,36

Key:
a. m/s
b. m^2/s

As is apparent from the results, calculations according to technique [9, 10] yield a greater value of σ_s. The differences in the amounts H, v_* and α do not exceed 10% of the actual values. The values of the turbulence coefficient that are computed according to two different techniques differ more significantly from each other. One can assume that closure of the PBL system of equations with the help of the generalized Karman hypothesis results in overestimation of the magnitude of the turbulence coefficient.

Analysis of the findings makes it possible to draw a conclusion on the expediency of using constants β=0.41; A_1=0.31; A_2=1.31; A_3=0.70 as optimal in the dimensionless equation for the balance of kinetic energy and the rate of dissipation.

The conclusions we obtained on the weak influence of numerical values of the constants (in the selected range) on the PBL characteristics refer to cases of stratification close to neutral. The correctness of this conclusion for stratification that significantly differs from the neutral was verified by us by solving the equation system (7)-(10) for the values μ_0 from -30 to 30 and ν from 300 to 1500 with variation in the sets of constants. It was found that for cases of stable and unstable stratification variation in the

numerical constant values, naturally, with observance of the correlation $A_2=1+A_1$ and the condition $\alpha_\theta=\alpha_\theta$ results in differences between the PBL parameters lying in the limits 10%--accuracy of their determination. This conclusion is illustrated in table 2 where dimensionless characteristics of turbulence are given that are computed for those two sets of constants that are indicated in the description of table 1. It also follows from table 2 that the turbulence characteristics significantly depend on the stratification conditions. The maximum turbulence coefficient is especially significantly altered during the transition of the system from a thermally stable to an unstable condition. The dependence of the geostrophic friction coefficient χ and the angle of complete rotation of the wind in the PBL α on lgRo for certain values μ_0 and ν (with optimal values of the constants) is given in figure 1.

TABLE 2 - CHARACTERISTICS OF TURBULENCE FOR DIFFERENT CONDITIONS OF STRATIFICATION

	(a) Параметр μ_0								
	30			0			−30		
	(a) Параметр ν								
	300	900	1500	300	900	1500	300	900	1500
$H_n\cdot10^3$	287 299	241 241	218 218	322 333	253 253	218 230	390 379	264 264	230 230
$(k_m)_n\cdot10^3$	20 21	16 18	15 16	36 38	25 25	21 21	192 169	58 55	38 37
lgRo=6									
$\chi\cdot10^3$	86 88	83 85	81 83	99 100	93 94	90 90	171 159	116 113	105 103
$-\alpha°$	28 28	31 31	33 33	26 26	31 31	34 33	28 28	32 32	35 34
lgRo=8									
$\chi\cdot10^3$	63 64	62 63	61 62	70 70	67 68	66 66	101 94	79 77	74 73
$-\alpha°$	20 20	22 22	24 24	18 18	22 22	24 23	16 16	21 21	24 23

Key:
a. Parameter

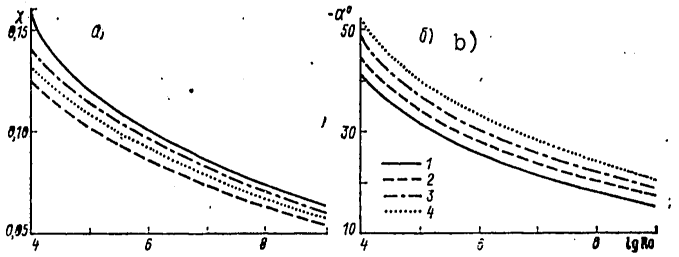

Figure 1. Dependence of (a) and α (b) on Ro, μ_0 and ν
Key:
1. $\mu_0=0$, $\nu=300$ 2. $\mu_0=30$, $\nu=300$ 3. $\mu_0=0$, $\nu=900$ 4. $\mu_0=0$, $\nu=1500$

Until now in studying the PBL structure we operated with the inner parameter of stratification μ_0 which cannot be defined according to the data of standard observations. Therefore in parametrization of the PBL effects in problems of dynamics of the atmosphere and ocean it is usually excluded with the help of the correlation [10]

$$M = \frac{\nu\chi H_n}{2\varkappa^2} + \mu_0 \frac{\chi \ln(\varkappa^2 H_n \mathrm{Ro}\,\chi)}{\varkappa^2}, \qquad (12)$$

where $M = g\delta\Theta(2\omega_z C_g \overline{T})^{-1}$ --integral dimensionless parameter of stratification computed according to standard aerosynoptic information.

As an example Table 3 includes the results of computations according to formula (12).

TABLE 3 - INTEGRAL PARAMETER OF STRATIFICATION M

lg R_0	ν	(a) Параметр μ_0 30	0	−30
6	300	172	33	−257
	900	200	73	−107
	1500	224	102	−53
8	300	182	23	−237
	900	205	53	−134
	1500	223	75	−101

Key:
a. Parameter

Recently in the laws of resistance and heat exchange the ratio of dynamic velocity v_* to the modulus of the wind velocity $\overline{C}$ that is the mean for the boundary layer is used. A number of authors [11-13] have focused attention on the expediency of using the mean wind in the problems of PBL parametrization.

We will show that the amount $\overline{C}$ can be computed according to the parameters C_g, α, χ and H_n known in the model. Since

$$u = C_g \cos\alpha + C_g \chi d\,\sigma_n/dz_n,$$
$$v = C_g \sin\alpha - C_g \chi d\,\eta_n/dz_n, \qquad (13)$$

then, by integrating equations (13) with regard for (11) we find

$$\overline{C} = C_g\left[1 + \left(\frac{\chi}{H_n}\right)^2 + \frac{2\chi\sin\alpha}{H_n}\right]^{1/2}. \qquad (14)$$

Now by analogy with the geostrophic friction coefficient we introduce the concept of the integral friction coefficient $\chi_1 = v_* / (\varkappa C)$. The dependence of χ_1 on Ro, μ_0 and ν is illustrated in Table 4.

TABLE 4 - INTEGRAL COEFFICIENT OF FRICTION $\chi_1 \times 10^3$

$\lg R_0$	(a) Параметр μ_0								
	30			0			−30		
	(a) Параметр ν								
	300	900	1500	300	900	1500	300	900	1500
6	96	95	95	109	107	107	194	145	127
8	66	66	66	73	72	72	105	84	81

Key:
a. Parameter

Relationship (14) can be used to solve the inverse problem: finding the velocity of the geostrophic wind according to the modulus of the mean wind velocity in the boundary layer. Such a task arises, for example, in the use of data on vertical profiles of temperature and wind obtained on high-altitude meteorological towers, to evaluate the turbulence parameters in the PBL. Then instead of the Rossby number one should assign the number $\overline{Ro} = \overline{C}/(2\omega_z z_0)$. The link between Ro and $\overline{Ro}$ is found with the help of correlation (14) for different stratification conditions.

Thus, the inclusion of an equation for the dissipation rate in the closed system makes it possible to develop a physically more substantiated PBL model. One can hope that the use of this advanced model for parametrization of the PBL effects in hydrodynamic schemes will result in an improvement in the quality of the forecasts. The results of the presented studies also will be useful in solving other applied problems associated with consideration of the peculiarities of the physical processes occurring in the atmospheric planetary boundary layer.

BIBLIOGRAPHY

1. Vager, B. G.; and Nadezhina, Ye. D. "Use of the Differential Equation for Dissipation Rate in Simulating the Atmospheric Ground Layer," IZVESTIYA AN SSSR. FIZIKA ATMOSFERY I OKEANA, vol 12, No 4, 1976.

2. Davydov, B. I. "Statistical Dynamics of Incompressible Turbulent Liquid," DOKLADY AN SSSR, vol 136, No 1, 1961.

3. Zilitinkevich, S. S. "Dinamika pogranichnogo sloya atmosfery" ["Dynamics of Atmospheric Boundary Layer"], Leningrad, Gidrometeoizdat, 1970.

4. Kochergin, V. P. "Teoriya i metody rascheta okeanicheskikh techeniy" ["Theory and Methods for Computing Oceanic Currents"], Moscow, Nauka, 1978.

5. Kochergin, V. P.; Sukhorukov, V. A.; and Tsvetova, Ye. A. "Simulation of the Processes of Vertical Turbulent Diffusion in the Ocean," "Chislennyye metody rascheta okeanicheskikh techeniy" ["Numerical Methods for Computing Oceanic Currents"], Novosibirsk, Computer Center of the Siberian Department of the USSR Academy of Sciences, 1974.

6. Laykhtman, D. L. "Fizika pogranichnogo sloya atmosfery," ["Physics of Atmospheric Boundary Layer"], Leningrad, Gidrometeoizdat, 1970.

7. Marchuk, G. I.; Kochergin, V. P.; Klimok, V. I.; Sukhorukov, V. A. "Mathematical Simulation of Surface Turbulence in Ocean," IZVESTIYA AN SSSR. FIZIKA ATMOSFERY I OKEANA, vol 12, No 8, 1976.

8. Monin, A. S.; and Yaglom, A. M. "Statisticheskaya gidromekhanika ["Statistical Hydromechanics"], part 1, Moscow, Nauka, 1965.

9. Tarnopol'skiy, A. G.; Shnaydman, V. A. "Parametrization of Planetary Boundary Layer in Forecasting Models," TRUDY GIDROMETTSENTRA SSSR, No 145, 1974.

10. Tarnopol'skiy, A. G.; Shnaydman, V. A. "Parametrization of Baroclinic Atmospheric Planetary Boundary Layer," TRUDY GIDROMETTSENTRA SSSR, No 180, 1976.

11. Chalikov, D. V. "Technique of Parametrization of Atmospheric Boundary Layer," METEOROLOGIYA I GIDROLOGIYA, No 8, 1977.

12. Arya, S. P. S. "Suggested Revisions to Certain Boundary Layer Parametrization Schemes Used in Atmospheric Circulation Models," MON. WEATHER REV., vol 105, 1977.

13. Deardorff, J. W. "Parametrization of Planetary Boundary Layer for Use in General Circulation Models," MON. WEATHER REV., vol 100, 1972.

14. Freeman, B. E., "Tensor Diffusivity of a Trace Constituent in a Stratified Boundary Layer," J. ATMOS. SCI., vol 34, 1977.

15. Hanjalic, K.; Launder, B. E. "A Reynolds Stress Model of Turbulence and its Application to Thin Shear Flow," J. FLUID MECH., vol 52, part 4, 1972.

16. Marchuk, G. I.; Kochergin, V. P.; Klimok, V. I.; Sukhorukov, V. A. "On the Dynamics of the Ocean Surface Mixed Layer," J. PHYS. OCEANOGR., vol 7, 1977.

17. Mellor, G. L.; Herring, H. J. "A Survey of the Mean Turbulent Field Closure Models," AAJA J., vol 11, No 3, 1973.

18. Ng, K. H.; Spalding, D. B. "Turbulence Model for Boundary Layer Near Walls," PHYS. FLUIDS, vol 15, No 1, 1972.

19. Rodi, W.; Spalding, D. B. "A Two-Parameter Model of Turbulence and its Application to Free Jets," THERMO AND FLUID DYNAMICS, vol 3, 1970.

20. Rotta, J. C. "Statistische Theoric Nichhomogener Turbulenz," ZEITR. PHYSIC., No 31, 1951.

21. Tsann-Wang, Ju. "A Comparative Study on Parametrization of Vertical Turbulent Exchange Process," MON. WEATHER REV., vol 105, 1977.

22. Volmers, S.; Rotta, J. C. "Equations for Mean Velocity, Turbulent Energy and its Scale," AAJA J., vol 15, No 5, 1977.

23. Wippermann, F. "The Planetary Boundary Layer of the Atmosphere," DEUTSCHER WETTERDIENTS ANN. D. MET., No 7, 1973.

24. Yamada, T.; Mellor, G. "A Simulation of the Wangara Atmospheric Boundary Layer Data," J. ATMOS. SCI., vol 32, No 12, 1975.

25. Zeman, O.; Tennekes, H. "A Selfcontained Model for Pressure Terms in Turbulent Stress Equations of Neutral Atmospheric Boundary Layer," J. ATMOS. SCI., vol 32, No 9, 1975.

26. Zeman, O.; Tennekes, H. "Parametrization of the Turbulent Energy Budget At the Top of the Daytime Atmospheric Boundary Layer," J. ATMOS. SCI., vol 34, No 1, 1977.

UDC 551.515.2

A TWELVE-LEVEL AXISYMMETRIC NUMERICAL MODEL OF A TROPICAL CYCLONE

Moscow METEOROLOGIYA I GIDROLOGIYA in Russian No 10, Oct 1979 pp 23-37

[Article by Candidate of Physical and Mathematical Sciences A. P. Khain, USSR Hydrometeorological Scientific Research Center, submitted for publication 3 Apr 1979]

Abstract: A twelve-level axisymmetric model of a tropical cyclone in z-coordinates is described. Parametrization of convective heating as a consequence of the release of latent condensation heat is used, as well as a new technique for parametrization of convective transfer of heat, water vapor and angular momentum. Parametrization of the boundary layer proposed by Deardorff is employed. In the initial moment a vortex is assigned in the gradient balance. The background temperature profile is considered to be identical to the tropical temperature profile in the tropical zone in the hurricane season. A comparison is made of the findings with the observational data.

[Text] In recent years numerical modeling of tropical cyclones (TC) has attained considerable advances. Besides the axisymmetric [13, 28, 30-32] a number of 3-dimensional models have appeared [15, 23]. A trend is observed towards modeling of the life cycle of specific TC. However the potentialities of the axisymmetric models have far from been exhausted. They are used to verify new ideas and methods in describing different physical processes [31, 33]. In addition, according to the dynamics and energetics the axisymmetric model TC are close to the 3-dimensional [22]. Finally, the use of the axisymmetric model makes it possible in reasonable periods to conduct a fairly large number of numerical experiments.

In our country work on simulating TC until recently was developed insufficiently intensively. One should isolate the cycle of works of V. V. Shuleykin [10,] based on the analytical presentations of meteorological parameters in the TC. In [2, 6] tasks are set on numerical modeling of axisymmetric TC. A more detailed survey of work linked to theoretical studies and numerical modeling of TC is given in [3, 6, 8, 12]. The given work presents results

on a model that is described in main details in [6]. The model differs from the majority of listed works in the regard for the hydrological cycle, presence of parametrization of convective transfer of heat, moisture and angular momentum in clouds, and parametrization of the boundary layer.

On the assumption of the axisymmetry and hydrostatic equilibrium the initial system of equations in the cylindrical z-system of coordinates looks like

$$\bar{\rho}\frac{\partial u}{\partial t}=\bar{\rho}v\left(f+\frac{v}{r}\right)-\frac{1}{r}\frac{\partial \bar{\rho}ru^2}{\partial r}-\frac{\partial \bar{\rho}\overline{wu}}{\partial z}-\frac{\partial \bar{\rho}\overline{w'u'}}{\partial z}-\bar{\rho}k_u^H\left(\frac{\partial^2}{\partial r^2}+\right.$$

$$\left.+\frac{1}{r}\frac{\partial}{\partial r}-\frac{1}{r^2}\right)u+\frac{\partial}{\partial z}\left(k_u^z\bar{\rho}\frac{\partial u}{\partial z}\right)-\bar{\rho}c_p\theta\,(1+0{,}61\,q)\frac{\partial \pi}{\partial r}, \qquad (1)$$

$$\bar{\rho}\frac{\partial v}{\partial t}=-\bar{\rho}u\left(f+\frac{v}{r}\right)-\frac{1}{r}\frac{\partial \bar{\rho}ruv}{\partial r}-\frac{\partial \bar{\rho}\overline{wv}}{\partial z}-\frac{\partial \bar{\rho}\overline{w'v'}}{\partial z}+$$

$$+\bar{\rho}k_v^H\left(\frac{\partial^2}{\partial r^2}+\frac{1}{r}\frac{\partial}{\partial r}-\frac{1}{r^2}\right)v+\frac{\partial}{\partial z}\left(k_v^z\bar{\rho}\frac{\partial v}{\partial z}\right), \qquad (2)$$

$$\bar{\rho}\frac{\partial \theta}{\partial t}=-\frac{1}{r}\frac{\partial \bar{\rho}ru\theta}{\partial r}-\frac{\partial \bar{\rho}\overline{w\theta}}{\partial z}-\frac{\partial \bar{\rho}\overline{w'\theta'}}{\partial z}+\bar{\rho}\frac{Q_k+Q_{кр}}{c_p\pi}+$$

$$+\frac{\bar{\rho}}{r\pi}k_\theta^H\frac{\partial}{\partial r}\left(r\frac{\partial \theta}{\partial r}\right)+\frac{1}{\pi}\frac{\partial}{\partial z}\left(\bar{\rho}k_\theta^z\frac{\partial \theta}{\partial z}\right), \qquad (3)$$

$$\bar{\rho}\frac{\partial q}{\partial t}=-\frac{1}{r}\frac{\partial \bar{\rho}ruq}{\partial r}-\frac{\partial \bar{\rho}\overline{wq}}{\partial z}-\frac{\partial \bar{\rho}\overline{w'q'}}{\partial z}-\bar{\rho}(P_k+P_{кр})+$$

$$+\frac{\bar{\rho}}{r}k_q^H\frac{\partial}{\partial r}\left(r\frac{\partial q}{\partial r}\right)+\frac{\partial}{\partial z}\left(\bar{\rho}k_q^z\frac{\partial q}{\partial z}\right), \qquad (4)$$

$$p=\bar{\rho}RT(1+0{,}61q), \qquad (5)$$

$$\pi=\left(\frac{p}{p_0}\right)^{R/c_p}=\frac{T}{\theta},\quad p_0=1000\ мб, \qquad (6)$$

$$\frac{\partial \pi}{\partial z}=-\frac{g}{(1+0{,}61\,q)\,c_p\theta}, \qquad (7)$$

$$\frac{\partial \bar{\rho}\bar{w}}{\partial z}=-\frac{1}{r}\frac{\partial \bar{\rho}ru}{\partial r}, \qquad (8)$$

where u--radial velocity component,
v--tangential velocity component,
w--vertical velocity,
T--temperature,
θ--potential temperature,
q--ratio of mixture of vapors--dry air,
p--pressure
$\bar{\rho}$--density,

Q_k--heat source as a consequence of condensation in cumulus clouds,
Q_{kp}--heat source as a consequence of large-scale condensation,
P_k--precipitation from cumulus clouds,
P_{kp}--large-scale precipitation,
k_u^H, k_v^H, k_θ^H, k_q^H--turbulence coefficients with respect to the horizontal for u, v, θ and q fields,
k_u^z, k_v^z, k_θ^z, k_q^z--turbulence coefficients with respect to the vertical for u, v, θ and q fields,
f--Coriolis parameter,
R--gas constant,
c_p--specific heat capacity with constant pressure,
g--acceleration of free fall.

In (1) the component with the pressure gradient is replaced according to (6) by an expression that is more convenient for computations with pressure analog (π); (5)--equation of state, (7)--equation of statics, (8)--continuity equation obtained in evaluating the order of magnitude of the components in the complete equation [16]. The use of the continuity equation in the form (8) jointly with the conditions of equality to zero of the vertical velocity on the upper and lower boundaries of the counted region filters out the inner gravity wave, and makes it possible to use large spacings in time in the process of integration [30]. The parametrization of the components $\frac{\partial \bar{\rho}\,\overline{w'v'}}{\partial z}$, $\frac{\partial \bar{\rho}\,\overline{w'\theta'}}{\partial z}$ and $\frac{\partial \bar{\rho}\,\overline{w'q'}}{\partial z}$, designating the transfer of the impulse of heat and moisture by pulsations of the scale of cumulus clouds will be discussed below.

Boundary Conditions

The region of counting--rectangle with lateral boundaries r=0 and $r=r_{max}$, and horizontal boundaries z=0 (surface of ocean) and $z=z_{max}$. The work used the following boundary conditions: on the upper boundary $z=z_{max}$

$$w=0;\quad k_v^z\frac{\partial v}{\partial z}=0;\quad k_u^z\frac{\partial u}{\partial z}=0;\quad k_\theta^z\frac{\partial \theta}{\partial z}=0;\quad k_q^z\frac{\partial q}{\partial z}=0; \qquad (9)$$

on the lower boundary w=0, the streams of heat, moisture and impulse are found with the help of parametrization of the boundary layer according to the Deardorff [17] method. A detailed description of the employed technique for parametrization of the boundary layer is given in [7] and is briefly described below.

The assumption of axisymmetry means that with r=0

$$u=0;\quad v=0;\quad \frac{\partial \theta}{\partial r}=0;\ \frac{\partial q}{\partial r}=0. \qquad (10)$$

With $r=r_{max}$ the selection of boundary conditions, generally speaking, depends on the amount r_{max}. In our case for the field T and q r_{max}=540 km, for the field u and v r_{max}=570 km. With such r_{max} for compensation of losses in the angular momentum M with friction on the earth's surface from outside the flow

M must be directed [12]. The question of the boundary layers with $r_{max} \approx 600$ km is examined in [27, 32]. The setting of the boundary layers is facilitated by the circumstance that with an increase in the radius the percentage of components with second derivatives in the equations rapidly drops. This permitted the authors of publications [27, 32] to obtain for the current function ψ the following boundary condition:

$$\frac{\partial \psi}{\partial r} = -\frac{\psi}{L}, \qquad (11)$$

where L--constant depending on selection r_{max}. With $r_{max} \approx 600$ km, as in [27, 28, 32] L=1800 km is assumed.

The current function ψ in the z-system of coordinates is assigned by the correlations

$$\bar{\rho} u = \frac{1}{r}\frac{\partial \psi}{\partial z}, \quad \bar{\rho} w = -\frac{1}{r}\frac{\partial \psi}{\partial r}.$$

It is easy to show that (11) is equivalent to the following conditions for the radial velocity component:

$$\frac{\partial ru}{\partial r} = -\frac{ru}{L}. \qquad (12)$$

The remaining boundary conditions with $r=r_{max}$ in the case of flow within the region ($u(r_{max}) < 0$) are assumed to be the following:

$$\frac{\partial rv}{\partial r} = 0; \quad T = T_\phi(z); \; q = q_\phi(z); \; \frac{\partial p_s}{\partial t} = 0, \qquad (13)$$

where T_ϕ and q_ϕ --background profiles of temperature and ratio of mixture, p_s--pressure at surface with $r=r_{max}$.

With outflow from the region ($u(r_{max}) > 0$) the values v, θ and q were determined on the boundary with the help of the method of so-called finite differences directed against the stream (the boundary conditions are not set).

Parametrization of Nonadiabatic Processes

The heat source Q and the velocity of condensation P were separated in (3) and (4) into two parts (Q_{kp}, Q_k and P_{kp}, P_k) governed by large-scale condensation and condensation in cumulus clouds (convective). It is believed that the large-scale condensation occurs when q, computed in one or several of the centers of the different grid increases the saturating value. It is assumed that the entire surplus moisture above the saturating value is momentarily condensed and comprises the large-scale precipitation. During condensation the temperature is increased (large-scale heating) so that the final saturating value, naturally, differs from the initial. Computation of Q_{kp}

and P_{kp} was made by the iteration method (Newton). In cumulus clouds condensation and precipitation occur when q does not reach the saturating value. During condensation of water vapor in the cumulus clouds an enormous quantity of latent heat is released. In addition, the cloud transfers upwards the heat, moisture and angular momentum. As a result of transfer of angular momentum the shift of the wind with altitude is lower than follows from the correlations of thermal wind [12]. In a number of models [14, 28] the transfer of the angular momentum is considered by selecting a large value for the turbulence coefficient with respect to the vertical in the zone of developed convection. However consideration of the transfer of the momentum by clouds is included more logically in the problem of convection parametrization.

For parametrization of atmospheric heating as a consequence of condensation in cumulus clouds the hypothesis is used for the conditions of instability of the second type (CISK) [16], as well as the consideration of Kuo [21] and Estogue [18] on the distribution of latent heat release with respect to the vertical. We will isolate the atmospheric column of unit area and break it down to horizontal planes on several layers. Assume in m lower layers the conditions for convection resistance are fulfilled: there is convergence of moisture (convergence of mass) and conditional instability ($\gamma > \gamma_{ea}$, where γ_{ea} is the moist-adiabatic gradient). (In typhoons in the zone of convergence as a consequence of the high air humidity the conditional instability coincides with the so-called convective instability [5]. The rising particles have a large supply of energy of instability. If the humidity is not great, as on the periphery of TC, the condensation level is located fairly high, the particles during elevation to this level along the dry adiabatic curve can become colder than the surroundings so much that above the condensation level its temperature becomes lower than the temperature of the surroundings. In such a situation deep convection, apparently is impossible, despite $\gamma > \gamma_{ea}$). For parametrization of the source Q_k in equation (3) we take into account the contribution of clouds that develop from each of the m lower layers. Assume I_β--quantity of moisture converged in a unit of time in the layer under the number $\beta \leqslant m$. As a result from the levels lying in this layer, in time Δt clouds emerge that occupy in the column above the base an area α'_β. Then $\alpha'_\beta = \frac{I_\beta \Delta t}{\delta q_\beta}$, where δ_{q_β}--quantity of moisture necessary for bringing to saturation the isolated atmospheric column from level β to the upper boundary of the clouds emerging from this level. The contribution to heating of the atmospheric column by clouds that emerge from level β, according to [21], can be computed as follows:

$$Q_{k_\beta} = \begin{cases} \frac{c_p a'_\beta}{\Delta t}(T_{o\delta_\beta} - \overline{T}) = \frac{I_\beta c_p}{\delta q_\beta}(T_{o\delta_\beta} - \overline{T}) & \text{with } T_{o\delta_\beta} > \overline{T} \\ 0 \quad \text{with } T_{o\delta_\beta} \leqslant \overline{T}, \end{cases} \tag{14}$$

where $T_{o\delta\beta}$--temperature of clouds emerging from level β (or according to the employed parametrization, the temperature of the moist adiabatic curve restored from level β).

The summary heating velocity Q_k is determined by the contribution of convective clouds that emerge from all m layers (the action of these types of clouds is considered to be independent from each other):

$$Q_k(z) = \sum_{\beta=1}^{m} Q_{k_\beta}. \qquad (15)$$

The velocity of convective condensation is determined from expression

$$P_k = \frac{Q_k}{L}, \qquad (16)$$

where L--specific heat condensation. Computation of Q_K according to formula (15) makes it possible to a certain degree to consider the change in the point of cloud cover (or rate of cloud formation) according to altitude.

We will now turn to parametrization of the components $\overline{w'\theta'}$, $\overline{w'q'}$ and $\overline{w'v'}$. We will use the following expressions as definitions:

$$w'_{o\delta} = w_{o\delta} - \overline{w}; \quad w'_{\delta o} = w_{\delta o} - \overline{w},$$

$$\theta'_{o\delta} = \theta_{o\delta} - \overline{\theta}; \quad \theta'_{\delta o} = \theta_{\delta o} - \overline{\theta}, \qquad (17)$$

$$\overline{w'\theta'} = \alpha w'_{o\delta}\theta'_{o\delta} + (1-\alpha)\, w_{\delta o}\theta_{\delta o},$$

$$\overline{w} = \alpha w_{o\delta} + (1-\alpha)\, w_{\delta o}; \quad \overline{\theta} = \alpha\theta_{o\delta} + (1-\alpha)\cdot\theta_{\delta o}. \qquad (18)$$

The dashes above mark the amounts obtained by averaging with respect to area, much greater than the scale of cumulus assemblies, but much smaller than the scale of TC. The strokes mark deviations from mean. The indices "oδ" and "δo" refer to the amounts in clouds and the cloudless surroundings respectively, α--percentage of space occupied by clouds.

From (17) and (18) with regard for the fact that $\alpha \ll 1$, we have

$$\overline{w'\theta'} = \frac{\alpha}{1-\alpha}(w_{o\delta} - \overline{w})(\theta_{o\delta} - \overline{\theta}) \approx \alpha w_{o\delta}(\theta_{o\delta} - \overline{\theta}). \qquad (19)$$

The simplification in (19) is linked to the fact that $w_{o\delta} \gg w$. For parametrization of expression (19) it is necessary to determine intensity of the cloud cover α, the vertical velocity in the clouds $w_{o\delta}$, and the potential cloud temperature. The values $\overline{w'\theta'}$, $\overline{w'q'}$ and $\overline{w'v'}$ were computed for the thickest clouds developed from the boundary layer $\beta=1$. The temperature of clouds was determined by the moist adiabatic curve restored from the level of condensation. The intensity was determined as follows.

The velocity of formation of the indicated clouds, according to (14) can be written as: $\frac{\tau_1}{\Delta t} = \frac{T_1}{\delta q_1}$. In order to determine the intensity the amount

$\frac{\alpha_1'}{\Delta t}$ was multiplied by the mean lifetime of the clouds t_{o6} (in the model $t_{o6}=30$ min). In computing the velocity w_{o6} of the cloud depending on altitude (the upper boundary of the clouds was considered to be the level where the moist adiabatic curve intersected the stratification curve) H_{o6} was separated into the following categories: 1) $H_{o6}>12$ km, 2) 12 km$\geqslant H_{o6}\geqslant 9$ km, 3) 9 km$> H_{o6}\geqslant 6$ km, 4) $H_{o6}<6$ km. It was considered that the velocity in the cloud rises linearly from 1 m/s on the lower boundary to the maximum value at the level $0.7\,H_{o6}$, and then drops linearly to zero on the upper boundary. The maximum velocity values with respect to categories were taken as follows: 1) $w_{o6\,max}=20$ m/s, 2) 15 m/s, 3) 10 m/s, 4) 7 m/s. These values correspond to the data [4] on velocities in thick cumulus clouds--"hot towers."

For the purposes of parametrization of expression $\overline{w'v'}$ included in (2) two assumptions were used: 1) the mass of air transferred in the "hot towers" preserves the angular momentum; 2) the shift in air elevated in the "hot towers" with respect to the radial coordinate is small.

A satisfactory fulfillment of the first assumption is indicated in [29]. The correctness of the second assumption follows from the smallness of the radial velocity components (1-3 m/s) as compared to the vertical velocity in clouds in the zone of developed convection of TC. From the indicated assumptions it follows that in the "hot towers" the tangential air velocity v_{o6} has a weak dependence on altitude, and equals the mean tangential air velocity at the level of the cloud base (level from which the moist adiabatic curve is restored). Thus we will consider

$$v_{o6}=v_{cp}. \tag{20}$$

Since $\bar{w}'\bar{v}'=\alpha\, w_{o6}(v_{o6}-\bar{v})$, then with regard for (20) we have

$$\overline{w'v'}=\alpha\, w_{o6}(v_{cp}-\bar{v}). \tag{21}$$

In the zone of developed convection of a TC the radial velocities are not great, therefore the component $\frac{\partial \bar{\rho}\,\overline{w'u'}}{\partial z}$ in (1) must be smaller than the remaining term of the equation, and is not considered in the computations. Observation of the condition for the presence of dry-stable stratification is controlled with the help of the method of dry convective adaptation. The method is stated in [9] and provides an unambiguous solution for the piecewise profile T(z) with preservation in the column of finite-difference analog (trapezoid method) of statistical energy of the entire atmospheric column

$$\int_0^{z_{max}} \bar{\rho}\,(c_v T+gz)\,dz,$$

where c_v--specific heat capacity with constant volume,
z_{max}--upper level of model.

Turbulent Exchange

In the given version of the model the coefficients of horizontal turbulence are assumed to be the same for all variables u, v, θ and q, and equal to 3×10^5 m^2/s. Such a considerable amount is linked to the great spacing in the finite-difference grid along the horizontal (Δr=60 km). The coefficients of turbulent viscosity, heat conductivity and moisture exchange were computed according to the same formula

$$k^z = c + l^2 \left| \frac{\partial V}{\partial z} \right|, \qquad (22)$$

where c--constant determined empirically. It is assumed c=10 m^2/s, l has the meaning of the path of shift and is computed according to the formula from [31]

$$l = \frac{0{,}4\ z}{1 + \frac{1480\ fz}{|V|}}, \qquad (23)$$

where V--complete wind velocity.

Interaction of Atmosphere and Ocean. Boundary Layer.

In [7, 25] the technique for parametrization of the boundary layer proposed by Deardorff [17] was employed under TC conditions, and a fairly good agreement was obtained between the computed amounts and those obtained from the balance correlations. It is known, that the Deardorff technique [17] makes it possible from the mean velocity values V_{bl}, potential temperature Θ_{bl}, and mixture ratio q_{bl} in the boundary layer (in the given case the so-called layer of mixing), its altitude z_B and temperature of water at the surface T_W to determine fluxes in impulse of the perceptible and latent heat from the surface. In the model the altitude z_B, as in [7, 25] was assumed to be equal to the altitude of the condensation level of the air that is adiabatically rising from the surface. This assumption is confirmed experimentally [26]. The values V_{bl}, Θ_{bl} and q_{bl} were defined on the level $z_B/2$. For closure of the parametrization equation to determine the level of irregularity the Charnok formula was used

$$z_0 = 0{,}035\ |V_*|^2/g, \qquad (24)$$

where V_*--friction velocity. The altitude of the near-water layer z_{sl} was considered to be linked to the altitude of the mixing layer by the correlation

$$z_{sl} = 0{,}025\ z_B. \qquad (25)$$

A detailed description of the technique for computing the fluxes and magnitudes on the level of the anemometer is given in [7].

Computation of the Pressure Field

Computation of the pressure field was made according to a technique analogous to [30]. From the continuity equation and condition w=0 on horizontal boundaries it is easy to obtain the expression

$$\int_0^{z_{max}} \bar{\rho} u \, dz = 0, \tag{26}$$

which is a consequence of the law of mass preservation. From (1) we have

$$\int_0^{z_{max}} c_p \Theta \bar{\rho} (1 + 0{,}61\, q) \frac{\partial \pi}{\partial r} \, dz = \int_0^{z_{max}} \left\{ \bar{\rho} v \left(f + \frac{v}{r} \right) - \frac{1}{r} \frac{\partial \bar{\rho} r u^2}{\partial r} + \right.$$

$$\left. + \bar{\rho} k_u^H \left(\frac{\partial^2}{\partial r^2} + \frac{1}{r} \frac{\partial}{\partial r} - \frac{1}{r^2} \right) u \right\} dz - c_D \bar{\rho} | V_a | u_a \equiv B(r). \tag{27}$$

In (27) the indices "a" marks the amounts on the so-called level of the anemometer which is the lower level of the model. Here the correlation is used

$$\bar{\rho} k_u^z \frac{\partial u}{\partial z} \Big|_{z=0} = c_D \bar{\rho} | V_a | u_a, \tag{28}$$

where c_D--resistance coefficient. The values c_D, u_a, V_a are located simultaneously with the fluxes in the block of the boundary layer.

From the statics equation (7) we have

$$\pi(z) - \pi_s = -g \int_0^z \frac{dz}{(1 + 0{,}61\, q) c_p \Theta} \equiv -H(z), \tag{29}$$

where $\pi_s = \pi(z=0)$.

From (29) it follows

$$\int_0^{z_{max}} c_p \bar{\rho} \Theta (1 + 0{,}61\, q) \frac{\partial \pi}{\partial r} \, dz = \frac{\partial \pi_s}{\partial r} c_p \int_0^{z_{max}} \bar{\rho} \Theta (1 + 0{,}61\, q) \, dz -$$

$$- \int_0^{z_{max}} c_p \bar{\rho} \Theta (1 + 0{,}61\, q) \frac{\partial H}{\partial r} \, dz. \tag{30}$$

From (27) and (30) we finally have the expression

$$\frac{\partial \pi_s}{\partial r} = \frac{B + c_p \int_0^{z_{max}} \bar{\rho} \Theta (1 + 0{,}61\, q) \frac{\partial H}{\partial r} \, dz}{c_p \int_0^{z_{max}} \bar{\rho} \Theta (1 + 0{,}61\, q) \, dz}. \tag{31}$$

From equation (31) and the value $\pi_s(r_{max})$ assigned on the boundary $\pi_s(r)$ is determined on the surface. Further, from (29) the entire field $\pi(r,z)$ is computed.

Numerical Technique

The difference grid consists of ten centers along the horizontal (Δr=60 km) and twelve levels along the vertical.

A fragment of the finite-difference grid is given in Figure 1. ω is computed at points z_j, where j=0, ..., 11, and r_i, where r=0, ..., 9; u and v are computed at points $z_{j+\frac{1}{2}}$, where j=0, ..., 10, and $r_{i+\frac{1}{2}}$, where i=0, ..., 9, and at points on the lower boundary z_j with j=0. θ, q and π are computed at points $z_{j+\frac{1}{2}}$, j=0, ..., 10, r_i, i=0, ..., 9.

Along the vertical the spacings of the grid are nonuniform. The heights of the corresponding level, mean pressure and mean air density are given in Table 1.

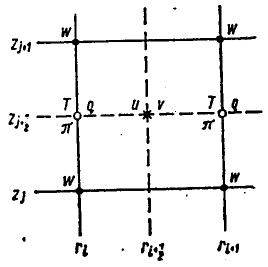

Figure 1.

In order to exclude the nonlinear calculation instability in recording the finite-difference approximations in the differential equations the box-method (1) is used.

As an example we will cite the finite-difference recording of a group of advective components in the equation of tangential velocity:

$$\left[\frac{1}{r}\frac{\partial\overline{\rho}ruv}{\partial r}-\frac{\partial\overline{\rho}wv}{\partial z}\right]=\frac{1}{r_{i+\frac{1}{2}}\Delta r}\left[\overline{\rho}_{j+\frac{1}{2}}\left(r_{i+1}\frac{u_{i+\frac{3}{2},\,j+\frac{1}{2}}+u_{i+\frac{1}{2},\,j+\frac{1}{2}}}{2}\times\right.\right.$$

$$\times\frac{v_{i+\frac{3}{2},\,j+\frac{1}{2}}+v_{i+\frac{1}{2},\,j+\frac{1}{2}}}{2}-r_i\frac{u_{i+\frac{1}{2},\,j+\frac{1}{2}}+u_{i-\frac{1}{2},\,j+\frac{1}{2}}}{2}\times$$

$$\left.\left.\times\frac{v_{i+\frac{1}{2},\,j+\frac{1}{2}}+v_{i-\frac{1}{2},\,j+\frac{1}{2}}}{2}\right)\right]+\frac{1}{z_{j+1}-z_j}\left(\overline{\rho}_{j+1}\frac{w_{i,\,j+1}+w_{i+1,\,j+1}}{2}\times\right.$$

$$\times\frac{v_{i+\frac{1}{2},\,j+\frac{3}{2}}+v_{i+\frac{1}{2},\,j+\frac{1}{2}}}{2}-\overline{\rho}_j\frac{w_{i,\,j}+w_{i+1,\,j}}{2}\times$$

$$\left.\times\frac{v_{i+\frac{1}{2},\,j+\frac{1}{2}}+v_{i+\frac{1}{2},\,j-\frac{1}{2}}}{2}\right)\qquad(32)$$

and heat influx:

$$\left[\frac{1}{r}\frac{\partial\overline{\rho}ru\theta}{\partial r}-\frac{\partial\overline{\rho}w\theta}{\partial z}\right]=\frac{1}{r_i\Delta r}\left[\overline{\rho}_{j+\frac{1}{2}}\left(r_{i+\frac{1}{2}}u_{i+\frac{1}{2},\,j+\frac{1}{2}}\times\right.\right.$$

$$\times\frac{\theta_{i+1,\,j+\frac{1}{2}}+\theta_{i,\,j+\frac{1}{2}}}{2}-r_{i-\frac{1}{2}}u_{i-1,\,j+\frac{1}{2}}\frac{\theta_{i,\,j+\frac{1}{2}}+\theta_{i-1,\,j+\frac{1}{2}}}{2}\left.\right)\Bigg]+$$

$$+\frac{1}{z_{j+1}-z_j}\left(\overline{\rho}_{j+1}w_{i,\,j+1}\frac{\theta_{i,\,j+\frac{1}{2}}+\theta_{i,\,j+\frac{3}{2}}}{2}-\right.$$

$$\left.-\overline{\rho}_jw_{i,\,j}\frac{\theta_{i,\,j+\frac{1}{2}}+\theta_{i,\,j-\frac{1}{2}}}{2}\right).\qquad(33)$$

TABLE 1.

(a) Номер уровня	(b) Высота, м	(c) Средняя плотность, кг/м³	(d) Среднее давление, мб	(a) Номер уровня	(b) Высота, м	(c) Средняя плотность, кг/м³	(d) Среднее давление, мб
1	0	1,165	1013	7	5105	0,708	550
2	574	1,117	950	8	7380	0,552	407
3	1042	1,069	900	9	9655	0,436	300
4	1530	1,019	850	10	11915	0,338	215
5	2042	0,968	800	11	14175	0,254	150
6	3154	0,865	700	12	16590	0,174	100

Key:
a. Number of level b. Altitude, m c. Mean density, kg/m^3
d. Main pressure, mbar

The remaining derivatives were recorded with the help of central differences. The scheme for integration with respect to time is close to the method of Natsuno [24]. It can be illustrated in the example of equation

$$\frac{\partial x}{\partial t} = A(x) + F(x),$$

where A--expression including the heat source from condensation in the cumulus clouds and rate of convective precipitation,
F--remaining components.

The computation of x on the next step with respect to time, consists of the following stages:

a) $x^{t+\frac{1}{2}} = x^t + \Delta t\,(A(x^t) + F(x^t))$;

b) computation of $x^{t+\frac{1}{2}}$ on the boundaries;

c) $x^{t+1} = x^t + \Delta t\,(A(x^t) + F(x^{t+\frac{1}{2}}))$;

d) computation of x^{t+1} on the boundaries.

The order of computations in the model is shown in the block diagram (Figure 2).

The spacing with respect to time was 1.5 min, the counting was stable without the use of special methods of smoothing.

Background Field and Parameters

The background values of temperature are close to the data [20] for the tropical atmosphere in the period of hurricanes. The background values of temperature, mixture ratio and relative humidity are given in Table 2. The temperature of the water surface was considered to be equal to 29°C, p_0=1013 mbar, f=5 x 10^{-5} s^{-1}.

TABLE 2.

z м	TK	g/kg q, z/кz	$\frac{q}{q_s} \times 100\%$	z м	TK	g/kg q z/кz	$\frac{q}{q_s} \times 100\%$
0	299,3	18,3	88%	4129	276,1	5,3	71%
287	298	17,0	87%	6242	263,6	2,6	67,5%
808	294,8	14,7	85,5%	8517	248,3	0,84	59%
1286	292	12,8	84%	10780	230.6	0,18	54%
1786	289,2	11,2	82,5%	13045	213,3	0,03	50%
2598	284,8	8,6	76,5%	15382	203,5	0,01	46%

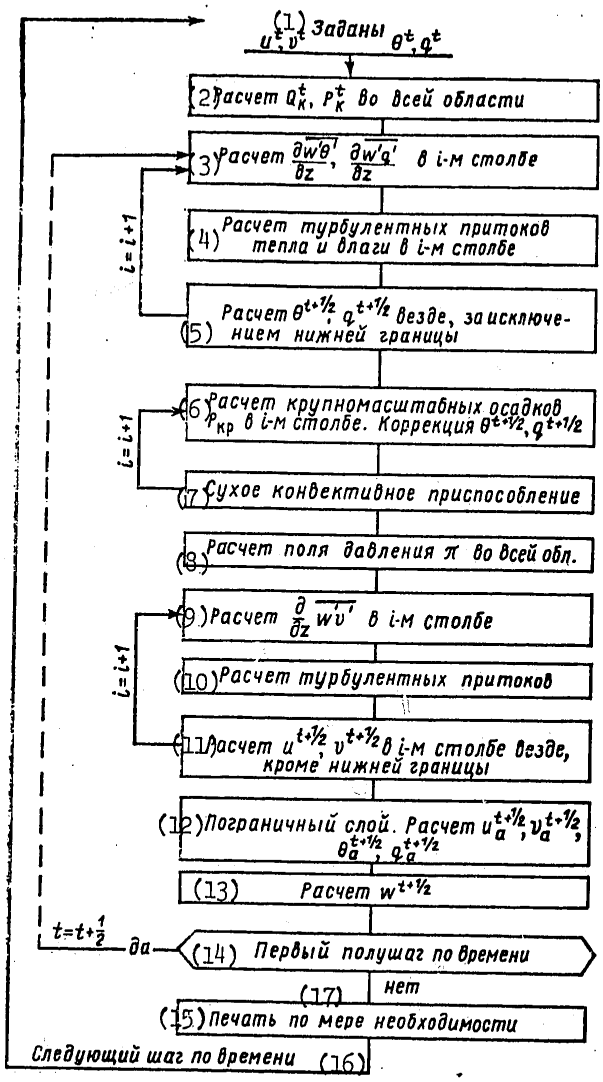

Figure 2.
Key:
1. Assigned
2. Computation of Q_k^t, P_k^t in entire region
3. Computation of $\frac{\partial \overline{w'\theta'}}{\partial z}$, $\frac{\partial \overline{w'q'}}{\partial z}$ in i-th column
4. Computation of turbulent influxes of heat and moisture in i-th column

5. Computation of $\theta^{t+\frac{1}{2}}$, $q^{t+\frac{1}{2}}$ everywhere, with the exception of the lower boundary
6. Computation of large-scale precipitations P_{kp} in i-th column. Correction $\theta^{t+\frac{1}{2}}$, $q^{t+\frac{1}{2}}$
7. Dry convective adaptation
8. Computation of pressure field π in entire region
9. Computation of $\frac{\partial}{\partial z}\overline{w'v'}$ in i-th column
10. Computation of turbulent influxes
11. Computation of $u^{t+\frac{1}{2}}$, $v^{t+\frac{1}{2}}$ in i-th column, everywhere, except the lower boundary
12. Boundary layer. Computation of $u_a^{t+\frac{1}{2}}$, $v_a^{t+\frac{1}{2}}$, $\theta_a^{t+\frac{1}{2}}$, $q_a^{t+\frac{1}{2}}$
13. Computation of $w^{t+\frac{1}{2}}$
14. First half step in time
15. Printing as necessary
16. Next step in time
17. No

The starting conditions were assigned as follows. According to the assigned profile $T_\phi(z)$ and $\overline{\pi_1}=\left(\frac{1013}{1000}\right)^{R/c_p}$ with the help of the static equation was the background value $\overline{\pi}(z)$ was determined. Further the background pressure $\overline{p}$ was determined, and from the equation of state--the mean air density $\overline{\rho}(z)$.

The starting temperature was assigned in the form

$$T_{i,j}=T_{\phi_j}+T_* \exp\left(-br_i/r_{max}\right)\sin\frac{\pi z_j}{z_{max}},$$

where T_* was assumed to be equal to 1K, b=5. From the equation of hydrostatics with $\pi(r, z_{max})=\overline{\pi}(z_{max})$ the starting field $\pi(r, z)$ was determined. The tangential velocity was found from the equation of gradient wind. The radial velocity with t=0 was assumed to be equal to zero. The ratio of the mixture was assumed to be the same along the horizontal and equal to the background value.

Results of Calculations

The main development of the model TC occurred in the first days. Further (roughly from 35 h) emergence to the quasistationary pattern occurred.

Figure 3 (on the right) gives a section in the field of tangential velocity component at the moment t=100 h. On the left for comparison the same field is given for the "mean" TC [19]. Figures 4 and 5 give the sections obtained in the model of the radial and vertical velocity component in the same moment of time. The minimum pressure in the center at the earth's surface was 979 mbar, the maximum wind velocity equals 40 m/s. On the whole the structure of the model TC agrees with the observed (see, for example, Figure 3). The storm winds were spread to great altitudes. In the upper part of the troposphere the cyclonic rotation is replaced by anticyclonic.

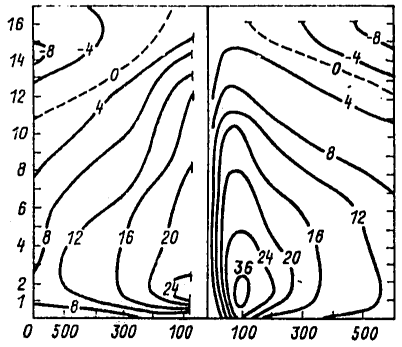

Figure 3

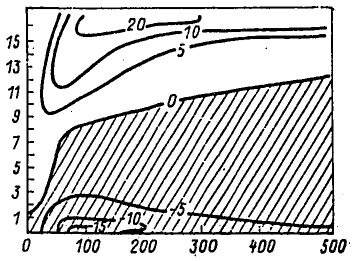

Figure 4

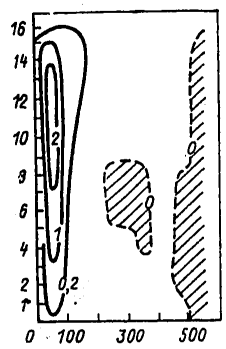

Figure 5

Due to the small resolution of the grid the radius of maximum winds is fairly great: 90 km. The field of tangential velocity for the given model was more real than, for example, in [28, 30] where the isoline v=10 m does not go beyond the limits of a region with radius 250 km [30] and 300 km [28].

The main influx into the TC region occurs in the boundary layer. The influx is spread to altitude 11-12 km (250-300 mbar) which agress with the empirical data [19], and differs from the results of publications [28, 30, 32] where the influx is replaced by outflow at level 500 mbar. The outflow is concentrated in the upper troposphere.

The vertical velocity field was fairly realistic. The maximum ascending movement (actually the wall of the TC eye) is located at distance 60 km from the center. The ascending vertical movements in the model occur up to considerable radii (r≈450 km), which agrees with the data for the mean TC [19] where the ascending movements occupy a region with radius 440 km.

Figure 6 on the right gives the field of temperature deviations in the background value, on the left the deviations for the mean TC from observational data [19]. The satisfactory agreement of the computation results of the observational data is apparent.

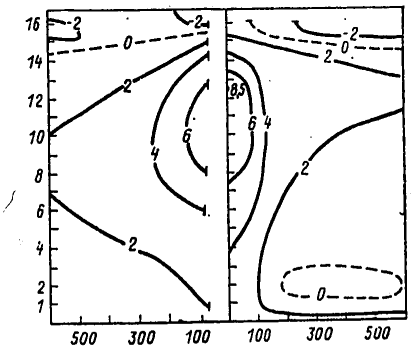

Figure 6.

Negative anomalies of temperature obtained in the lower troposphere were observed in a number of TC, for example in Hilda 1964. In the computations negative temperature anomalies were obtained in the upper troposphere-lower stratosphere. These anomalies exist also in real TC. On the whole the field of temperature anomalies in the given work were much more realistic than in [28, 30], where, for example, the isoline 2°C does not go beyond the limits of the region with radius 150 km. In [28] the isoline 4°C reaches the earth's surface. In these same publications, as well as in [32] negative temperature anomalies were not obtained in the upper troposphere.

We note that in the boundary layer with r<300 km the temperature practically does not depend on the radial distance, as occurs in actuality. Figure 7,a presents the dapences of pressure, coefficients of resistance c_D and heat exchange c_H, as well as altitude of the mixing layer on the distance to the center of the TC. Figure 7,b shows the relationships of the streams of perceptible and latent heat and the impulse stream. Since the extant models either do not include the hydrological cycle, or the boundary layer, then the amounts of the computed streams usually are not given.

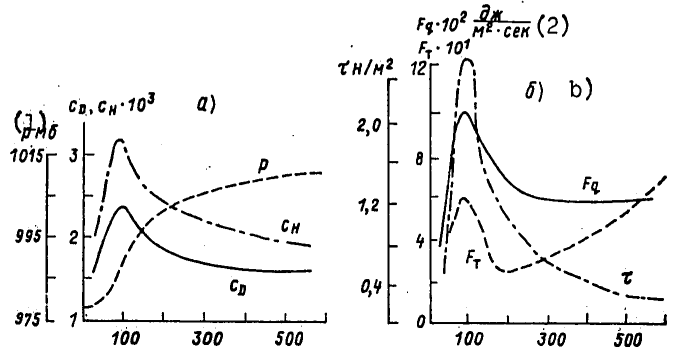

Figure 7. 1. mbar 2. $J/m^2 \cdot s$

As is apparent in Figure 7,a the altitude of the mixing layer (altitude of the condensation level) increases with an increase in radius from 200 to 500 m, which agrees with the observational data. Thus in hurricane Hilda 1964 (in the limits of radius 100 km) the altitude of the condensation level increased from 260 to 408 m [7], and in hurricane Inez 1966 in the same region--from 440 to 70 m. The computed coefficients c_D and c_H are also close to the observational data [7, 25]. The computed values for the streams of latent heat and impulse agree well with the observations. The computed heat flows as compared to the data [7, 25] are somewhat lower (roughly 1.5-fold).

Figure 8 presents a section in the field of relative humidity that is also fairly close to the observed.

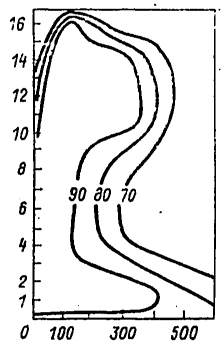

Figure 8.

A more detailed analysis of the results and comparison with the observational data will be made in the future.

The author expresses his gratitude to V. V. Yepikhin for valuable notes and discussions.

BIBLIOGRAPHY

1. Brayyen, K. "Scheme of Numerical Integration of Motion Equations on Irregular Grid Free of Nonlinear Instability," "Chislennyye metody resheniya zadach dinamiki atmosfery i okeana" [Numerical Methods for Solving the Problems of Atmospheric and Ocean Dynamics], Leningrad, Gidrometeoizdat, 1968.

2. Zakharov, V. Ye.; Sapronov, Yu. T. "Multiple-Level Axisymmetrical Model of Tropical Cyclone," "Tayfun-75" [Typhoon-75], 1978.

3. Zakharov, V. Ye. "Mathematical Models of Life Cycle of Tropical Hurricanes," TRUDY IEM, No 3 (37), 1973.

4. Malkus, Dzh. A. "Modern Development of Studies of Penetrating Convection and Their Application to Towers of Cumulonimbus Clouds," "Dinamikh kuchevykh oblakov" [Dynamics of Cumulus Clouds], Moscow, Mir, 1964.

5. Fal'kovich, A. I. "Thermodynamic Parameters and Convective Instability of Tropical Atmosphere," METEOROLOGIYA I GIDROLOGIYA, No 9, 1977.

6. Khain, A. P.; and Sitnikov, I. G. "Numerical Model of Evolution of Axisymmetrical Tropical Cyclone (Statement of Problem)," TRUDY GIDROMETTSENTRA SSSR, No 203, 1978.

7. Khain, A. P.; and Agrenich, Ye. A. "Peculiarities of Boundary and Near-Water Layers in Tropical Cyclones," METEOROLOGIYA I GIDROLOGIYA, No 1, 1978.

8. Khain, A. P. "Methods of Parametrization of Convection Used to Model Tropical Cyclones," "Tayfun-75", 1978.

9. Khain, A. P.; Gevorkyan, K. Kh. "Method of Dry Convective Adaptation," TRUDY GIDROMETTSENTRA SSSR, 1979.

10. Shulykin, V. V. "Development and Attenuation of Tropical Hurricane in Different Thermal Conditions," IZV. AN SSSR. FIZIKA ATMOSFERY I OKEANA, vol 8, No 1, 1972.

11. Shulykin, V. V. "Computation of Trajectories of Tropical Hurricanes," IZV. AN SSSR. FIZIKA ATMOSFERY I OKEANA, vol 9, No 12, 1973.

12. Anthes, R. A. "The Dynamics and Energetics of Mature Tropical Cyclones," REV. GEOPHYS. AND SPACE PHYS., vol 12, No 3, 1974.

13. Anthes, R. A. "Hurricane Model Experiments With a New Cumulus Parametrization Scheme," MON. WEATHER REV., vol 105, No 3, 1977.

14. Anthes, R. A.; Rosenthal, S. L.; Trout, J. W. "Preliminary Results From an Asymmetric Model of the Tropical Cyclone," MON. WEATHER REV., vol 99, 1971.

15. Anthes, R. A. "The Development of Asymmetries in a Three-Dimensional Numerical Model of the Tropical Cyclone," MON. WEATHER REV., vol 100, No 6, 1972.

16. Charney, J. G.; Eliassen, A. "On the Growth of the Hurricane Depression," J. ATMOS. SCI., vol 21, No 1, 1964.

17. Deardorff, J. W. "Parametrization of the Planetary Boundary Layer for Use in General Circulation Models," MON. WEATHER REV., vol 10, 1972.

18. Estogue, M. A. "Vertical Mixing Due to Penetrative Convection," J. ATMOS. SCI., vol 25, No 6, 1968.

19. Frank, W. M. "The Structure and Energetics of the Tropical Cyclone I-Storm Structure," MON. WEATHER REV., vol 105, No 9, 1977.

20. Jordan, C. L. "Mean Soundings for the West Indies Area," J. APPL. METEOROL., vol 15, 1976.

21. Kuo, M. L. "On Formation and Intensification of Tropical Cyclones Through Latent Heat Release by Cumulus Convection," J. ATMOS. SCI., vol 22, No 1, 1965.

22. Kurihara, U. "Budget Analysis of a Tropical Cyclone Simulated in an Axisymmetric Numerical Model," J. ATMOS. SCI., vol 32, No 1, 1975.

23. Kurihara, Y.; Tuleya, R. E. "Structure of a Tropical Cyclone Developed in a Three-Dimensional Numerical Simulation Model," J. ATMOS. SCI., vol 31, No 5, 1974.

24. Matsuno, Y. "Numerical Integrations of Primitive Equations by Use of Simulated Backward Difference Method," J. METEOROL. SOC. JAPAN, vol 44, 1966.

25. Moss, M. S.; Rosenthal, S. L. "On the Estimation of Planetary Boundary Layer Variables in Mature Hurricanes," MON. WEATHER REV., vol 103, 1975.

26. Moss, M. S.; Merceret, F. J. "A Note on Several Low-Layer Features of Hurricane Eloise (1975)," MON. WEATHER REVL, vol 104, No 7, 1976.

27. Ooyama, K. "Numerical Simulations of the Life-Cycle of Tropical Cyclones," J. ATMOS. SCI., vol 26, No 1, 1969.

28. Peng, L. I.,; Kuo, H. L. "A Numerical Simulation of the Development of Tropical Cyclones," TELLUS, vol 27, No 2, 1975.

29. Riehl, H.; Malkus, J. S. "Some Aspects of Hurricane Daisy, 1958," TELLUS, vol 13, 1961.

30. Rosenthal, S. L. "A Circulary Symmetric Primitive Equation Model of Tropical Cyclone Development Containing an Explicit Water Vapor Cycle," MON. WEATHER REV., vol 98, No 9, 1970.

31. Rosenthal, S. L. "Numerical Simulation of Tropical Cyclone Development With Latent Heat Release by the Resolvable Scales I: Model Description and Preliminary Results," J. ATMOS. SCI., vol 35, 1978.

32. Sundquist, H. "Numerical Simulation of the Development of Tropical Cyclones With a Ten-Level Model, P. I.," TELLUS, vol 22, 1970.

33. Yamasaki, M. "A Preliminary Experiment of the Tropical Cyclone Without Parametrizing the Effects of Cumulus Convection," J. METEOROL. SOC. JAPAN, vol 55, 1977.

UDC 532.52+551.513

CONSIDERATION OF THE EFFECT OF ROTATION AND MOTION OF VORTICES ON THE BASIC FLOW OF LIQUID

Moscow METEOROLOGIYA I GIDROLOGIYA in Russian No 10, Oct 1979 pp 38-47

[Article by Candidate of Physical and Mathematical Sciences A. S. Kabanov and B. Ya. Shmerlin, Institute of Experimental Meteorology, submitted for publication 14 May 1979]

Abstract: The physical mechanism is examined for the impulse transfer from regions with lower mean flow velocity value into regions with greater value. Such a transfer can be implemented by the vortices emerging in the liquid. A system of equations is written that describes the combined movement of vortices and the liquid, and their mutual effects. As an example stationary zonal circulation in the earth's atmosphere is examined that emerges as a consequence of cyclonic and anticyclonic activity in the atmosphere. A profile is obtained for zonal wind velocity that agrees qualitatively with that observed in the atmosphere.

[Text] As measurements show, for certain types of currents in rotating systems both under laboratory and under natural conditions, the viscosity coefficient values are systematically negative [5], that is, the impulse is transferred from regions with a lower mean flow velocity value to regions with a greater value of the mean flow velocity. A real example of such a current can be, for example, rotation of the earth's atmosphere.

In [5] it is indicated that the reason for such an "anomalous" impulse transfer can be the constantly emerging vortical movements, whereby the impulse transfer is governed by a certain orientation of the corresponding current lines. However currently there is no theory which would describe the systematic orientation of current lines.

Another mechanism for impulse transfer is possible that is associated not with a certain orientation of the current lines, but with movement of the vortices

in relation to the basic flow. Assume, for example, (Figure 1) with y=0 vortices are generated that are twisted clockwise and counterclockwise. The interaction of vortices with the flow, and the effects linked to the rotation of the liquid, result in the fact that the vortices twisted to different sides begin to be shifted in different directions from the site of their generation.

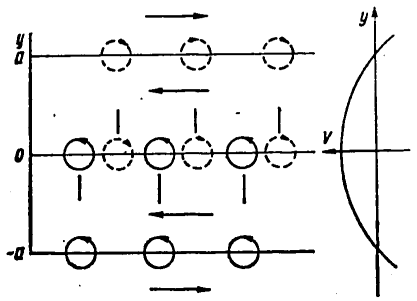

Figure 1. Schematic Illustration of Generation, Movement and Filling of Vortices and Formation of Velocity Profile of Basic Flow

Assume that the vortices that are twisted clockwise are shifted in a direction $y>0$, counterclockwise--in a direction $y<0$. Due to the friction on the basic flow the vortices attenuate, for example, with $y=\pm a$ correspondingly. As is apparent from the figure, the friction of the vortices rotating with $y=\pm a$ on the basic flow results in the fact that in the band $-a<y<a$ the flow velocity will be directed to the left, and in the region $|y|>a$ the flow velocity will be directed to the right in accordance with the velocity profile given in the figure. Thus, the emergence and movement of the vortices results in the establishment of a certain flow velocity profile, even if no external forces will act on the flow. In order to describe the establishment of such a velocity profile the coefficient of negative viscosity was introduced. Its physical meaning is evident from the discussions given above.

Consequently, it is important to write a system of dynamic equations that describe the rotation and movement of vortices and their effect on the basic flow.

As a model of liquid we will examine a model made of three mutually-penetrating continuums: the basic liquid, vortices rotating clockwise, and vortices rotating counterclockwise. The movement of such a 3-phase mixture will be examined on the assumption that the distances at which the parameters of the basic flow are significantly altered are much greater than the characteristic dimensions of the vortices. We will consider the vortices to be cylinders interacting with the basic flow and not interacting with each other. Assume that the specific volumetric content of the basic liquid in

the mixture α, its density ρ. Then the movement of the basic liquid in the mixture with velocity V_0 and density ρ is identical to the movement in free space with velocity V_0 and mean density $\alpha\rho$. (An analogous approach is employed in the mechanics of multiple-phase mixtures, for example, in [2]). In the system of coordinates rotating with angular velocity Ω, the equations for the basic liquid adopt the following appearance:

continuity equation

$$\frac{\partial \alpha\rho}{\partial t} + \frac{\partial}{\partial X_i} \alpha\rho V_{0i} = I; \tag{1}$$

equation of motion

$$\alpha\rho \frac{dV_{0i}}{dt} + V_{0i} I = -\alpha \frac{\partial P}{\partial X_i} + \frac{\partial}{\partial X_j} \alpha\tau_{ij} + \frac{\partial}{\partial X_j} \tau^a_{ij} - 2\alpha\rho e_{ikl} \Omega_k V_{0l} + F_i + I_i, \tag{2}$$

equations of angular momentum

$$\tau^a_{ij} = \frac{1}{2} e_{kij} (G_k - e_{kmn} X_m I_n). \tag{3}$$

We will designate

$$Q_k = G_k - e_{kmn} X_m I_n.$$

In these equations e_{ikl}--Levi-Chivit tensor;
X_i--coordinates;
V_{oi}--relative velocities of basic flow of liquid;
P--pressure of basic liquid;
τ_{ij}--symmetrical part of stress tensor;
τ^a_{ij}--antisymmetrical part of stress tensor.

The cited equations differ from the generally accepted in the fact that they have terms that describe the effect of vortices on the basic liquid. In their generation and development vortices "draw out" the angular momentum from the basic flow, and give it to the basic flow in the process of filling as a consequence of ordinary friction, but already in different places, shifted in relation to the basic flow. Thus, the vortices are a source for angular momentum for the basic flow; here the stress tensor of the basic flow becomes asymmetric (see, for example, [1]), and additional volume-distributed force appears that acts on the main liquid governed by the antisymmetric part of the stress tensor τ^a_{ij}, and takes into consideration the effects associated with rotation of the vortices. G_k in (3) is the source of the angular momentum in a unit of volume in the mixture, F_i in (2) is the forces acting

on the basic liquid on the part of the vortices in a unit of mixture volume governed by the movement of the vortices in relation to the basic liquid, I_1 is the source of impulse in a unit of mixture volume governed by the fact that at the moment of generation of the vortex the impulse is taken from the basic liquid, and at the moment of destruction it is given back to the basic liquid. Analogously to this I is the source of mass in a unit of mixture volume governed by generation and destruction of the vortices.

Further the movement of the liquid will be examined on the surface of a rotating sphere with radius R. Following [3], we average equations (1), (2), with regard for (3) according to altitude, assuming here that for the basic liquid the equation of quasistatics is fulfilled and the vertical velocities are much lower than the horizontal; we will consider, in addition, that the basic liquid is adiabatic. The assumption on the adiabatic nature of the basic liquid corresponds to the fact that the influx of heat in the system from external forces is localized in the vortices, by means of which the vortices "are untwisted," while the basic liquid receives energy only in the form of mechanical from the vortical movements.

We obtain the expressions:

$$\frac{d\alpha}{dt} + \alpha\frac{d\gamma}{dt} + \alpha \operatorname{div} \mathbf{V}_0 = \frac{g}{P_0} I^*, \tag{4}$$

$$\alpha\left(\frac{dV_{0\Theta}}{dt} - \frac{V_{0\Phi}^2}{R}\operatorname{ctg}\Theta\right) + I^* V_{0\Theta}\frac{g}{P_0} = -gH_0\frac{\alpha}{R}\frac{\partial\gamma}{\partial\Theta} + $$
$$+ 2\alpha\Omega\cos\Theta V_{0\Phi}(1+\gamma) + \frac{g}{P_0}F_\Theta^* +$$
$$+ \frac{1}{2R\sin\Theta}\frac{g}{P_0}\frac{\partial Q_r^*}{\partial\Phi} + \frac{g}{P_0}I_\Theta^* + F_{\text{тр}\,\Theta}, \tag{5}$$

$$\alpha\left(\frac{dV_{0\Phi}}{dt} + \frac{V_{0\Theta}V_{0\Phi}}{R}\operatorname{ctg}\Theta\right) + I^* V_{0\Phi}\frac{g}{P_0} = -gH_0\frac{\alpha}{R}\frac{\partial\gamma}{\partial\Phi} -$$
$$- 2\alpha\Omega\cos\Theta V_{0\Theta}(1+\gamma) + \frac{g}{P_0}F_\Phi^* -$$
$$- \frac{1}{2R}\frac{g}{P_0}\frac{\partial Q_r^*}{\partial\Theta} + \frac{g}{P_0}I_\Phi^* + F_{\text{тр}\,\Phi}. \tag{6}$$

In these equations Θ--addition of latitude;
Φ--longitude increasing to the east;
$V_{0\Theta}$, $V_{0\Phi}$--corresponding velocities averaged with respect to altitude of the liquid $r(\bar{V}=\int_R^\infty V\rho\,dr/\int_R^\infty \rho\,dr)$;
g--analog of acceleration of freefall;
P_0--mean pressure on surface of sphere;
H_0--altitude of uniform atmosphere, $H_0=P_0/g\rho_0$, where ρ_0--mean density on surface of sphere;

$\chi = \frac{P(\Theta, \Phi, 0) - P_0}{P_0}$ --characterizes the deviation of pressure on the sphere surface and its mean value;

F_{tp}--viscous forces in basic liquid; amounts with asterisks are integrated with respect to the previously introduced amounts without asterisks;

$$\frac{d}{dt} = \frac{\partial}{\partial t} + \frac{V_{0\Theta}}{R}\frac{\partial}{\partial \Theta} + \frac{V_{0\Phi}}{R\sin\Theta}\frac{\partial}{\partial \Phi}, \quad \operatorname{div} \mathbf{V}_0 = \frac{1}{R}\frac{\partial}{\partial \Theta} V_{0\Theta} +$$

$$+ \frac{1}{R\sin\Theta}\frac{\partial}{\partial \Phi} V_{0\Phi} + \frac{V_{0\Theta}}{R}\operatorname{ctg}\Theta.$$

In order to describe the rotation and movement of the vortices we introduce the function $f(\Theta, \Phi, V_\Theta, V_\Phi, \omega, L, \tau, t)$ separately for vortices rotating clockwise, and separately for vortices rotating counterclockwise, such that $fd\Theta d\Phi dV_\Theta dV_\Phi d\omega dL d\tau$ are the number of vortices, whose lifetime lies in the interval $d\tau$ around τ; the coordinates are included in the interval $d\Theta$, $d\Phi$ around Θ and Φ, the velocities are included in the intervals dV_Θ, dV_Φ around V_Θ, V_Φ; the angular velocity in the interval $d\omega$ around ω and the dimensions in the interval dL around L.

In the expressions given above V_Θ, V_Φ--components of velocity of vortical movement in relation to sphere; ω--angular velocity of vortex rotating on the surface of the sphere in relation to the sphere.

We will call the functions f for brevity the distribution functions.

For the distribution functions we will write continuity equations in seven-dimensional space $\Theta, \Phi, V_\Theta, V_\Phi, \omega, L, \tau$ which express the preservation of the number of vortices;

$$\frac{\partial f}{\partial t} + \frac{\partial f}{\partial \tau} + \frac{1}{R} V_\Theta \frac{\partial f}{\partial \Theta} + \frac{1}{R\sin\Theta} V_\Phi \frac{\partial f}{\partial \Phi} + \frac{dV_\Theta}{dt}\frac{\partial f}{\partial V_\Theta} +$$

$$+ \frac{dV_\Phi}{dt}\frac{\partial f}{\partial V_\Phi} + \frac{d\omega}{dt}\frac{\partial f}{\partial \omega} + f\left\{\frac{\partial}{\partial V_\Theta}\left(\frac{dV_\Theta}{dt}\right) + \frac{\partial}{\partial V_\Phi}\left(\frac{dV_\Phi}{dt}\right) +\right.$$

$$\left. + \frac{\partial}{\partial \omega}\left(\frac{d\omega}{dt}\right)\right\} + \frac{dL}{dt}\frac{\partial f}{\partial L} + f\frac{\partial}{\partial L}\left(\frac{dL}{dt}\right) = Z(\Theta, \Phi, V_\Theta, V_\Phi, \omega, L, \tau, t). \quad (7)$$

Here $Zd\Theta d\Phi dV_\Theta dV_\Phi d\omega dL d\tau$ --number of vortices generated (lost) in a unit of time, whose lifetime is included in the interval $d\tau$ around τ; the coordinates lie in the interval $d\Theta$, $d\Phi$ around Θ, Φ; the velocities in the intervals dV_Θ, dV_Φ around V_Θ and V_Φ; the angular velocities in the interval $d\omega$ around ω, the radius in the interval dL around L.

Accelerations of the vortices included in (7) are found from the equations

$$m\frac{d\mathbf{V}}{dt} = \sum_{i=1}^{6} \mathbf{f}_i. \qquad (8)$$

where m--mass of vortex,

f_i--forces acting on vortex on the part of the basic flow and the underlying surface (Stokes' force; Zhukovskiy force; force governed by pressure gradients in the basic flows; effect of added mass; friction on underlying surface; Coriolis force). Without giving specific expressions for the forces, we note that all the forces are determined through previously introduced characteristics of the basic flow $(\mathbf{V}_0, \chi)$ and vortices (V, ω, L). Analysis demonstrates that in the western zonal flow the cyclonic vortices under the influence of these forces are shifted to the north from the sites of their generation, the anticyclonic to the south.

The angular acceleration of the vortex is obtained from equation

$$K\frac{d\omega}{dt} = \sum_{i=1}^{5} M_i, \qquad (9)$$

where K--moment of inertia of vortex in relation to vertical axis passing through the center of the vortex;

M_1--moment of friction force in relation to vortical axis emerging through rotation of the vortex in relation to the basic flow,

$$M_1 = l_1(\omega_0 - \omega);$$

M_2--moment of friction force in relation to vortical axis governed by vortical friction on the underlying surface,

$$M_2 = -l_2\omega;$$

M_3 is linked to the vortical movement over the spherical surface and with the dependence of the Coriolis parameter on latitude,

$$M_3 = l_3\dot{V}_\theta \sin\theta\Omega;$$

M_4 is linked to the change in the moment of vortical inertia with a change in the altitude of the vortex, and consequently, its radius during movement of the vortex over the surface of the sphere

$$M_4 = l_4\frac{d'\chi}{dt}(\omega + \Omega_\perp).$$

We note that the terms M_3 and M_4 express the known law of preservation of potential vortex.

The term M_5 is linked to the fact that as a consequence of the internal processes the vortex "draws out" rotation from the surrounding basic flow during

its development. In order to write it in a certain specific form it is necessary to know the mechanism "of unwinding" of the vortex. At the given stage it is assumed that $M_5=M(\tau)$, where τ--time passing from moment of generation of the vortex. One can assume, for example, that $M_5=M\theta(\tau^*-\tau)$, where M is constant, θ--Heaviside function, τ^*--time of "unwinding" of vortex.

We note that only M_1 and M_5 result in the appearance of the asymmetric part of the stress tensor of the basic flow, since only they describe the exchange of angular momentum between the vortices and the basic liquid.

The expressions for the coefficient l_1-l_4 and the forces f_1 include the radius of the vortex L. This governs the fact that L needs to be included in the number of variable distribution functions f in addition to the remaining variables which determine the acceleration of angular velocity of the vortex.

A change in the radius of the vortices in a unit of time looks like

$$\frac{dL}{dt}=\frac{L}{2}\frac{d''\chi}{dt}. \qquad (10)$$

Equation (10) reflects the preservation of the vortical mass during change in the altitude of the vortex in the process of its movement over the sphere.

The terms $\frac{\partial}{\partial V_\mu}\left(\frac{dV_\mu}{dt}\right)$, $\frac{\partial}{\partial\omega}\left(\frac{d\omega}{dt}\right)$, and so forth that are included in (7) are found by differentiating with respect to the corresponding variables (8)-(10).

Z is included in (7) which must consider the generation and disappearance of the vortices after their filling. Since the vortices do not interact with each other, it is easy to show that Z can be presented in the form

$$Z=\dot{Z}_1-f\delta(T-\tau). \qquad (11).$$

In (11) Z_1 considers only the generation of vortices, and must be assigned. Here it is suggested that with the passage of time $T\gg\tau^*$ from the moment of vortical generation the velocity and angular velocity of the vortex almost coincides with the velocity and angular velocity of the basic liquid, that is, the vortex is filled. Thus, when the "age" T is reached the vortices disappear, supplementing the basic liquid. $f\delta(T-\tau)$ represents the run-off of the vortices, δ--Dirac function.

Through the distribution functions of vortices f the functions Z that describe the generation and destruction of the vortices, by using where necessary, the expressions for forces f_i and moments of forces M acting on the liquid on the part of an individual vortex, it is easy to express now all the terms α, I^*, I^*_μ, I^*_ϕ, F^*_θ, F^*_Φ and Q^*_r included in the equation for the basic liquid (4)-(6), and describing the effect of vortices on the basic liquid. Due to the awkwardness of the obtained expressions we will not present here all the expressions, and for example we will give the expressions only for Q^*_r.

The source of the angular momentum governed by the rotation of the vortices can be presented in the form of a sum of two terms

$$Q_r^{\cdot} = Q_{r1} - Q_{r2}. \qquad (12)$$

The source Q_{r1} is governed by the fact that the vortices can be generated and be lost with angular velocity ω, which differs from the angular velocity of the surrounding liquid ω_0:

$$Q_{r1}(\theta, \Phi) = \frac{1}{R^2} \sum_{i=1}^{2} (\int K(L)(\omega_0 - \omega)\, Z dV_\theta\, dV_\Phi\, d\omega\, dL\, d\tau)_i.$$

The source Q_{r2} is governed by the fact that the vortices draw out the angular momentum from the basic liquid during their development and give it back to the basic liquid as a consequence of the viscous friction during dissipation

$$Q_{r2}(\theta, \Phi) = -\frac{1}{R^2} \sum_{i=1}^{2} [\int M_5(\tau) f dV_\theta\, dV_\Phi\, d\omega\, dL d\tau]_i -$$

$$-\frac{1}{R^2} \sum_{i=1}^{2} [\int l_1(L)(\omega_0 - \omega) f dV_\theta\, dV_\Phi\, d\omega\, dL d\tau]_i.$$

The index i=1,2 refers to the vortices rotating clockwise and counterclockwise; the region of integration includes the entire region of change in the variables of the f function.

The expressions for α, I* and so forth have an analogous appearance.

Thus, if one assigns a priori the mechanism for untwisting of the vortex $M_5(\tau)$ and the function for generation of vortices $Z_1(\Theta, \Phi, V_\theta, V_\Phi, \omega, L, \tau, t)$, the system of equations (4)-(11) and the expression analogous to (12) becomes closed. This means that from it one can, by knowing only $M_5(\tau)$ and Z_1 determine the "self-consistent" field of velocity of the basic liquid V_0 and the distribution functions of the vortices $f(\Theta, \Phi, V_\theta, V_\Phi, \omega, L, \tau, t)$: the moving and rotating vortices form a field of velocity of the basic liquid, here the movement and rotation of the vortices themselves determine the field of velocity of the basic liquid.

As an example we will examine the following maximum simplified problem. From the long established synoptic observations in the Northern Hemisphere it is known [4] that the number of cyclones and anticyclones generated at the given latitude on the average equal each other, whereby the maximum of both cyclogenesis and anticyclogenesis is observed near 38°n.l. in winter, and about 48° n.l. in summer, i.e., at the same latitudes where the maximum mean-tropospheric western transfer dominates. In the cyclones after their formation there exists a strong trend to move in a direction towards the poles; thus in

winter the maximum of cyclone frequency is observed near 55°n.l., in summer--near 60°n.l. The cyclones have a somewhat weaker trend to move towards the equator from the site of their formation, so that the maximum of anticyclone frequency is located near 30°n.l. in winter and near 43°n.l. in summer. In accordance with the described experimental data we will construct the following model. We consider that the cyclones and anticyclones are generated at a certain latitude θ_0, whereby their number and intensity are the same, and then momentarily are redistributed with respect to the latitudes according to the law

$$n^+(\theta)=\begin{cases}0 & \text{with } \theta<\theta_1\\ \frac{N}{4\pi}\sin 2\pi\frac{\theta-\theta_1}{\theta_2-\theta_1} & \text{with } \theta_1<\theta<\theta_2\\ 0 & \text{with } \theta>\theta_0,\end{cases}$$

$$n^-(\theta)=\begin{cases}0 & \text{with } \theta<\theta_0\\ -\frac{N}{4\pi}\sin 2\pi\frac{\theta-\theta_1}{\theta_2-\theta_1} & \text{with } \theta_0<\theta<\theta_2\\ 0 & \text{with } \theta>\theta_2,\end{cases}$$

where N--complete number of cyclones (+) (anticyclones (-)) on earth; $\theta_0=\frac{\theta_2+\theta_1}{2}$.

We will consider the redistributed cyclones and anticyclones to be immobile and rotating with angular velocity ω.

Since the number and intensities of the generated cyclones and anticyclones is the same, their generation does not make a contribution to Q_T^*. However damping of the cyclones and anticyclones due to friction makes a contribution to Q_T^*. Since the cyclones and anticyclones are shifted in relation to each other. For Q_T^* we obtain

$$Q_r^*=\begin{cases}-\frac{\mu_1 H_0 L^2}{R^3}\omega\frac{N}{2}\sin 2\pi\frac{\theta-\theta_1}{\theta_2-\theta_1} & \text{with } \theta_1<\theta<\theta_2\\ 0 \text{ with } \theta<\theta_1 \text{ and } \theta>\theta_2.\end{cases}$$

We will consider that the distribution with respect to latitude of the cyclones and anticyclones is the only source of zonal circulation. Equation (6) for the case of purely zonal stationary circulation yields

$$\frac{\mu_3 H_0}{R^2}\frac{\partial^2 V_{0\Phi}}{\partial\theta^2}-\frac{\mu_1 V_{0\Phi}}{h}=\begin{cases}\frac{1}{2}\frac{\mu_1 H_0 L^2}{R^3}\omega N\frac{\pi}{\theta_2-\theta_1}\cos 2\pi\frac{\theta-\theta_1}{\theta_2-\theta_1}\\ \qquad\qquad \text{with } \theta_1<\theta<\theta_2\\ 0 \text{ with } \theta<\theta_1 \text{ and } \theta>\theta_2,\end{cases}\quad (13)$$

where μ_1, μ_3, μ_4--turbulent analogs of coefficients of dynamic viscosity that determine the friction of vortices on the zonal flow, friction in the zonal

flow and friction of the zonal flow on the underlying surface. μ_1, μ_3 and μ_4 generally differ, since they are determined by different scales of turbulence; h--characteristic of altitude at which the velocity of the zonal flow is altered. We will designate

$$\frac{\mu_3 H_0}{R^2} = \beta_1, \quad \frac{\mu_4}{h} = \beta_2, \quad \frac{1}{2}\frac{\mu_1 H_0 L^2}{R^3}\,\omega N \frac{\pi}{\theta_2 - \theta_1} = G.$$

Equations (13) will be solved with the following boundary conditions:
$V_{0\Phi}=0$ with $\Theta=0$--at the pole the zonal velocity must be nullified, so that infinite gradients do not emerge.

$V_{0\Phi}=u$ with $\Theta=\Theta_3$. This boundary condition must be set on the boundary with the Hadley circulation cell, since the mechanism of motion of the air masses in the limits of the Hadley cell significantly depend on the vertical convection, and for its description the monolayer model is insufficient.

With Θ_1 and Θ_2 we use continuity $V_{0\Phi}$ and continuity $\frac{\partial V_{0\Phi}}{\partial \theta}$ as the joining conditions.

The relationship $V_{0\Phi}(\theta)$ is presented in figure 2 for three cases $\frac{\beta_1}{\beta_2} \ll 1, \frac{\beta_1}{\beta_2} \gg 1, \frac{\beta_1}{\beta_2} \sim 1$. In the case $\beta_1/\beta_2 \sim 1$ the relationship $V_{0\Phi}(\theta)$ qualitatively coincides with that observed in the atmosphere: in the environs of the latitude θ between θ_1 and θ_2 there is a maximum of the western zonal wind, in the environs $\Theta=0$ an easterly wind occurs. The maximum value of the westerly wind

$$V_{0\Phi\max} = \frac{G}{\beta_1\left(\frac{2\pi}{\theta_2-\theta_1}\right)^2+\beta_2} = \frac{\frac{1}{2}\mu_1 H_0 L^2 \omega N \frac{\pi}{\theta_2-\theta_1}}{R^3\left\{\frac{\mu_3 H_0}{R^2}\left(\frac{2\pi}{\theta_2-\theta_1}\right)^2+\frac{\mu_4}{h}\right\}}. \qquad (14)$$

On the condition $\beta_1 \sim \beta_2\left(\frac{\mu_3}{\mu_4} \sim \frac{R^2}{H_0 h}\right)$ we obtain

$$V_{0\Phi\max} = \frac{1}{2}\frac{\mu_1}{\mu_3}\frac{\theta_2-\theta_1}{2\pi}\frac{N}{2}\frac{L}{R}L\omega. \qquad (15)$$

In (15) $\frac{\theta_2-\theta_1}{2\pi} \simeq \frac{1}{10}$, $\frac{L}{R} \sim \frac{1}{6}$,

$L\omega \approx V_s$--velocity of wind in cyclone, $N \approx 20$.

Thus $V_{0\Phi\max} \simeq \frac{1}{12}V_s\frac{\mu_1}{\mu_3}$. . If the viscosity that determines the horizontal friction in free atmosphere is five times lower than the viscosity that determines the friction of the cyclone on the free atmosphere, then $V_{0\Phi\max} \simeq \frac{1}{2}V_s$, which will be found in agreement with the experiment.

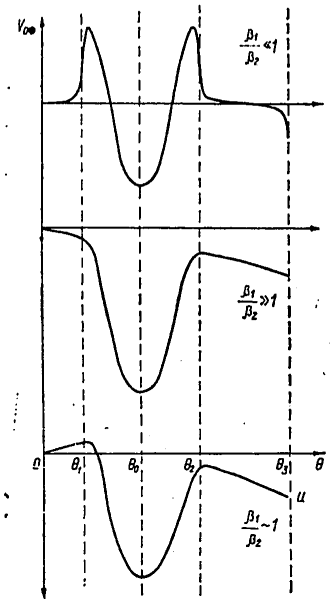

Figure 2. Dependence on Zonal Velocity of Wind Averaged With Respect to Altitude $V_{0\Phi}$ on Addition of Latitude θ for Different Values of Ratio β_1/β_2.
The negative values $V_{0\Phi}$ correspond to the westerly wind.

As is apparent from (15) the westerly transfer is proportional to $\frac{\theta_2-\theta_1}{2\pi}$. In the Northern Hemisphere $\frac{\theta_2-\theta_1}{2\pi}$ strongly alters from winter to summer and in summer is approximately 1.5-fold lower than in winter. At the same time the number of cyclones in the atmosphere is insignificantly altered from season to season [4]. This, possibly, is the reason for the significant attenuation in the summer maximum of the western transfer as compared to the winter [4].

We note that the zonal transfer must increase with an increase in the number of cyclones and anticyclones and their intensity. The extremum study of such a relationship is of definite importance.

We note that the maximum of the zonal transfer corresponds to the latitude θ_0. For summer $\theta_0=48^\circ$s.l. and for winter $\theta_0=40^\circ$s.l., which is located in accordance with the data of experimental observations.

We stress that in the simple example we examined the self-consistent problem of determining the profile of the zonal velocity and the distribution of vortices with respect to latitude has not been solved. The distribution of vortices was assigned a priori in the same way that this is observed in the atmosphere, and according to the assigned distribution of the vortices the profile of zonal velocity that is governed by this distribution was found.

Thus the proposed model is in qualitative agreement with the synoptic experiment.

The authors express gratefulness to V. A. Bogomolov for notes made.

BIBLIOGRAPHY

1. Afanas'yev, Ye. F.; and Nikolayevskiy, V. N. "Construction of Asymmetric Hydrodynamics of Suspensions With Rotating Solid Particles," "Problemy gidrodinamiki i mekhaniki sploshnoy sredy" [Problems of Hydrodynamics and Mechanics of Continuum], Moscow, Nauka, 1969.

2. Nigmatulin, R. I. "Methods of Continuum Mechanics to Describe Multiple-Phase Mixtures," PRIKLABNAYA MATEMATIKA I MEKHANIKA, vol 34, No 6, 1970.

3. Obukhov, A. M. "Question of Geostrophic Wind," IZV. AN SSSR. SER. GEOGRAFICHESKAYA I GEOFIZICHESKAYA, vol 13, No 4, 1949.

4. Pal'men, E.; and N'yuton, Ch. "Tsirkulyatsionnyye sistemy atmosfery" [Atmospheric Circulation Systems], Leningrad, Gidrometeoizdat, 1973.

5. Starr, V. "Fizika yavleniy s otritsatel'noy vyazkost'yu" [Physics of Phenomena With Negative Viscosity], Moscow, Mir, 1971.

UDC 551.(509.313:558.29)

NUMERICAL MODELING OF DEEP CONVECTION PROCESSES

Moscow METEOROLOGIYA I GIDROLOGIYA in Russian No 10, Oct 1979 pp 48-55

[Article by M. Alautdinov, USSR Hydrometeorological Scientific Research Center, submitted for publication 15 February 1979]

Abstract: A scheme for numerical solution of deep convection equations is presented based on the principle of introducing "artificial compressibility." Results are given of computation of convective currents for unstable stratified layers of varying thickness. Results are compared of computations on a computational grid that is uniform and nonuniform with respect to the vertical.

[Text] In solving a number of meteorological problems such as modeling thick convective cloud cover or local circulation in the atmosphere as an initial system it is convenient to use deep convection equations in which thermodynamic characteristics are linearized in relation to the main hydrostatic state, but in contrast to the Bussinesk simplifications the change in hydrostatic density with altitude $\bar{\rho}=f(z)$ is considered.

The system of deep convection equations was obtained for the first time in the work of Ogura and Phillips [6] and looks like:

$$\frac{d\vec{u}}{dt} = -\frac{1}{\bar{\rho}}\operatorname{grad} p' + \nu\nabla^2\vec{u} + g\alpha\theta'\vec{k}, \qquad (1)$$

$$\operatorname{div}(\bar{\rho}\vec{u}) = 0, \qquad (2)$$

$$\frac{d\theta'}{dt} = -\frac{\partial\bar{\theta}}{\partial z}w + \varkappa\nabla^2\theta'. \qquad (3)$$

here $\vec{u}$--velocity vector with components u, v, w along x, y, z, respectively,
p'--deviation of pressure from static value $\bar{p}(z)$,
θ'--deviation of potential temperature from undisturbed state $\bar{\theta}(z)$,

$\tilde{\rho}=f(z)$--density in undisturbed state,
$\nu=\mu\tilde{\rho}^{-1}$--coefficient of kinematic viscosity,
μ=const--coefficient of dynamic viscosity,
$\varkappa=\chi\tilde{\rho}^{-1}c_p^{-1}$--coefficient of temperature conductivity,
χ=const--coefficient of heat conductivity,
c_p--specific heat capacity of air with constant pressure,
$\tilde{\alpha}$--coefficient of temperature expansion,
$\vec{k}$--unit vector directed along z axis.

In the overwhelming majority of works the system (1)-(3) is solved in a two-dimensional situation which makes it possible to exclude from the initial system pressure, and to solve the problem by using the equation of vortex and the function of current. In the three-dimensional situation the pressure is not successfully excluded and it becomes necessary to numerically integrate the initial system (1)-(3).

In the numerical solution of the system of equations (1)-(3) in the Bussinesk approximation ($\tilde{\rho}$=const) the method of introducing artificial compressibility is successfully used (Chorin [4], Somerville [7], Vel'tishev and Zhelnim [2], Belotserkovskiy et al. [1], Lipps [5]). Since the introduction of the hydrostatic compressibility does not limit the possibility of this method, we extended it for the case of solving deep convection equations.

The initial system of equations (1)-(3) is brought to the dimensionless form with the use of the scales

$$\tilde{x}_i = h, \quad \tilde{t} = h^2 \nu_0^{-1}, \quad \tilde{u}_i = \nu_0 h^{-1}, \quad \tilde{p} = \rho_0 \nu_0^2 h^{-2}, \quad \tilde{\Theta} = \Delta\bar{\Theta}, \quad \tilde{\rho} = \rho_0.$$

here h--thickness of convective layer,
$\Delta\bar{\Theta}$--difference in potential temperature on lower and upper boundaries of layer,
ρ_0--density on lower boundary,

$$\nu_0 = \mu\rho_0^{-1}, \quad \varkappa_0 = \chi\rho_0^{-1}.$$

By employing the scaling indicated above we obtained the initial system of equations (1)-(3) in the dimensionless form

$$\frac{d\vec{u}}{dt} = -s^{-1}\operatorname{grad} p + s^{-1}\nabla^2\vec{u} + \operatorname{Gr}\Theta\vec{k}, \tag{4}$$

$$\operatorname{div}(s\vec{u}) = 0, \tag{5}$$

$$\frac{d\Theta}{dt} = w + \operatorname{Pr}^{-1} s^{-1}\nabla^2\Theta. \tag{6}$$

Here the strokes to designate the disturbances in temperature and pressure are omitted,

$s=\bar{\rho}\rho_0^{-1}$--dimensionless characteristic of hydrostatic compressibility,
Gr=RaPr--Grashof number,
$Ra=g\alpha\Delta\bar{\Theta}\bar{h}^3\varkappa_0^{-1}\nu_0^{-1}$ --Rayleigh number,
$Pr=\nu_0\varkappa_0^{-1}$ --Prandtl number.

In the two-dimensional variant the system (4)-(6) is solved with the following conditions on the lower and upper boundaries:

$$u=w=\Theta=0 \quad \text{with } z=0 \text{ and } z=1 \tag{7}$$

On the lateral boundary the condition of periodicity of all functions is assumed, and the motion at the initial moment is excited by the arbitrary temperature impulse

$$\Theta_0=f(x). \tag{8}$$

For numerical solution of the equation system (4)-(6) with boundary and starting conditions (7) and (8) the method of introducing artificial compressibility was employed that was previously used to solve the problem of viscous incompressible liquid. This method is based on splitting in which at the first stage the auxiliary velocity u_i^* and temperature θ^{n+1} is implemented from equations of the following type

$$f^* = f^n + \tau(s^{-1}\nabla^2 f^* - u_i^n \nabla f^* + E). \tag{9.}$$

Here n--number of temporal step,
τ--step in time,
f*--auxiliary velocities of temperature,
E--free terms in corresponding equations.

Computation of the auxiliary velocities is made without consideration for the forces of pressure and the continuity equation. This results in the fact that the equation for mass preservation (5) is not fulfilled.

Therefore the next step in the computation is calculation of pressure and correction of the auxiliary velocities with respect to the iteration plan

$$p^{n+1,\,m+1} = p^{n+1,\,m} - \lambda \operatorname{div}(\vec{s u}_i^{n+1,\,m+1}), \tag{10}$$

$$\vec{s u}_i^{n+1} = s\vec{u}_i^* - \tau \frac{\partial}{\partial x_i} p^{n+1,\,m+1}. \tag{11}$$

Here λ--parameter, m--number of iteration.

The iteration is made until

$$\max_D |p^{n+1,\,m+1} - p^{n+1,\,m}| < \varepsilon, \tag{12}$$

where D--region of computation,
ε--small amount assigned in advance.

The convergence of the iteration process indicates that in the plan the condition of mass preservation is guaranteed, i.e., $\operatorname{div}(\vec{su}^{n+1})=0$ independently of the amount of divergence of the auxiliary velocities. A detailed description of this method can be found in the work of Vel'tishev and Zhelnina [2].

To compute the auxiliary velocity a monotonic plan is used with perturbed coefficients proposed in the work of Samarskiy [3]. By using this plan we obtain the difference analog of equation (9) in the form

$$f_i^* = f_i^n + \tau \left[s^{-1} R \left(f^*_{\overline{x}_j}\right)_j + \frac{r^-}{2} f^*_{x_j} - \frac{r^+}{2} f^*_{\overline{x}_j} + \right.$$
$$\left. + \frac{h_{i-1}\left(E_i^n + E_{i-1}^n\right) + h_i \left(E_{i+1}^n + E_i^n\right)}{2\left(h_i + h_{i-1}\right)} \right]. \qquad (13)$$

Here $R = [1 + 0{,}25\ (h_i r^- + h_{i-1} r^+)]^{-1}$,

$$r^- = |r| - r, \quad r^+ = |r| + r, \quad r = u_j^n, \quad j = 1, 2$$

$$f^*_x = \frac{1}{h_i}\left(f^*_{i+1} - f^*_i\right), \quad f^*_{\overline{x}} = \frac{1}{h_{i-1}}\left(f^*_i - f^*_{i-1}\right),$$

where h--spacing of grid.

According to the analysis made in the work of Samarskiy [3] the difference operator (13) is absolutely stable and yields the second order of accuracy with respect to the spatial coordinates and the first order of accuracy with respect to time. This yields significant advantages as compared to the method of central differences that possesses conditional stability.

In order to solve the equation system (4), (6) with the use of the difference approximation (13) the method of variable directions is used. The difference equations are solved by the method of normal passage in a vertical direction and the method of cyclic passage in a horizontal direction.

Pressure and the final velocities are computed according to the iteration scheme (10) and (11).

Computations are made on a grid 57 x 19 in size in a horizontal and vertical direction. The size spacing of the grid along the horizontal is constant and is 1 km. Along the vertical the spacing of the grid decreases from top to bottom in the lower kilometric atmospheric layer. The maximum grid spacing equals 1 km, the minimum--2 m. In addition, to compare the results of

computations calculations are made on uniform grids with size 65 x 21 and 33 x 9.

In computing pressure according to the iteration scheme (10)-(11) it was found that on the employed significantly nonuniform grid the parameter λ strongly varies in limits of the examined region. This results in the fact that pressure on different sections of the region is computed with varying accuracy. In order to avoid this computation of pressure is made on a grid that is uniform with respect to the vertical with spacing 1 km. On this same grid the final velocities are also computed. In the lower kilometer layer pressure and velocity are linearily interpolated.

This work followed two main goals:
1) To approve the technique of numerical modeling of deep convection processes with the use of the method of artificial compressibility.
2) To study the differences in the solutions emerging as a consequence of the use of different methods for approximation of operator (9), as well as a consequence of the use of a grid significantly nonuniform with respect to the vertical.

Computations were made in an initially quiescent liquid with assigned linear temperature profile. In each numerical experiment (a list of the experiments is given in Table 1) the values of the dimensionless parameters Ra and Pr (the task was solved at establishment) were fixed, as well as the starting conditions.

TABLE 1 - LIST OF NUMERICAL EXPERIMENTS

(1) Номер эксперимента	(2) Сетка	(3) Схема	(4) Мощность слоя, км	s_h	$Ra \cdot 10^{-3}$	Pr	$\lvert u_{max} \rvert$	$\lvert w_{max} \rvert$	$\lvert T_{max} \rvert$	$\overline{Nu}$
1	65×21	ЦР	1	1	4	0,7	17,9	19,1	0,383	1,887
2	"	"	1	0,93	то же (5)	то же (5)	17,6	18,8	0,377	1,864
3	"	"	2	0,87			17,4	18,3	0,368	1,835
4	"	"	3	0,80	"	"	17,1	17,9	0,357	1,800
5	"	"	5	0,66	"	"	16,0	16,5	0,327	1,699
6	"	"	10	0,33	"	"	11,8	10,8	0,208	1,323
7	33×9	"	8	1	"	"	15,5	17,6	0,360	1,756
8	"	МСС	"	1	"	"	14,3	16,2	0,318	1,670
9	65×21	ЦР	10	1	6	1	17,6	20,1	0,427	2,240
10	57×19	МСС	10	1	6	1	21,9	21,0	0,519	2,379
11	65×21	ЦР	10	0,33	6	0,7	20,8	19,9	0,316	1,522
12	33×9	МСС	10	0,33	6	0,7	19,9	18,4	0,302	1,453
13	57×19	МСС	10	0,33	6	0,7	29,3	24,0	0,452	1,698

Key:
1. Number of experiment
2. Grid
3. Plan
4. Thickness of layer, km
5. The same

ЦР--central differences, МСС monotonic scheme of Samarskiy (1977), s_h ratio of density on upper boundary of layer to density on lower boundary, $\lvert u_{max} \rvert$, $\lvert w_{max} \rvert$, $\lvert T_{max} \rvert$ absolute values of horizontal and vertical components of velocity and pulsations in temperature in dimensionless units, Nu -- Nussel't number.

The fields of temperature, velocities, pressure that were averaged with respect to the period of the temperature profile, inner and kinetic energy, as well as the streams of heat expressed by the dimensionless Nussel't number were analyzed

$$\mathrm{Nu} = 1 + \frac{-\frac{\partial \overline{\theta'}}{\partial z} + \mathrm{Pr}\,\overline{w'\theta'}\,\bar{s}}{\frac{\partial \bar{\theta}}{\partial z}}.$$

Here the dash above designates averaging with respect to the horizontal.

Results of Computations

Analysis of the computation results showed that the employed numerical plan is stable also for the case of compressible liquid and the modeled movements emerge onto a stationary pattern. With the establishment with sufficient degree of accuracy integral laws of conservation are fulfilled. Imbalances in the expenditures and inner energy are the maximum in the sixth experiment. The first of them comprises 1% from the characteristic values of velocity, and the second does not exceed 4%.*

The maximum deviation in the Nussel't number computed in individual layers within the region, from their mean value in the entire convective layer do not exceed 10%, which additionally indicates the stationariness of the process and the fairly high quality of the computation scheme. The computations show that consideration of compressibility results in a decrease in intensity of the convective currents, temperature pulsations and diminishing in the summary heat flows (see Table 1 and Figure 1).

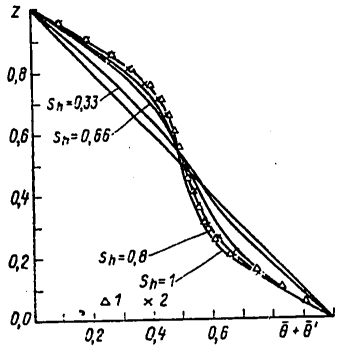

Figure 1. Vertical Profile of Resulting Temperature $\bar{\theta}+\bar{\theta}'$
Key:
1. S_h=0.93 2. S_h=0.87

*Here and further the values of all variables are given in dimensionless units.

The same as in the case of incompressible liquid, the movements acquire the shape of rollers whose horizontal dimension is two times larger than the thickness of the convective layer, however the symmetry is lost between the ascending and descending branches of the currents: the area occupied by the ascending currents becomes greater than the area occupied by the descending currents. For example, the intensity of the descending movements becomes greater than the intensity of the ascending movements.

It is known that in approximation of equation (9) by the scheme that uses directed differences a countable viscosity emerges, which, naturally, distorts the obtained solutions. Approximation of equation (9) by the difference operator (13), i.e., the use of a monotonic Samarskiy scheme with perturbed coefficients, as was indicated in publication [3] is absolutely stable and somewhat "dampens" this countable viscosity as a consequence of the introduction of perturbing coefficients. To compare the computation results with the use of operator (13) and the standard central differences experiments 7 and 8 were conducted. The computation shows that approximation (13) guarantees with great degree of accuracy the fulfillment of the laws of conservation, however the mean kinetic energy of convective movements is 15% lower, while the mean in the layer of temperature pulsation--by 10-15% lower than with the use of central differences.

Thus, the monotonic Samarskiy scheme with perturbed coefficients completely does not exclude the countable viscosity, however its magnitude is comparatively small.

Experiments 9-10 were carried out in order to reveal the effect of nonuniformity in the computation grid. Analysis of the computation results demonstrated with the use of a nonuniform computation grid the scheme also is stable and the movements emerge onto a stationary pattern. Whereby in experiment 10 (nonuniform grid) the rate of convection development and emergence onto the steady-state pattern occur faster than in experiment 9 (uniform grid). Thus in experiment 10 the time for establishment of movements equals 0.559, while in experiment 9 0.660. Yet another peculiarity of the computations on a nonuniform grid consists of the fact that the intensity of the simulated movements is higher than in the case of computation on a uniform grid. This can be seen from Table 1 according to the extremum magnitudes of velocity pulsations and temperature and according to the mean kinetic energy which in the steady-state pattern remains constant, and in experiment 10 is roughly 20% greater than in experiment 9.

With a fair degree of accuracy the law of mass conservation is fulfilled in the scheme--the mean on the levels of the value of pulsations in the vertical velocity component have an order 10^{-6} in experiment 10 and order 10^{-4}-10^{-5} in experiment 9. The internal energy is preserved also with fairly high degree of accuracy (imbalance on the grid with variable spacing does not exceed 10^{-3}).

In order to evaluate the absolute error in the scheme comparisons were made of numerical solutions with the accurate for the particular case Ra=0, s=1.

The initial scheme (4)-(6) in this case acquires the appearance

$$\frac{d\vec{u}}{dt} = -\operatorname{grad} p + \nabla^2 \vec{u}, \tag{14}$$

$$\operatorname{div} \vec{u} = 0. \tag{15}$$

It has precise solutions:

$$u = -\cos x \sin z\, e^{-2t}, \quad w = \sin x \cos z\, e^{-2t},$$

$$p = -\frac{1}{4}(\cos 2x + \cos 2z)\, e^{-4t} \tag{16}$$

Comparison of the numerical computations on a nonuniform grid with analytical solutions (16) demonstrated that the maximum differences in the solutions for velocities and kinetic energy do not exceed 2%.

Experiments 11-12 follow the same goal as experiments 7-8 with only the difference that they examine the case of a compressible liquid.

Analysis of the computation results and the constructed graphs (see figure 2) demonstrate that the introduction into the scheme of the compressibility factor s sharply reduces the differences in the solutions which occurred in experiments 7 and 8. Thus, if in experiments 7 and 8 the mean values for temperature pulsations differ by 10-15%, then in experiments 11-12 (see figure 2a) the mean profiles practically coincide. Small differences in temperature pulsations occur in the regions of ascending and descending movements, the maximum differences do not exceed 8%.

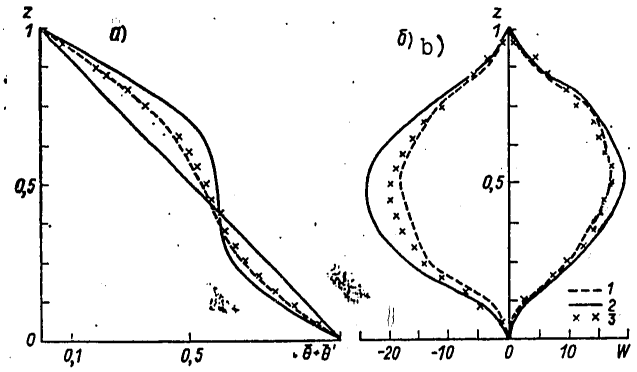

Figure 2. Vertical Profile of Resulting Temperature $\bar{\theta}+\bar{\theta}'$ (a) and Profiles of Vertical Velocity Component w in Regions of Maximum Ascending and Descending Motions (b).

Key:
1. Experiment 12
2. Experiment 13
3. Experiment 11

The differences in the vertical components of velocity in experiments 11 and 12 in the zones of descending currents do not exceed 16%, and in the zones of ascending currents there are practically no differences (see figure 2b). In comparing the results of experiments 11 and 12 it is necessary to recall that the dimensions of the computation grids in these experiments varied (see table 1).

In experiment 13 computations were made according to Samarskiy monotonic scheme with perturbed coefficients on a significantly nonuniform grid in a convective layer 10 km deep. Analysis of the computation results showed that the computation scheme remained stable, the simulated movement merged onto a stationary pattern. The integral laws of conservation are fulfilled. The computed value on the levels of the vertical velocity component value do not exceed the values on the order 10^{-5}-10^{-6}, i.e., the equation of mass conservation is well fulfilled in the system. The inner energy of the system is preserved (the imbalance is 10^{-3}). The maximum deviation in the Nussel't number computed in individual layers from their mean value do not exceed 1%. The extremum values of velocity pulsations in temperature are presented in table 1.

The mean temperature profile are given in figure 2a. From this figure it is apparent that the mean temperature values in experiments 13 and 11, 12 significantly differ (maximum differences ≈50%). The temperature pulsations differ by roughly the same amount in the regions of maximum ascending and descending currents. As compared to experiments 11 and 12 the maximum differences in the profiles of vertical velocity component are observed in the region of maximum descending currents and reached 3%.

The conducted numerical experiments made it possible to formulate the following conclusions.

1. The method of numerical solution with introduction of artificial compressibility successfully employed in the problems of simulating convection of an incompressible liquid can be used also to solve the problem of deep convection. The method yields stable solution and guarantees the fulfillment of the integral laws of conservation with fairly high accuracy.

2. With an increase in the compressibility of liquid the rate of development and intensity of the process of convection are reduced, asymmetry emerges in movements in relation to the middle of the layer, and also asymmetry between the ascending and descending branches of the currents.

3. With an increase in the compressibility of the liquid deformation of the starting temperature profile is reduced.

4. The monotonic plan with perturbed coefficients does not "dampen" the countable viscosity that emerges as a consequence of the use of directed differences, however the maximum errors emerging here do not exceed 10-15%.

5. The use of a significantly nonuniform grid results in a noticeable increase in the amplitudes of convective movement, especially with consideration for the hydrostatic compressibility.

BIBLIOGRAPHY

1. Belotserkovskiy, A. M.; Gushchin, V. A.; and Shchepnikov, V. V. "Method of Splitting in Application to Solution of Problems of Dynamics of Viscous Incompressibility of Liquid," ZHURNAL VYCHISLITEL'NOY MATEMATIKI I MATEMATICHESKOY FIZIKI, vol 15, No 1, 1975.

2. Vel'tishchev, N. F.; and Zhelnin, A. A. "Numerical Model of Convection in Stream With Vertical Shift," TRUDY GIDROMETTSENTRA SSSR, No 110, 1973.

3. Samarskiy, A. A. "Teoriya raznostnykh skhem" [Theory of Difference Schemes], Moscow, Nauka, 1977.

4. Chorin, A. "Numerical Solution of the Navier-Stokes Equations," MATHEM. COMPUT., vol 22, No 104, 1968.

5. Lipps, F. B. "Numerical Simulation of Three-Dimensional Benard Convection in Air," J. FLUID MECH., vol 75, Part 1, 1976.

6. Ogura, Y. and Phillips, N. A. "Scale Analysis at Deep and Shallow Convection in the Atmosphere," J. ATMOS. SCI., vol 19, No 2, 1962.

7. Somerville, R. C.J. "Numerical Simulation of Small-Scale Thermal Convection in the Atmosphere," LECT. NOTES PHYS., vol 19, 1973.

UDC 551.510.72

REGULARITIES IN THE BEHAVIOR OF RADIOACTIVE AEROSOLS IN THE NEAR-GROUND ATMOSPHERE

Moscow METEOROLOGIYA I GIDROLOGIYA in Russian No 10, Oct 1979 pp 56-61

[Article by Candidates of Physical and Mathematical Sciences K. P. Makhon'ko and A. S. Avramenko, V. P. Martynenko, A. A. Volokitin, and F. A. Rabotnova, Institute of Experimental Meteorology, submitted for publication at 9 Oct 1978]

Abstract: The link is examined between the power of nuclear explosions and the average annual magnitudes of near-ground concentrations and atmospheric fallouts of long-lived isotopes, products of these explosions. The role is shown of the Chinese nuclear explosions in atmospheric pollution over the territory of the USSR. The regularities are discussed in the annual course of concentrations of nuclear explosion products in the atmosphere, time of onset of the seasonal maximum, peculiarities in the concentration distribution over the USSR territory, and the effect of quantity and type of atmospheric precipitation on the formation of radioactive fallouts.

[Text] As is known after the conclusion in 1963 of the Moscow agreement on banning tests of nuclear weapons in three spheres the levels of radioactive atmospheric pollution began to drop quickly. The improvement in atmospheric purity was promoted by agreements concluded between the USSR and the United States on limiting underground tests of nuclear weapons and the use of nuclear explosions for peaceful purposes. However, further radioactive atmospheric pollution by nuclear explosion products ceased to drop, and in individual periods of time even began to rise again which was a consequence, first of all, of the nuclear weapon tests in the People's Republic of China. As indicated by the newspaper PRAVDA, "...radioactive dust from nuclear weapon tests in China...precipitate in Japan, the United States, and countries of Southeast Asia,"* Fallout of products of these explosions is observed also in other countries, including in the USSR.

After 1963 the average annual concentrations of long-lived isotopes on the territory of the USSR diminished according to the exponential law with

*"Peking: Course to Disrupt International Detente Under the Cover of 'Anti Sovietism'," PRAVDA, No 134 (21469), 14 May 1977.

period semi-decrease roughly 10 months. Deviations from this law were governed by additional injections of isotopes into the atmosphere of the Northern Hemisphere whose magnitude is proportional to the power of explosions $W_{дел}$, corresponding to the yield of fission products. Since after 1962 the percentage of $W_{дел}$ in the total power W of explosions of the megaton rank was roughly constant, one can speak of the existence of proportionality between the entrance of isotopes into the atmosphere and the total power W in this period of time. The empirical correlation between the concentration q_{i-1} of the isotope in the near ground atmosphere on the average for the country for the year when the powerful explosion was made whose products were discharged into the stratosphere, and the concentration q_i for the next year after the explosion looks like

$$q_i = aq_{i-1} + bW_{i-1}, \quad \text{Ci/m}^3 \qquad (1)$$

where the power W taken from [5] is expressed in megatons, concentration q--in Curie/m^3; for cesium-137 a=0.44; b=0.7 x 10^{-15} Ci/(m^3 x MT), for strontium-90 a=0.42, b=0.5 x 10^{-15} Ci/(m^3 x MT), and for cerium-144 a=0.19, b=8 x 10^{-15} Ci/(m^3 x MT).

The second component in (1) gives us an evaluation of the additional atmospheric pollution caused by a nuclear explosion. The summing of these additions with regard for the natural process of self-cleaning of the atmosphere occurring in parallel makes it possible to evaluate the role of nuclear explosions, first of all the Chinese, made after 1966 to the radioactive atmospheric pollution of the Northern Hemisphere.

Figure 1a gives a picture of the change with time in the average annual concentrations of cesium-137 on the average for the USSR; it also gives for comparison data for the United States that we computed from [4]. The experimental points for the United States are located higher than the points for the USSR, as a consequence of the fact that the United States is located in a more southern latitudinal belt where the concentrations of radioactive products are increased. Certain peculiarities in the latitudinal effect will be examined below.

Figure 1b presents the change computed from the data of Figure 1a with time in the contribution of Chinese nuclear explosions to USSR atmospheric pollution by the examined isotope. It is apparent from Figure 1b that already in 1968 concentration of cesium-137 due to explosions in the People's Republic of China was two times greater than the values expected in the absence of explosions. In 1969-1970 this excess reached already the order of magnitude and in subsequent years continued to increase. In 1977 the contribution of the Chinese nuclear explosions to pollution of the near-ground atmosphere with cesium-137 on the average for the USSR was roughly 4,000 times greater than the concentration which should have been expected if all the nuclear powers accepted the Moscow agreement. The contribution of transfer to the Northern Hemisphere of products of explosions made in the Southern Hemisphere

was not great. Similar results were obtained also for atmospheric pollution of the United States.

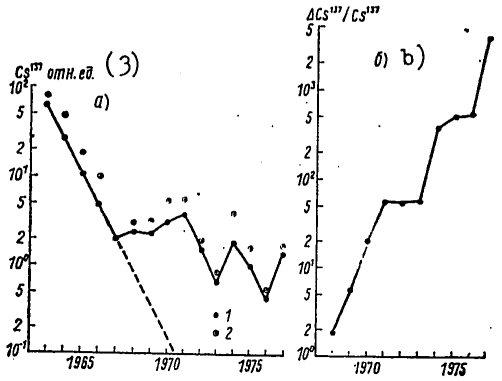

Figure 1. Change With Time in Average for Country Average Annual Concentration of Cesium-137 (a) and Contribution of Chinese Nuclear Explosions to Atmospheric Pollution (b)

Key:
1. USSR 2. United States 3. Relative unit

If as the global background one takes the concentration of radioactive products in a period directly preceding the nuclear explosion, then after the explosion made in the People's Republic of China on 26 September 1976 the maximum daily average concentration observed on the territory of the USSR was 300 times greater than the global background, while the magnitude of radioactive fallout was 1,000 times greater (according to the summary beta-activity). After the explosion made in the People's Republic of China on 17 September 1977 the maximum diurnal magnitude of radioactive fallout exceeded the background fallout by 600 times. In both mentioned cases the maximum of radioactive fallouts were associated with the passage of a cyclone accompanied by atmospheric precipitation. The main mass of radioactive explosion products was spread high above the earth and was subject to capture by cloud drops, while the near-ground concentrations were comparatively small. This resulted in a sharp growth in the parameter v_g, that represents the ratio of radioactive fallouts to the concentration of radioactivity in the air, and has dimensions of velocity. The amount v_g increased in these cases to three orders and became close to the rate of fall of rain drops.

We will examine the regularity and the change of average monthly concentrations of individual isotopes in the near-ground atmosphere on the average for the Soviet Union in recent years. In 1975 when no nuclear explosions were made in the atmosphere the usual annual course concentration was observed with one maximum in the spring time. For short-lived isotopes the maximum occurred

somewhat earlier than for long-lived. In the remaining years when nuclear explosions were made in the atmosphere the annual course of concentration was subject to distortions to a varying degree, depending on the half-life of the isotope. Thus the position of the spring maximum of long-lived cesium-137 in 1976 was not altered, but the absolute maximum of concentration was observed not in May, but in November, after the tropospheric September explosion in the People's Republic of China. In other years nuclear explosions were more powerful and their products entered mainly into the stratosphere, from which they began to be removed only the next year. Therefore, in contrast to short-lived isotopes no additional maximums in near-ground concentrations of long-lived isotopes were observed.

After September tropospheric explosions in the People's Republic of China in 1976 the maximum average monthly concentrations of cerium-144, zirconium--with niobium-95 and cerium-141 were observed in October, they exceeded by more than 16, 200 and 400 times respectively the concentration for the previous month. In October 1977 the concentration of cerium-141 was by an order greater than the background, but the concentrations of more long-lived isotopes practically were not increased, since the contribution of the September explosion to atmospheric pollution in fall 1977 was not great as compared to the contribution from the powerful thermonuclear explosion made in November 1976.

We will examine in more detail a typical annual course of near-ground concentrations of long-lived cesium-137. As shown by an analysis of the material of many years of observations the magnitude and time formation of the spring-summer maximum concentrations of this isotope practically do not depend on the periods of its entrance into the atmosphere. The ratio of maximum monthly concentration to the average annual on the average for the country has a weak tendency to diminish with a shift in the moment of onset of the maximum at later months, and monotonically altered from 2.3 for the maximum in April to 2.0 for the maximum in July, which lies within the limits of spread of the data. In individual points of the country the seasonal maximum of near-ground concentrations for cesium-137 can be observed in different months, however in the majority of points of the period of observation the maximums coincide. The frequency of periods of onset of the seasonal maximum of cesium-137 concentration obtain in averaging observational data in individual points for the entire country in 10 years is a normal distribution parameter σ=1.7 month and the maximum at the end of May-beginning of June. The fact that was experimentally observed in individual years of a comparatively early appearance of the seasonal maximum (in relation to the mean periods of seasonal reconstruction of the tropopause) indicates the presence of additional mechanisms for transfer of isotopes from the stratosphere to the troposphere. Among such mechanisms one can, for example, include those emerging under the influence of winter stratospheric warmings.

The isotope concentration whose source is a stratospheric reservoir is noted above, increases in the direction from north to south. Here in the latitudinal belt 55-60°n.l. a secondary maximum of concentrations is observed that

is comparatively small in magnitude. The rate of change in concentrations q with latitude x can be characterized by the steepness of the concentration curve i.e., by the magnitude of the derivative dg/dx. It is important to note that the latitudinal belt from 57°n.l. to 50°n.l. in which the derivative dq/dx alters its sign to the opposite corresponds to the limits of the seasonal oscillations in the zone of maximum deviations in the meridianal component of geostrophic wind from the mean value, which can be a measure of turbulent mixing of the atmosphere [3].

The normal distribution law and position of seasonal maximum (May-June) are preserved also for the southern regions of the country (located to the south of 50°n.l.). On the other hand in the central belt of the USSR corresponding to the change in sign of the derivative dq/dx (50-57°n.l.) the maximum concentration occurs in July, and in the northern regions (to the north of 57°n.l.) in May; the distribution functions for the periods of onset of the maximum with respect to time for these two regions acquire an asymmetrical, but mirror-reflected appearance. Thus, the seasonal maximum occurs in the beginning in the north of the country, than in the south, and only after this, in the central belt of the USSR, in the zone of maximum deviation of meridional component of geostrophic wind. The meaning of the last coincidence is not yet completely clear, and apparently must serve as the theme of an individual study.

Besides the latitudinal effects it is important to examine the peculiarities in the distribution of the field of isotope concentration between individual regions of the country. Table 1 presents the average annual concentrations of cesium-137 and cerium-144 averaged for individual regions of the USSR, and relative to the mean for the entire country. For the calculations 1975 was selected when there were no injections of radioactive products into the atmosphere. From the cited data it follows that the highest concentrations of isotopes of global origin are observed in the Transcaucasus, in Southern Siberia and especially in Central Asia. In the direction from west to east the cesium-137 and cerium-144 concentrations are not significantly altered, although in Southern Siberia considerably higher concentrations of isotopes are observed than in the southern European territory of the country, where the locality is lower. This pattern agrees with the known data that isotope concentrations increase with a rise in the altitude above sea level.

TABLE 1 - DISTRIBUTION OF RELATIVE CONCENTRATIONS OF CESIUM-137 AND CERIUM-144 OVER TERRITORY OF THE USSR IN 1975

Region	Cesium-137	Cerium-144
Northern European territory of the USSR	0.51	0.68
Central European territory of the USSR	0.99	0.98
Southern European territory of the USSR	0.82	0.82
Transcaucasus	1.21	1.02
Central Asia	1.82	1.94
Southern Siberia	1.21	1.12
Far East	0.68	0.71

In the absence of stratospheric injection of radioactive products the magnitude of fallouts of these products from the atmosphere annually decreases in proportion to the reduction in supply of the corresponding isotope in the stratosphere. If one examines the pattern of reduction in annual fallouts of cesium-137, strontium-90 and cerium-144 on the territory of the USSR, then one can conclude that the experimental values for the average annual fallout fall fairly well on the exponents with periods of half-reduction 1.12 years for strontium-90, 0.90 years for cesium-137, and 0.55 years for cerium-144. This makes it possible to employ formula (1) for radioactive fallout if the concentration q in it is replaced by fallout P. The empirical values of the parameters in this formula then will be the following: for cesium-137 a=0.46, b=0.27 mCi/(km^2 x year x MT), for strontium-90 a=0.54, b=0.20 mCi/(km^2 x year x MT), for cerium-144 a=0.29, b=3.38 mCi/(km^2 x year x MT).

In the middle latitudes the main portion of the fallout arrives at the earth with atmospheric precipitation. In the course of many years in the region near Moscow we made observations of the magnitude of radioactive fallout with atmospheric precipitation ("wet fallout") and without precipitation. On the average the percentage of wet fallout of radioactive products was 74±7%, and for individual years the magnitude fluctuated from 60 to 90% [2].

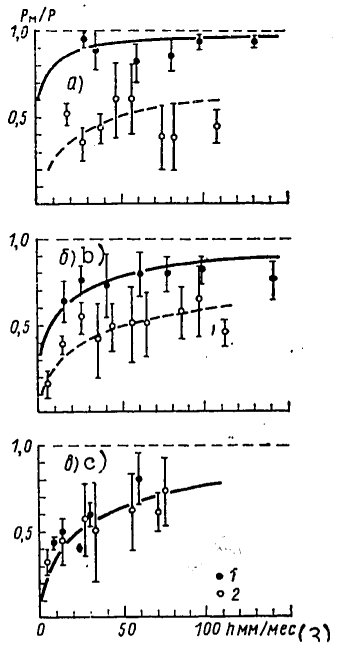

Figure 2. Dependence of Percentage of Wet Fallouts in Moscow Region on Quantity of Precipitation Falling in Form of Rain With Snow (a), Rain (b) and Snow (c)

Key:
1. Summary beta-activity
2. Minimal dust
3. mm/month

Depending on the quantity of atmospheric precipitation and their type the percentage of wet fallout is altered. Figure 2 presents curves for the dependence of the percentage of wet radioactive fallout P_m/P on the monthly quantity of precipitation for rain, snow and rain with snow, it also plots data on the percentage of mineral dust falling from the atmosphere on days with precipitation, in the total quantity of fallout of this dust. The last data are results of averaging for 1966-1973.

As is apparent from the figure, with an increase in the quantity of atmospheric precipitation the percentage of wet fallout rapidly rises, and then its growth is slowed down. With fallout of precipitation in the form of snow the percentage of wet fallout both of radioactive products and mineral dust with different quantities of precipitation practically coincide. But with rain mixed with snow the values of the percentage of wet fallout of mineral dust are located noticeably lower than the corresponding curve for radioactive products. This is explained by the fact that washing of aerosol particles from the cloud layer of the atmosphere occurs more efficiently than from the subcloud layer [1]. Radioactive products enter the layer of wash-out both in the cloud and in the subcloud layers. The source of mineral dust to a considerable measure is soil, when it is not covered with snow, therefore the dust in spreading downwards does not always completely reach the level of clouds, and the contribution of wash-off in the subcloud layer increases for it, which results in a decrease in the percentage of wet fallout of mineral dust as compared to the radioactive products.

BIBLIOGRAPHY

1. Makhon'ko, K. P. "Osedaniye radioaktivnoy pyli i yeye udaleniye iz atmosfery osadkami" ["Settling of Radioactive Dust and its Removal From the Atmosphere By Precipitation"], Moscow, Atomizdat, 1968.

2. Makhon'ko, K.P.; Rabotnova, F. A.; Reut, G. M.; and Chumichev, V. B. "Link Between Radioactive Fallout and Atmospheric Precipitation," TRUDY IEM, No 6 (64), 1977.

3. Flon, G. "Meridional Transfer of Particles and a Standard Vector of Deviation of Upper Winds," "Atmosfernyye aerozoli i radioaktivnoye zagryazneniye vozdukha ["Atmospheric Aerosols and Radioactive Air Pollution"], Leningrad, Gidrometeoizdat, 1964.

4. ENVIRONMENTAL QUARTERLY, EML-335, Appendix, 1978.

5. Zander, I.,; Araskog, R. "Nuclear Explosions 1945-1972. Basic Data," FOA4, Rep. A 4505-A1, April, 1973.

UDC 551.(507.321.2:511.6)

ANALYSIS OF MOTION OF A CONSTANT-LEVEL BALLOON IN ORDER TO DETERMINE CERTAIN TURBULENT ATMOSPHERIC CHARACTERISTICS

Moscow METEOROLOGIYA I GIDROLOGIYA in Russian No 10, Oct 1979 pp 62-67

[Article by P. F. Demchenko, Corresponding Member of the USSR Academy of Sciences G. S. Golitsyn, Institute of Atmospheric Physics, USSR Academy of Sciences, submitted for publication 7 November 1979]

Abstract: Based on an analysis of decisive parameters that figure in a system of equation describing the motion of a constant-level balloon in a turbulent atmosphere evaluations are made of dispersion in the rotation and acceleration angles of the balloon. The possibilities are indicated for evaluating the rate of dissipation of turbulent kinetic energy and Väisälä frequency if the balloon has a sufficiently sensitive accelerometer.

[Text] Currently sounding balloons, balloons and aerostats are used not only to obtain data about the temperature, wind velocity, altitude of the geopotential surface on the flight level, but also to study Lagrange turbulence characteristics [9]. This work on the basis of an analysis of balloon motion in a turbulent stratified atmosphere evaluated the amounts of angular and vertical oscillations in the system, and established the possibility of using a balloon with acceleration sensor to evaluate the rates of turbulent kinetic energy dissipation, Väisälä frequency, and mean vertical wind velocity gradient if the balloon has a sufficiently long cable with a car.

A balloon suspended in free atmosphere on the average moves with velocity of the mean wind $\langle u \rangle$. However due to the nonstationariness of the flow it experiences random hydrodynamic effects that result in random rotations and fluctuations in the velocity of the system as a whole. In the system of metering moving with velocity of the mean wind, the turbulence can be viewed as uniform, isotropic and stationary on the average for a sufficiently large interval of temporal and spatial scales. Then, according to the hypotheses of Kolmogorov, the [illegible] characteristics of fields of wind and pressure are defined only by three parameters: specific dissipation of kinetic energy $\varepsilon[L^2/T^3]$, kinematic viscosity $\nu[L^2/T]$ and atmospheric density $\rho_{ao}[M/L^3]$

(see for example, [4], section 21). Here L, T and M are dimensions of length, time and mass. Corrections for the nonisotropicity of the large scales will be discussed further.

The change in time of the generalized coordinates of the balloon are described by the Lagrange equations of the second type [2]. In the case where the balloon can be viewed as a solid body, these will be three equations of motion for the center of mass and three equations for the change in Euler's angles (equations of moments). In the presence of additional degrees of freedom (hinged securing of the car with the cable, cable with the balloon and so forth) the number of equations is increased, while the selection of generalized coordinates is dictated by considerations of convenience. The system of decisive parameters for the balloon of the assigned geometrical and weight scales, besides ε, ν and ρ_{a0} includes: mass m, characteristic size of the system R, acceleration of freefall g, as well as the characteristics of the cable for bending and torsion, and the friction coefficients in the possible hinged fastenings. In light of the presence of a vertical density gradient $d\rho_a/dz$, Archimedes' force acting on the balloon will be altered in time, resulting in oscillations in the system in relation to the mean flight level. Examination of this movement is contained in publication [8]. By adding $d\rho_a/dz$ to the amounts listed above we obtain a complete system of decisive parameters.

In order to reduce the number of parameters in the problem further a model is suggested with rigid fastening of the balloon and the car which makes it possible to avoid the mechanical characteristic of linking in the system. The suitability of this simplified model is explained by the fact that in the first place we are interested in the extremum evaluations of rotations of the system around the horizontal axes. Since the main hydrodynamic reactions are applied to the balloon, then the movable connections only weaken the link between the car and the balloon, and reduce these rotations. Moreover, as noted in [1] they are weakly linked to the rotation around the vertical axis, which makes it possible not to consider the torsion of the cable. Thus, the results obtained on such a simplified model for the studied motions are extremum evaluations, although they must not strongly differ from reality.

If one digresses from rotation of the balloon around the vertical axis, then its position will be determined by the coordinates of the mass center and two angles $\varphi_{1,2}$, formed by the vertical axis Oz with projections of the balloon axis of symmetry on the vertical planes Ozy and Oxz. For dispersions in acceleration of the mass center σ^2_{ai} and dispersions of the angular deviations $\sigma^2_{\varphi_i}$ we obtain the dependence on seven parameters that have three independent dimensions:

$$\sigma^2_{ax} = \sigma^2_{ay} = \sigma^2_a(\varepsilon, R, \nu, m, \rho_{a0}, g, d\rho_a/dz), \quad (1)$$

$$\sigma^2_{az} = \sigma^2_{az}(\varepsilon, R, \nu, m, \rho_{a0}, g, d\rho_a/dz), \quad (2)$$

$$\sigma^2_{\varphi_1} = \sigma^2_{\varphi_2} = \sigma^2_{\varphi}(\varepsilon, R, \nu, m, \rho_{a0}, g, d\rho_a/dz). \quad (3)$$

By using the P-theorem [6] we obtain

$$\sigma_a^2 = (\varepsilon^2/R)^{2/3} F_a\left[\frac{(\varepsilon R^4)^{1/3}}{\nu},\ \frac{1}{g}(\varepsilon^2/R)^{1/3},\right.$$
$$\left.\left(\frac{g}{\rho_{a0}}\frac{d\rho_a}{dz}\right)^{1/2}\left(\frac{\varepsilon}{R^2}\right)^{-1/3},\ \frac{\rho_{a0}R^3}{m}\right] \qquad (4)$$

and so forth.

Taking into consideration in light of the neutral constant-level of the balloon in the atmosphere the last parameter in correlations (4) is a constant amount for the balloons of assigned weight and geometric proportions, they can finally be written in the form

$$\sigma_a^2 = (\varepsilon^2/R)^{2/3} f_a(\Pi_\nu, \Pi_g, \Pi_\rho), \qquad (5)$$

$$\sigma_{az}^2 = (\varepsilon^2/R)^{2/3} f_{az}(\Pi_\nu, \Pi_g, \Pi_\rho), \qquad (6)$$

$$\sigma_\varphi^2 = f_\varphi(\Pi_\nu, \Pi_g, \Pi_\rho). \qquad (7)$$

Here $\Pi_\nu=(\varepsilon R^4)^{1/3}/\nu$--Reynolds number for turbulent formations of size R equal to $(R/l_\nu)^{4/3}$, where $l_\nu=\varepsilon^{-1/4}\nu^{3/4}$--inner scale of turbulence [4], $\Pi_g=\frac{1}{g}\left(\frac{\varepsilon^2}{R}\right)^{1/3}$ --ratio of vortical acceleration of size R to acceleration of freefall g proportional to the square of the ratio of the characteristic frequency of these formations $\omega_R=(\varepsilon/R^2)^{1/3}$ to the frequency of the natural oscillations in the system under the influence of the gravity force $\omega_0\sim(g/R)^{1/2}$, $\Pi_\rho=\left(\frac{g}{\rho_{a0}}\frac{d\rho_a}{dz}\right)^{1/2}\left(\frac{\varepsilon}{R^2}\right)^{-1/3}$ --ratio of frequency of vertical balloon oscillations-Väisälä frequency--to the characteristic frequency ω_R.

The correlations (5)-(7) still contain many dimensionless similarity criteria. For ordinary aerostats and sounding balloons in the free atmosphere $\Pi_g \ll 1$. This means that the oscillations around the horizontal axes are small, while their frequency is significantly greater than the characteristic frequency of turbulent formations. One can also ignore the dependence of σ_a^2 on Π_ρ, i.e., the dependence of the horizontal velocities on the density gradient. Then the correlation (5) is transformed into

$$\sigma_a^2 = (\varepsilon^2/R)^{2/3}\,\alpha(\Pi_\nu). \qquad (8)$$

In the correlations (6)-(7) such simplifications cannot be made, however it is qualitatively clear that with $\Pi_g \to 0$, which corresponds with fixed g and R to the approach of ε to 0, $\sigma_\varphi^2 \to 0$, and with $\Pi_g \to \infty$ (which corresponds to small gravity and slow natural time of the system) the task is reduced to the classic problem of random wandering on a sphere [5]. However this case will not interest us because it practically does not happen in the atmosphere.

We will examine the case $\Pi_g \ll 1$. If we assume that the hydrodynamic reactions are applied to the sphere (its area is usually two orders greater than the area of the car), while the angular deviations are small (the smallness of Π_g is an indirect indication of the latter circumstance), then the Lagrangian equation for angles [2] can be written as:

$$\frac{d^2\varphi_i}{dt^2} + \omega_0^2 \varphi_i = \frac{dv_i}{at} \frac{\omega_0^2}{g}, \quad i = 1, 2. \tag{9}$$

Here $\omega_0 = \left(\frac{kR}{g}\right)^{1/2}$ --frequency of natural oscillations in balloon-car system,

k--amount that is constant for balloons of assigned weight and geometrical scales,

v_i--velocity of mass center.

In correlation (9) terms on the order φ^2 are ignored, as well as the shift in the center of action of hydrodynamic forces. Correlation (9) makes it possible according to the known spectrum of accelerations of mass center in the system $S_a(\omega)$ to determine the spectrum of angular deviations $S_\varphi(\omega)$ having used the formulas given in [6]:

$$S_\varphi(\omega) = \frac{\omega_0^4}{g^2 (\omega^2 - \omega_0^2)^2} S_a(\omega). \tag{10}$$

In correlation (10) the possibility of resonance is visible, but in fact the system is far from it, since the condition $\Pi_g \ll 1$ means that $\omega_R \ll \omega_0$, while ω_R, as we will see further is the characteristic damping frequency of the acceleration spectrum of the balloon. Since $\omega_R \ll \omega_0$, then from (10) it follows that

$$\sigma_\varphi^2 = \frac{\sigma_a^2}{g^2} = (\varepsilon^2/R)^{2/3} \frac{1}{g^2} \alpha(\Pi_\nu). \tag{11}$$

Thus, to find σ_a^2 and σ_φ^2 in the case $\Pi_g \ll 1$ it is sufficient to determine only one universal function of one dimensionless parameter Π_ν. However with the help of simple hypotheses one can evaluate σ_φ^2 also without knowing $\alpha(\Pi_\nu)$.

Being in a turbulent flow the balloon is carried away by major vortices, slightly distorting them. The balloon integrates vortices of size of much smaller radius than the balloon, i.e., averages their action over its surface, so that the contribution of pulsations with frequency much greater than ω_R equals zero (which does not lessen their possible role in the law of flow-around). The sphere distorts and does not average the intermediate scales. However as a first approximation one can take the following form of the acceleration spectrum:

$$\text{I}\quad S_a(\omega)=\begin{cases}S_0(\omega) & \omega<\omega'_R\\ 0 & \omega>\omega'_R\end{cases}\quad \text{with}\quad \omega'_R\ll\omega_\nu, \tag{12}$$

$$\omega'_R=c\,\omega_R, \tag{13}$$

$$\text{II}\quad S_a(\omega)=\begin{cases}S_0(\omega) & \omega<\omega_\nu\\ 0 & \omega>\omega_\nu\end{cases}\quad \text{with}\quad \omega'_R\gg\omega_\nu. \tag{14}$$

Here $\omega_\nu\sim(\nu/\varepsilon)^{1/2}$ --upper boundary of turbulent frequencies [4], $S_0(\omega)$--Lagrangian spectrum of acceleration of liquid particle. According to [4], in a uniform and isotropic turbulent flow

$$S_0(\omega)=B_0\varepsilon, \tag{15}$$

where B_0--universal constant of order 1.

In the region of frequencies $\omega\sim1/T_{\Lambda}$, where T_{Λ}--outer time Lagrangian turbulence scale. $S_0(\omega)\to0$, which shows the extremum nature of the evaluation for σ_φ^2 in the model of isotropic turbulence. By approximating $S_a(\omega)$ by formulas (12)-(15), we obtain:
with $\omega'_R\ll\omega_\nu$,

$$\sigma_a^2=c_1(\varepsilon^2/R)^{2/3},\quad \sigma_\varphi^2=\frac{c_1}{g^2}(\varepsilon^2/R)^{2/3}\sim\Pi_g^2; \tag{16}$$

with $\omega'_R\gg\omega_\nu$

$$\sigma_a^2=c_2(\varepsilon^2/\nu)^{1/2},\quad \sigma_\varphi^2=\frac{c_2}{g^2}(\varepsilon^2/\nu)^{1/2}\sim\Pi_g^2\Pi_\nu^{1/2}. \tag{17}$$

Here c_1 and c_2 are constant for balloons of the given weight and geometric scales. Formulas (16) and (17) are easy to obtain, having required that σ_a^2 from formula (8) does not depend on Π_ν with $\Pi_\nu\to\infty$, and does not depend on R with $\Pi_\nu\to0$, which corresponds to the following asymptotics of the function $\alpha(\Pi_\nu)$: $\alpha\to c_1$ with $\Pi_\nu\to\infty$ $\alpha(\Pi_\nu)\sim\Pi_\nu^{1/2}$ with $\Pi_\nu\to0$. We will be interested in the asymptotics (16), since it corresponds to the real constant-level balloons. For them $R\sim10^2$-10^3 cm, in the free atmosphere $\varepsilon\leq1$ cm^2/s^3, $g\approx10^3$ cm/s^2 and from the second formula (16) we find that $\langle\varphi^2\rangle^{1/2}\sim10^{-4}$ rad, i.e., the root-mean-square angles of torsion are obtained on the order of a minute. With these same values ε and R the first of the formulas (16) yields the root-mean-square acceleration $\sigma_a\sim0.1$ cm/s^2, which is quite permissible for modern accelerometers [3].

In order to take into consideration the real resistance of the balloon to the flow, one can examine the model equation

$$\frac{dv_i}{dt} + \lambda v_i = \lambda u_i, \quad i = 1, 2. \tag{18}$$

Here u_i--velocity of flow,

λ-friction coefficient (although in actuality the friction is clearly nonlinear, the relative velocity of the balloon and the flow often pass through zero and such an approximation is possible). After differentiating (18) with respect to time, and having adopted for the spectrum du_i/dt a graduated form, corresponding to (12) for the acceleration spectrum we obtain

$$S_a(\omega) = \begin{cases} \frac{B_0 \varepsilon}{1 + (\omega/\lambda)^2} & \omega < \omega'_R \\ 0 & \omega > \omega'_R \end{cases} \tag{19}$$

Thus, an evaluation according to formula (16) preserves the property of extremality. However for more precise evaluations the value of function α (Π_V) is required, whose appearance can be determined experimentally.

Although during flight in free atmosphere, as we explained, the angular deviations are small, during take-off and the nonstationariness associated with it a resonance oscillation of the balloon is possible. In the given case the Lagrangian description of turbulence is inapplicable, and for the characteristic frequency of pulsations one should assume U/R, where U--velocity of elevation. For real values $\omega_0 \sim 1$Hz and $R \sim 10^2$ cm the resonance occurs with velocities U on the order of several meters per second.

In the case where the balloon enters the layer of constant shift in wind velocity with altitude du/dz, it acquires a systematic deviation from the vertical by angle φ. Assuming the law of resistance is quadratic, and the angle φ is small, the forces of hydrodynamic resistance acting on the sphere (F_1) and the car (F_2) can be written as

$$F_i = \frac{1}{2} \rho_{a0} c_i S_i \left(L_i \frac{du}{dz} \right)^2, \quad i = 1, 2. \tag{20}$$

Here $L_{1,2}$--distance from balloon and car to that point in the system which is at rest in relation to the flow,

$c_{1,2}$ and $S_{1,2}$--respectively the coefficients of resistance and the area of the cross section of the balloon and the car.

By designating the Archimedes' force acting on the sphere, F_a and ignoring the Archimedes' force acting on the car, we write the equation of moment balance in relation to the fixed point:

$$\varphi L_1 F_a + L_2 m_2 g \varphi = L_1 m_1 g \varphi + L_1 F_1 + L_2 F_2. \tag{21}$$

Here m_1 and m_2--masses of balloon and car.

By adding to (20) and (21) the equations of force balance

$$F_a = m_1 g + m_2 g, \qquad F_1 = F_2 \tag{22}$$

and considering the distance between the balloon and car ($L=L_1+L_2$) and assigned amount, we find the angle φ:

$$\varphi \approx \frac{1}{2} \frac{\rho_{a0} c_2 S_2 \left(\frac{du}{dz}\right)^2 L^2}{2\left(1+\sqrt{\frac{c_2 S_2}{c_1 S_1}}\right) m_2 g}. \tag{23}$$

In deriving (23) the resistance and mass of the cable were ignored.

In conclusion we note the possibility of resonance for vertical oscillations in the system with $\Pi_\rho \ll 1$ (i.e., with $\omega_R > \left(\frac{K}{\rho_{a0}} \frac{d\rho_a}{dz}\right)^{1/2}$). Publication [7] successfully experimentally found the spectrum maximum of vertical shift on frequencies of the order of the Väisälä frequency. This effect makes it possible to have additional estimates of $d\rho_a/dz$. In this same work the upper boundary of the spectrum was experimentally obtained that coincides with ω_R with accuracy to a multiplier on the order of one (if one assumes that $\varepsilon \sim 1$ cm^2/s^3, $R \sim 10^2$ cm).

Conclusions

1. The main criterion for evaluating the angular deviations in the balloon is $\Pi_g = g^{-1}\varepsilon^{2/3}R^{-1/3}$. In the case $\Pi_g \ll 1$, which occurs in reality, the angular deviations are small ($\alpha_\varphi \sim \Pi_g$). We note that the smoothness of flight in preatmosphere was noted by all the astronauts with whom the authors spoke (N. Z. Pinus, A. S. Masenskis, V. I. Tatarskiy, A. M. Obukhov, R. Engel'man).

2. Based on calibration measurements of universal functions that describe the behavior of a balloon and with installation of sufficiently sensitive accelerometers, it can be used as a source of information about the turbulent kinetic energy dissipation rate ε and the vertical density gradient $a\rho_a/dz$.

BIBLIOGRAPHY

1. Danilov, A. M.; Dul'kin, P. Z.; Zemlyakov, A. S.; Matrosov, V. M.; and Srezhnev, V. A. "Dynamics of Stratospheric Observatory," "Problemy analiticheskoy mekhaniki i teorii ustoychivosti i upravleniya dvizheniyem" [Problems of Analytical Mechanics and Theory of Stability and Control of Motion], vol 1, Nauka, 1975.

2. Landau, L. D.; and Lifshits, Ye. M. "Mekhanika" [Mechanics], Moscow, Fizmatgiz, 1973.

3. Malov, V. V. "P'yezorezonansnyye datchiki" [Piezo-Resonance Sensors], Moscow, Energiya, 1978.

4. Monin, A. S.; Yaglom, A. M. "Statisticheskaya gidromekhanika" [Statistical Hydromechanics], Part II, Moscow, Fizmatgiz, 1967.

5. Rytov, S. M. "Statisticheskaya radiofizika" [Statistical Radiophysics], Part I, Moscow, Fizmatgiz, 1976.

6. Svefhnikov, A. A. "Prikladnyye metody teorii sluchaynykh funktsiy" [Applied Methods of Theory of Random Functions], Moscow, Fizmatgiz, 1968.

7. Sedov, L. I. "Metody podobiya i razmernosti v mekhanike" [Methods of Similarity and Dimensionality in Mechanics], Moscow, Fizmatgiz, 1965.

8. Massman, W. I. "On the Nature of Vertical Oscillations of Constant Volume Balloons," J. APPL. METEOROL., vol 17, No 19, 1978.

9. Santomauro, L.; Bacci, P.; Longhetto, A.; Anbossi, D. and Richiardone, R. "Experimental Evaluation of Diffusion Parameters on Local Scale by Means of No-lift Balloons," J. APPL. METEOROL., vol 17, No 10, 1978.

UDC 551.509.314

EXPERIMENTAL EVALUATION OF THE QUALITY OF OPERATIONAL AEROLOGICAL INFORMATION

Moscow METEOROLOGIYA I GIDROLOGIYA in Russian No 10, Oct 1979 pp 68-71

[Article by Candidate of Physical and Mathematical Sciences Yu. M. Liberman and V. P. Tarakanova, Main Geophysical Observatory, submitted for publication 30 Jan 1979]

Abstract: Aerological telegrams that entered the USSR Hydrometeorological Center in the space of 4 days have been subjected to complex static-time control. The detected rough errors in the values of geopotential and temperature of standard isobaric surfaces have been analyzed with respect to types, frequency of occurrence and combinations. It is shown that complex control possesses considerable potentialities not only for finding, but also for correcting such errors.

[Text] Aerological telegrams containing data on the temperature-wind sounding of the atmosphere on a network of ground and ship stations is the main form of information for compiling hydrodynamic forecasts. The reliability of this information is characterized by errors of two types: systematic and random. The systematic errors are governed by the limited accuracy in the radio sounding as a method for measuring the free atmospheric parameters; these errors have been studied by the authors (see, for example, [1]). As for the random errors, then it is impossible as a rule to establish the fact of the error of such type and to unambiguously determine its reason. This, however, can also be expedient if we are concerned with a rough error. Experience has demonstrated that rough errors comprise a noticeable percentage of all the random errors. They emerge as errors in counting during the processing of observational materials at stations, or are a consequence of inevitable distortion during the transmission of information and communications channels. In the process of automatic primary processing of data in the forecasting center (reception, accumulation, sorting and decoding) individual rough errors can also appear. Information about their number and types, as well as the effectiveness of control are insufficient. This report presents results of an experiment to reveal and to classify rough errors in aerological telegrams.

We analyzed 3,294 telegrams from the stations of the Northern Hemisphere. These telegrams entered the USSR Hydrometeorological Center in the space of eight operational sessions of information accumulation with periods 00 and 12.00 from 12 to 15 September 1977. They were prepared in the form of a file on a magnetic tape and kindly presented for our disposal by A. N. Bagrov and Ye. A. Loktionova.

Analysis was made on the computer BESM-6 with the help of the algorithm of complex static-time control. This algorithm is designed for processing information for pattern purposes. Its significant peculiarity is the use during control of data of each period not only of the previous, but also the subsequent information that enters from the station being checked. Under operational conditions such an approach, of course, is impossible. The values of geopotential H and temperature t of each of the 10 standard isobaric surfaces from 1,000 to 100 mbar and which are contained in part A of the telegram were controlled. When an error was found diagnosis and correction were put on print together with the initial data of the telegram and certain additional information. Based on this information a final judgment was formed on the correctness or erroneousness of the values H and t, on the correctness of the correction made and the type of error. These a posteriori judgments were based to a considerably greater degree than the decisions taken in operational conditions. Therefore the conclusions based on them are fairly reliable.

The obtained evaluations for the quality of the telegrams should be viewed as an evaluation from below. The reasons for this are the following. First, the static-time control, despite its power, cannot find all the actual errors: like any other control it does not react to errors below a certain level. Second, if during a subjective analysis of the information put in print doubt arises as to the correctness of the diagnosis, then the data of the telegram were considered to be without error. Third, it is known that in the telegrams often errors are found in which the equation of statics is not violated (sometimes by the named errors in radio sounding); their diagnosis was not provided for in the used algorithm. Finally, in the models of telegrams available at our disposal there was no information about the altitude of the station above sea level, as well as about the near-ground values of pressure and temperature. This circumstance did not make it possible to unambiguously judge the correctness or erroneousness of the values H_{1000} and t_{1000}. In particular, their absence in the telegram could be justified (if the near-ground pressure is less than 1000 mbar) or erroneous., but this was not successfully established. Therefore further in the statistics of errors the level 1000 mbar is not considered.

Analysis of the quality of telegrams begins with an evaluation of their completeness. We will call complete such a telegram in which in addition to other levels there is a value if but of one element H or t also on the level 100 mbar. Otherwise one can assume that the radiosonde did not reach the level 100 mbar or the corresponding numerical groups of the telegram have been lost. The number of such incomplete telegrams, cut off from above, was equal to 353 (11% of the total number of telegrams). Their distribution with

respect to the upper level is given below.

p, mbar	700	500	400	300	250	200	150
Number of telegrams	24	44	26	44	46	62	107

The completeness of the telegram in the indicated sense does not mean that at all the available levels values of both H and t are present; both these values or one of them on individual levels are missing. There were 127 such missing values H and t.

From the available values 457 were erroneous. Thus, the total number of defective--missing and erroneous--values equals 584. These defects were found in 417 telegrams, which is 13% of the total number of telegrams. Table 1 presents an idea about the types of defects and distribution with respect to levels. Most often errors are found of one of two elements, whereby the errors H are roughly 40% greater than the errors t.

TABLE 1 - DISTRIBUTION OF NUMBER OF DEFECTS WITH RESPECT TO TYPES AND ISOBARIC LEVELS

	(1) р мб 850	700	500	400	300	250	200	150	100	(2) Всего
(3) Отсутствие *H* при наличии *t*	3	4	9	12	8	6	4	5	1	52
(4) Отсутствие *t* при наличии *H*	1	6	4	5	5	3	4	4	1	33
(5) Отсутствие *H* и *t*	—	3	1	4	5	2	2	4	—	21
(6) Ошибочность *H* при верном *t*	16	27	28	29	23	34	19	24	16	216
(7) Ошибочность *t* при верном *H*	20	15	23	13	13	21	22	13	13	153
(8) Ошибочность *H* и *t*	1	1	4	6	10	11	6	1	4	44
(2) Всего	41	56	69	69	64	77	57	51	35	

Key:
1. mbar
2. Total
3. Absence of H with presence of t
4. Absence of t in presence of H
5. Absence of H and t
6. Erroneous H with true t
7. Erroneous t with true H
8. Erroneous H and t

Table 1 does not take into consideration the errors permitted at the station during computation of the relative geopotential of any layer. There were six such errors. It is significant that each of them results in distortion not only of one, but many values of H. Precisely, values that respond to the upper boundary of the corresponding layer and all the underlying isobaric surfaces. Therefore errors in computing relative geopotential produced actually the appearance of 39 erroneous values H.

Among the detected distortions the following characteristic groups are isolated:
--in 105 cases the values H or t were distorted by an amount, a multiple of 10 or 100;
--in 21 cases the oldest or youngest decimal sign of the number was lost;
--in 24 cases the decimal signs of the same number changed places;
--in 53 cases the "plus" sign was ascribed erroneously to the number, and in 15 cases--the "minus" sign.

Based on the obtained estimates one can assert that in 12-15% of the aerological telegrams individual values H and t on the isobaric surfaces are erroneous or lost.

TABLE 2 - EFFECT OF STATIC-TIME CONTROL

		(1) *p мб*									(2)
		850	700	500	400	300	250	200	150	100	Всего
(3) Число дефектных значений	*H*	20	35	42	51	46	53	31	24	21	333
	t	22	25	32	28	33	37	34	22	18	251
(4) Число исправленных значений	*H*	12	25	32	31	24	32	24	28	8	216
	t	9	18	16	13	14	19	26	15	4	134

Key:
1. p, mbar
2. total
3. Number of defective values
4. Number of corrected values

The urgent need for such control of aerological information is evident; this would permit not simply filtering out of rough errors, but also correction of as great a number of them as possible. In this sense the effectiveness of statics-time control is fairly high. Besides the errors in computation of the relative geopotential 350 defective values of the 584 were successfully unambiguously corrected, that is, 60% (table 2).

In addition in 59 cases two or three variants of correction were proposed. Apparently, after perfection of the algorithm of control the percentage of positive corrections can be brought to 75-80% of all the detected defects. Only a comparatively small number of telegrams were subject to such strong distortions that their correction becomes impossible and it is necessary to be limited only to rejection of the data. In this relationship it is characteristic to have a distribution of telegrams with respect to the number of discrepancies found in them in the equation of statics exceeding the critical values. The overwhelming majority of the distorted telegrams contain 1, 2

or 3 discrepancies, i.e., the probability of their correction is very great. Below the distribution is given of telegrams with respect to number of discrepancies (without consideration for the layer 1000/850 mbar).

Number of discrepancies	1	2	3	4	5	6	7	8
Number of telegrams	94	253	45	20	9	2	1	1

In conclusion we recall the desirability of the fastest development of the methods for complex control of the information contained in telegrams on the deficit of the dew point and wind. Up until now this information has not been used in the plans of numerical forecasting, and therefore the corresponding control remains undeveloped. However the need for it is sharply intensified due to the automated processing of aerological information for pattern purposes.

BIBLIOGRAPHY

1. Marfenko, O. V. "Evaluation of Accuracy of Radio Sounding Results on Aerological Network of the Soviet Union," METEOROLOGIYA I GIDROLOGIYA, No 3, 1969.

UDC 551.(465.11+466.3)

NUMERICAL MODELING OF WIND-DRIVEN WAVES

Moscow METEOROLOGIYA I GIDROLOGIYA in Russian No 10, Oct 1979 pp 72-80

[Article by V. K. Makin, and Candidate of Physical-Mathematical Sciences D. V. Chalikov, Leningrad Department of Institute of Oceanology, submitted for publication 20 March 1979]

Abstract: A general approach to the wind-driven wave numerical modeling problem is described, and the method of deriving the initial model equations is given. Basic results are discussed of a laboratory experiment simulation in an aerodynamic canal of traveling monochromatic waves, of numerical experiments to study the mechanism of energy and impulse transfer to the wave, and modeling the structure of the near-water atmospheric layer with developed waves.

[Text] Waves on the surface of a liquid, and in particular, wind-driven waves are one of the most studied natural hydrodynamic phenomena. The number of experimental studies of wind-driven waves continually rises. Wind-driven waves are effectively reproduced under laboratory conditions. The theory of wind-driven waves is an actively developed section of geophysical hydrodynamics. The progress in this field can be judged by comparing the survey article of Ursell [14] that were published in 1956, and Barnett and Kenyon [6] published 20 years later. The most important result obtained during this period is the discovery of the mechanism for generation and growth of waves made by Phillips [11] and Miles [10]. These theories that provide a clear qualitative interpretation of two methods of wave energy supply are in satisfactory agreement with the experimental data. At the same time, since both mentioned authors, in the same way as their numerous followers, were under pressure of the need to obtain a result in analytical form the initial set-up of the task was subject to a number of simplifications. Of them the strongest, probably, is the assumption on the smallness of the amplitude. The results obtained later on the basis of complete nonlinear models (see for example, [2, 3]) indicate that linearization of the problem in the most interesting cases results in irreparable losses of the physical content of the process.

In this respect the application of methods of mathematical modeling to the problem of small-scale (wave) interaction of the ocean and the atmosphere that makes it possible to reduce to a minimum the limitation in the statement of the problem is a natural step in the study of this phenomenon.

The main difficulty in construction of the model of wind-driven waves is the presence of a solid interface preventing the averaging of the Navier-Stokes equations in the Euler coordinate system. These difficulties are removed if the vertical coordinate ζ is counted not from a fixed level, but from the interface, i.e., one assumes $\zeta=z-\eta$, where z--Euler vertical coordinate counted from the undisturbed level, while η--elevation in water surface.

The main advantage of the ζ-coordinate consists of the fact that in it particles with equal altitudes always belong to the same medium, therefore in averaging the equation the difficulties associated with the existence of an interface, at least formally, do not arise, although the initial equations, of course, are complicated; in them a group of new terms appears which, by the way, has a clear physical interpretation. Based on the fact that in the future only a two-dimensional case will be examined we immediately will be concerned with two-dimensional equations (consideration for three-dimensionality in no point of the subsequent discussions will produce any basic difficulties):

$$\begin{aligned} u_t+(uu)_x+(wu-\eta_t u-\eta_x uu)_\zeta&=-\rho^{-1}P_x+\rho^{-1}\eta_x P_\zeta,\\ w_t+(uw)_x+(ww-\eta_t w-\eta_x uw)_\zeta&=-\rho^{-1}P_\zeta+g,\\ u_x+(w-\eta_x u)_\zeta&=0, \end{aligned} \qquad (1)$$

to which the kinematic condition on the surface is added

$$\eta_t=w_0-u_0\eta_x. \qquad (2)$$

In (1), (2) u, and w--longitudinal and vertical Euler velocity components,
u_0, w_0--their values on the surface $\zeta=0$,
$\rho=\rho_a$--air density with $\zeta>0$,
$\rho=\rho_w$--water density with $\zeta\leqslant 0$,
P--complete pressure.

Equation (2) guarantees the nonpenetration of the advective mass, impulse and energy transfer through the interface; on the left sides of the first two equations (1) the group of terms that can be differentiated with respect to ζ, with $\zeta=0$ turns to 0.

Assuming beforehand that the surface can be of fairly complicated shape, we introduce a procedure for averaging equations with respect to the assembly of surfaces close to each other (for more detail on this subject see [5] and [7]). By using further the standard idea of random amounts in the form of a sum of random deviations from them that are averaged with respect to

assembly, we will average the equation system (including the kinematic condition (2)). The average amounts $\bar{u}$, $\bar{w}$, $\bar{P}$, obtained by such averaging reflect the effect of the average excited surface $\bar{\eta}$, while the deviations from them--u', w', P'--the pulsations governed, in the first place, by the natural turbulence of the velocity field $\bar{u}$, $\bar{w}$, and secondly generated by the high-frequency components η'. In [5] and [7] considerations are given on the fact that the two-point moments containing pulsations η', must rapidly attenuate the farther from the surface. This makes it possible to omit from the equations the terms that contain such moments in the entire region, with the exception of the thin near-surface layers above and below, where it is necessary to consider their effect in the parametric form.

The selected method of averaging assumes that the task which it remains to solve consists of a clear description of large-scale wave components in water and in air. High-frequency (grid) components of waves and turbulence must be considered in the parametrical form. We note that here one cannot speak about turbulence as a grid phenomenon since its scales reach dimensions of the entire boundary layer.

In sum, we approach the Reynold's equation ascribed in the curvilinear system of coordinates (x,ζ), where altitude ζ is computed from the smoothed G--by averaging of the surface $\bar{\eta}$ (the averaging sign for the moments of first order is omitted):

$$u_t + (uu + \overline{u'u'})_x + (wu + \overline{w'u'} - \eta_t u - \eta_x uu - \eta_x \overline{u'u'} - M^u)_\zeta = \\ = -\rho^{-1} P_x + \rho^{-1} \eta_x P_\zeta,$$

$$w_t + (uw + \overline{u'w'})_x + (ww + \overline{w'w'} - \eta_t w - \eta_x uw - \eta_x \overline{u'w'} - M^w)_\zeta = \\ = -\rho^{-1} P_\zeta + g, \qquad (3)$$

$$u_x + (w - \eta_x u)_\zeta = 0, \qquad (4)$$

$$\eta_t = w_0 - \eta_x u_0 - \overline{\eta'_x u'_0}, \qquad (5)$$

where M^u and M^w designate the sums of the second and third moments which we will not compute (see, however, [5]).

Single-point moments of the second order are presented in the form of the product of deformation tensor components $\Phi_{i,j}$ (in the system of coordinates (x,ζ)) and the isotropic turbulent viscosity coefficient K, expressed through the turbulence scale l, that linearly rises the farther from the surface, and kinetic turbulence energy e (KTE)

$$l = \varkappa|\zeta|, \; K = l(e/c_1)^{1/2}, \qquad (6)$$

($\varkappa$=0.4--Karman constant, c_1=4.6--constant).

Due to the first of formulas (6) K formally with $\zeta=0$ converts into zero. This standard difficulty is eliminated by parametrization of the near-surface friction, which is discussed in detail in [5, 7]. The final recommendations are reduced to the fact that with $\zeta=0$ the terms $\rho K u_\zeta$ and $\rho K w_\zeta$ are replaced respectively by τ_s and $\eta_x \tau_s$, where τ_s--local tangential to friction surface computed according to formula

$$\tau_s = \rho_a \Delta u_\tau |\Delta u_\tau| c_s, \tag{7}$$

where $\Delta u_\tau = (u^+ - u^-) + \eta_x (w^+ - w^-)$ (u^+, w^+--velocity component directly above interface, u^-, w^---under it), c_s--resistance coefficient. Under real conditions the approved c_s is determined by the surface shape at high frequencies, so that, based, for example on the Phillips' spectrum for the inertia interval of gravity waves, for c_s the evaluation is obtained $c \sim \varkappa^2 [\ln(c_2 z^+/\delta x)]^{-2}$ (z^+--altitude of parametrized boundary layer, δx--horizontal resolution of numerical model, c_2--constant on the order 10[3]). Under laboratory experiments the surface often can be considered smooth so that $c_s \sim \varkappa^2 [\ln(c_3 z^+ v_*/\nu)]^{-2}$ (ν-molecular air viscosity, c_3--constant 10). If the depth of the liquid is low, parametrization is required of the near-bottom boundary layer. Here a relationship of type (7) is used in which instead of the velocity drop the actual near-bottom velocity will already figure.

The considerations that explain the possibility of ignoring the moments that contain pulsation η' are inapplicable to the last term in equation (5) since it is computed on the actual surface. It is easy to understand that the term describes the effect of grid components of wave action on the large-scale, clearly described portion of the spectrum. A discussion of this effect is given in [7].

The final system of equations in the two-dimensional variant looks as follows:

$$u_t + \left(uu + \frac{2}{3}e - 2Ku_x + 2K\eta_x u_\zeta\right)_x + \left(wu - \eta_t u - \eta_x uu - \right.$$
$$\left. - Ku_\zeta - Kw_x + K\eta_x w_\zeta - \frac{2}{3}\eta_x e + 2K\eta_x u_x - 2K\eta_x^2 u_\zeta\right)_\zeta =$$
$$= -\rho^{-1} p_x + \rho^{-1}\eta_x p_\zeta + g_1 \eta_x, \tag{8}$$
$$w_t + \left(uw - Ku_\zeta - Kw_x + K\eta_x w_\zeta\right)_x + \left(ww - \eta_t w - \eta_x uw + \right.$$
$$\left. + \frac{2}{3}e - 2Kw_\zeta + K\eta_x u_\zeta + K\eta_x w_x - K\eta_x^2 w_\zeta\right)_\zeta = -\rho^{-1} p_\zeta, \tag{9}$$
$$u_x + (w - \eta_x u)_\zeta = 0, \tag{10}$$
$$\eta_t = w_0 - \eta_x u_0 - J, \tag{11}$$
$$e_t + (eu - Ke_x - K\eta_x e_\zeta)_x + (ew - \eta_t e - \eta_x ue - Ke_\zeta -$$
$$- K\eta_x e_x + K\eta_x^2 e_\zeta)_\zeta = K[(u_\zeta + w_x - \eta_x w_\zeta)^2 + (2w_\zeta)^2] - \varepsilon \tag{12}$$

Here J designates the rate of change in the level as a consequence of the waves falling down,

$p = P - g\int_{\zeta}^{H_a} \zeta\, d\zeta + g\rho_a\eta$ --deviation of pressure from hydrostatic,

g_1--modified acceleration of freefall ($g_1=0$ with $\zeta>0$ and $g_1=g\,(1-\rho_a/\rho_w)$ with $\zeta\leqslant 0$),

$\varepsilon = (e/\rho c_1)^{3/2} l^{-1}$ --velocity of turbulent energy dissipation.

The system of equations (8)-(12) is solved in the rectangular ζ-coordinate of the region of extent L and altitude H_a+H_w (H_a and H_w--orders of wavelength). The periodicity of the function and the necessary derivatives are assumed along the x axis. Thus if the adopted grid is counted along the horizontal of m centers, the surface can be presented by superposition m/2 of harmonic waves.

On the upper boundary in the self-modeling region the turbulent impulse flow $\tau=\rho_a v_*^2$ is assigned, the turbulent energy determined by it, and damping of the vertical velocity and pressure perturbations are assumed:

$$\begin{array}{ll} \text{with} & \zeta = H_a \quad \overline{u'w'} = -v_*^2,\ e = c_1\rho_a v_*^2,\ w = 0,\ p = 0; \\ \text{with} & \rho = -H_w \quad u = 0,\ w = 0,\ e = c_1\tau_b. \end{array} \qquad (13)$$

Here τ_b--near-bottom friction.

It follows from equations (8) and (9) that the vertical impulse flow $\overline{F}$ is described by the expression

$$\overline{F} = \overline{u\tilde{w}} + \overline{u'w'} - \eta_x\overline{u'u'} - M^u - \rho^{-1}\eta_x p, \qquad (14)$$

Here $\tilde{w}=w-\eta_t-\eta_x u$--vertical velocity counted from moving surface; the upper here and below designates averaging with respect to the horizontal. As is apparent, the impulse flow in the ζ-coordinate is created by an individually described velocity field (first term), turbulence (mixed three terms) and pressure. Above the waves of small curvature the impulse transfer is implemented mainly by turbulent viscosity. With a rise in the curvature the contribution of streams created by the wave components of velocity of pressure is increased. This is illustrated in figure 1 where the vertical distribution of impulse flow components in (14) is presented. The computations were made of two variants: with regard for the advective terms in the motion equations and without them. As is apparent, with fairly great curvature the impulse transfer mechanism in the absence of nonlinear terms is strongly distorted. In figure 1,d for ak=0.4 (a--wave amplitude, k--its wave number) results are given of analogous computations for the Stokes' wave for two variants of spatial resolution.

By comparing figures 1d and 1c one can conclude that even for fairly steep waves the differences in flow-around of the sinusoidal wave and the Stokes'

wave are not very significant. Figure 1d shows that a double improvement in the spatial resolution does not result in a significant change in the results.

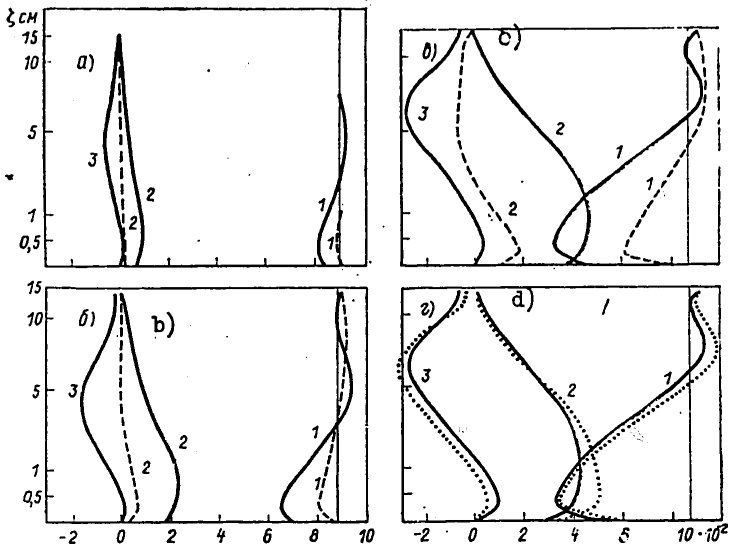

Figure 1. Vertical Distribution of Impulse Flow Components

Key: a. ak=0.1
b. ak=0.2
c. ak=0.4
d. ak=0.4, above Stokes' wave
1. $-\rho_a\overline{u'w'}+\eta_x\overline{u'u'}$,
2. $\eta_x p$
3. uw

Dashed line gives results of computations without advective terms in equation. Dotted line shows results of computations with horizontal spacing, halved.

We note that from (15) it follows as a kinematic condition that w=0, and also $\overline{u'w'}-\eta_{1x}\overline{u'u'}-M^u=\tau_s$, so that the impulse F_0 is transmitted to the water only by pressure and surface friction forces

$$\overline{F_0}=\overline{\tau_s+p\eta_{1x}}. \qquad (15)$$

We also cite the formula for energy flow from one medium to another:

$$\overline{A_0}=\overline{u_0\tau_s-w_0\eta_x\tau_s+p\eta_{1t}}. \qquad (16)$$

As the first task we examined the use of the numerical model developed above for simulating the Stewart laboratory experiment [13] that measured velocity and aerodynamic canal above traveling monochromatic waves created by a wave-producer. The results given in [1, 4, 7] indicated that the model quite satisfactorily reproduces many fine peculiarities of wind field above the waves and the spread of the wave itself. As a result such a difficult to measure characteristic was successfully obtained as the spectra of velocity field wave components at different altitudes above the waves. Calculations demonstrated that the monochromatic wave generates all possible modes in the numerical model already on a comparatively low altitude above the waves. The model correctly reproduced the difference in the wind velocity profiles in different phases of the wave.

Publication [2] found interesting peculiarities in the turbulent energy distribution. The most specific of them is the presence of four extremums: two surface and two at the altitude on the order 1/10 of wavelength. The surface maximum is located to the left of the crest, and the minimum to the left of the foot. The raised maximum is shifted roughly by 180° from the crest. In magnitude it somewhat exceeds the surface maximum. It is curious that the elevated extremum can easily be found by pulsation measurements with the use of phase averaging. This possibility, as far as we know, has not yet been realized. It is curious that qualitatively close results were obtained in publication [8, 9].

The most unexpected result was obtained in studying the pressure field in [3] with different values c/v_* (c--phase velocity of wave). With $c/v_*=23.7$ the distribution of surface pressure is described by a single-modal curve of asymmetric form. The value $\beta_1 = (p_{max} - p_{min})/\rho v_*^2$ equals 30.9. With $c/v_*=20$ the pressure is described already by a two-modal curve. Up to $c/v_*=8$ the two modes are preserved, altering their shape. β_1 is reduced from 14.9 with $c/v_*=20$ to 5.3 with $c/v_*=10$. With $c/v_*=8$ the pressure profile again is described by one mode, while β_1 rises to 9.4. The pressure becomes symmetric with $c/v_* \leqslant 6$. Thus, the energy transfer as a consequence of pressure is implemented by the complex interaction of the surface pressure field with the surface. This effect basically cannot be studied on the basis of the linear theory.

The results given below were obtained in the next cycle of computations that covers the study of the near-water atmospheric layer with developed wave action. In the same way as in publication [2, 3, 8, 9], to simplify the computations here a single-layer task is solved consisting of integration of the system of equations (8)-(12) above the assigned surface. The difference of the mentioned works consists of the fact that the surface was a system of dispersing gravitation waves with the assigned spectrum, each of which is described by the theory of low amplitude waves.

As the initial the Pierson and Moskovits spectrum [12] was selected that corresponds, in the opinion of the authors, to the conditions of completely developed waves

$$F = \alpha g^2 \omega^{-5} \exp[-\beta (g/U\omega)^4]. \qquad (17)$$

Here ω--frequency,
U--wind velocity at altitude of measurements H,
$\alpha=8.1 \times 10^{-3}$, $\beta=0.74$--empirical coefficients.

By introducing the dimensionless frequency $\hat{\omega}=\omega v_*/g$ and spectral density $\hat{F}=Fg^3/v_*^5$, and by presenting the velocity U in the form

$$U=\frac{v_*}{\varkappa}\ln\frac{H}{z_0}, \text{ where } z_0=0{,}035\ \frac{v_*^2}{g}, \tag{18}$$

we obtain

$$\hat{F}=\alpha\hat{\omega}^{-5}\exp(-\beta Q\hat{\omega}^{-4}), \tag{19}$$

where Q--slightly altering dimensionless parameter.

$$Q=\left(\varkappa\ln\frac{Hg}{0{,}035\,v_*^2}\right)^4 \tag{20}$$

where typical conditions of the component $Q\approx 10^{-6}$.

By using the velocity scale v_* of length v^2/g and time v_*/g we bring equations (3)-(5) to the dimensionless form. After this the entire task as a whole depends only on one dimensionless parameter Q, which, taking into consideration the approximateness of formulas (17), with complete substantiation can be considered fixed.

We will present dimensionless elevation $\hat{\eta}$ in the form

$$\hat{\eta}(\hat{x},\hat{t})=\sum_1^N A_k\cos(\hat{k}\hat{x}-\hat{\omega}\hat{t}). \tag{21}$$

Here A_k--dimensionless harmonics amplitude with wave number $\hat{k}$ and frequency $\hat{\omega}$, linked by the dispersion correlation $\hat{k}=\hat{\omega}^2$. The amplitudes A_k are selected such that the successive set of realizations at each point has a frequency spectrum (20). Here one should immediately indicate the defect in the proposed interpretation of the spectrum which becomes completely stripped only in the case when the process is actually linear. In the case of nonlinear waves for reproduction of the realization the information about one spectrum is insufficient.

As new boundary conditions on the surface $\zeta=0$ the components of surface velocity are assigned

$$\hat{u}_0(\hat{x},\hat{t})=\sum_1^N A_k\hat{k}^{1/2}\cos(\hat{k}\hat{x}-\hat{\omega}\hat{t}),$$

$$\hat{w}_0(\hat{x},\hat{t})=\sum_1^N A_k\hat{k}^{1/2}\sin(\hat{k}\hat{x}-\hat{\omega}\hat{t}). \tag{22}$$

In the discussed computation N=16 is assumed. With this value the initial spectrum is described with fairly high accuracy: the discrepancy between the integral characteristics $\bar{\eta}^2 = \sum_{\omega_{min}}^{\omega_{max}} \hat{F} \Delta\omega$, where ω_{min} and ω_{max}, respectively, the minimum and maximum wave frequency included in the summary elevation (22) and the theoretical amount $\int_0^\infty F d\omega$ is 5%. Integration of system (3)-(5) was carried out up to time $\hat{t}$=500 with spacing with respect to time $\delta\hat{t}$=1. The statistically equilibrium pattern was achieved roughly with $\hat{t}$=50. The solution was traced according to the series of integral characteristics. An important characteristic of the interaction--dimensionless velocity of energy exchange between media $\bar{A}_0$ was obtained. This amount during the entire period of integration was stably negative, which corresponds to the stream of energy from water to air. The mean amount $\hat{A}_0$ was roughly 1.5. The energy stream due to the normal forces was about 70% of the total. The sign for the energy flow indicates that the Pierson-Moskovits spectrum is overestimated in the region of low frequencies. This situation can be explained, for example, by the presence of swell components in the measurements placed at the basis of the approximation (17). The impulse flow through the surface is governed, mainly, by the turbulent viscosity that is no less than 90% of the total. Currently analogous studies are being made of other types of approximation of a completely developed spectrum. As an illustration of the possibilities of the proposed method figure 2 presents momentary distribution of turbulent energy and the current function above the surface. We will stress that these distributions, of course, cannot be obtained by simple superposition of the results for individual harmonics, since flow-around of the complex surface is a significantly nonlinear process.

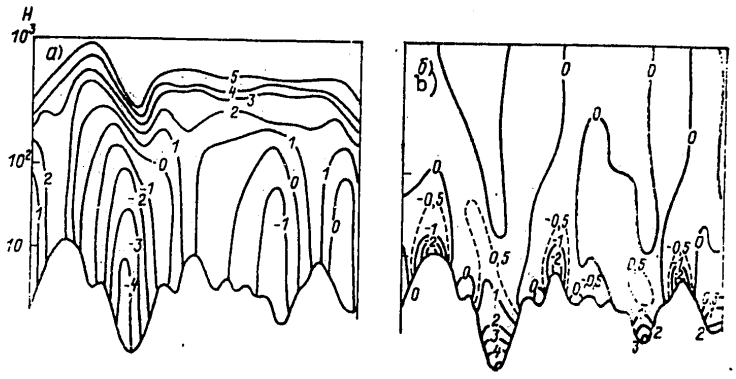

Figure 2. Fields of Current Function (a) and Dimensionless Energy of Turbulence (Deviation from 4.6) (b) above Surface Assigned by Formula (22).

Thus, we have described the general approach and the main results of numerical modeling of wind-driven waves. Now it is apparent that it is still early to speak of how suitable the proposed method is for solving the main problem of wind-wave interaction. At the same time it seems that the findings do not repudiate the expediency of further steps in this direction.

BIBLIOGRAPHY

1. Makin, V. K.; and Chalikov, D. V. "Numerical Modeling of Air Flow Above Waves," IZV. AN SSSR. FIZIKA ATMOSFERY I OKEANA, No 5, 1979.

2. Makin, V. K. "Wind Field Above Waves," OKEANOLOGIYA, No 2, 1979.

3. Makin, V. K. "Energy Transfer to Waves," IZV. AN SSSR. FIZIKA ATMOSFERY I IKEANA, 1979.

4. Chalinkov, D. V. "Mathematical Model of Wind-Driven Waves," DOKL. AN SSSR, No 229, 1976.

5. Chalinkov, D. V. "Matematicheskaya model' vetrovogo volneniya," [Mathematical Model of Wind-Driven Waves], Leningrad, Gidrometeoizdat, 1979.

6. Barnett, T. P.; Kenyon, K. E. "Recent Advances in the Study of Wind Waves," REPORTS ON PROGRESS IN PHYSICS, vol 38, 1975.

7. Chalikov, D. V. "The Numerical Simulation of Wind-Wave Interaction," J. FLUID MECH., vol 87, 1978.

8. Gent, P. R.; and Taylor, P. A. "A Numerical Model of the Air Flow Above Waves," J. FLUID MECH., vol 77, 1976.

9. Gent, P. R. "A Numerical Model of the Air Flow Above Water Waves. Part II," J. FLUID MECH., vol 82, 1977.

10. Miles, J. W. "On the Generation of Surface Waves by Shear Flows," J. FLUID MECH., vol 3, 1957.

11. Phillips, O. M. "On the Generation of Waves by Turbulent Wind," J. FLUID MECH., vol 2, 1957.

12. Pierson, W. S.; and Moskovits, L. "A Proposed Spectral Form for Fully Developed Wind Seas Based on the Similarity Theory of S. A. Kitaigorodskii," J. GEOPHYS. RES., vol 69, 1964.

13. Stewart, R. H. "Laboratory Studies of the Velocity Field Over Deep-Water Waves," J. FLUID MECH., vol 42, 1970.

14. Ursell, F. "Wave Generation by Wind," "Surveys in Mechanics," London, 1956.

UDC 551.463.7:537.31(265/266)

ELECTRICAL CONDUCTIVITY FIELD OF SEAWATER IN NORTH PACIFIC OCEAN

Moscow METEOROLOGIYA I GIDROLOGIYA in Russian No 10, Oct 1979 pp 81-87

[Article by S. A. Oleynikov, and Candidate of Geographical Sciences D. M. Filippov, All-union Scientific Research Institute of Hydrometeorological Information, World Data Center, submitted for publication 12 March 1979]

Abstract: From materials of deep-sea observations made in the period from 1920 through 1970 a three-dimensional field of specific electrical conductivity of seawater in situ in the ocean is calculated on a computer. On the example of the northern Pacific Ocean a general climatological-statistical description of this field is given, the main peculiarities of its structure and most characteristic elements of the vertical stratification are noted (uniform layer of electrical conductivity, its extremum layers, and so forth).

[Text] One of the most important physical and chemical properties of the ocean and seawater as complex multiple-component solutions of strong electrolytes is their electrical conductivity, in particular, the specific electrical conductivity of water in situ, currently observed with the help of probes. It is known that the electrical conductivity of seawater is determined by a number of factors, of which the main is the concentration of salts dissolved in water, water temperature, and hydrostatic pressure [7, 8, 12]. For the ranges existing in the World Ocean of changes in temperature, salinity and pressure with their increase a specific electrical conductivity arises. The functional link of electrical conductivity with the parameters determining it has been fairly widely studied under laboratory conditions by many authors [5, 6, 10, 11]. A large number of works have covered questions of perfecting instruments and methods for determining salinity and density of seawater with respect to its electrical conductivity [9]. At the same time no published information is found about the electrical conductivity in situ both of the oceanographic field, the vertical structure, stratification elements, spatial-temporal variability in electrical conductivity and so forth.

The data of full-scale observation on electrical conductivity in situ do not make it possible as yet to obtain a general pattern of the field of specific

conductivity in the World Ocean, since they still bear a fragmentary, occasional nature and are limited mainly to the surface and intermediate structures of the ocean zones. However the fairly accurately established dependence of electrical conductivity on the temperature, salinity and pressure that makes it possible to approximate its real distribution in the ocean, permits this field to be obtained by computation on a computer. Such work was done in the Center of Oceanological Data on technique of the Institute of Oceanology of the USSR Academy of Sciences for the Pacific and Atlantic Oceans based on deep-water data file that encompasses the period of observations from 1920 through 1970, by the authors and L. A. Golovanova. The algorithms, descriptions of the programs and technology of processing of deep-water information on a computer are given in [1, 3].

As a computation formula the semi-empirical expression was used that was compiled according to the data of the works of E. Aceerboni and F. Mosetti [6] and A. Bradshow and K. Schleicher [7]

$$D_i = D'_i [1 + | (W_1W_2 + W_3W_4)(1 + W_5W_6) | \cdot 10^{-8}], \quad (10^{-1}\ Cm/m),$$

where D_i--specific electrical conductivity of seawater on observed level i;
D'_i--electrical conductivity of seawater on observed level with atmospheric pressure (6) as a function of temperature (t^oC) and salinity (S^o/oo);

$$D'_i = \left(2{,}1923 + 0{,}12842 \frac{t_i^{1{,}032}}{1 + t_i^{0{,}032}} e^{0{,}0029\, t_i}\right) \frac{S_i}{1 + S_i^{0{,}1243}} e^{-0{,}000978\, S_i} \times$$

$$\times e^{-0{,}0000165\,(S_i - 35)\,(t_i - 20)};$$

$| (W_1W_2 + W_3W_4)(1 + W_5W_6) | \cdot 10^{-2}$ --correction multiplier that takes into consideration the effect of hydrostatic pressure on electrical conductivity depending on salinity S and temperature t of seawater [7] on the observed level;

$$W_1 = 1{,}5192 - 4{,}5302 \cdot 10^{-2}\, t_i + 8{,}3089 \cdot 10^{-4}\, t_i^2 - 7{,}9 \cdot 10^{-6}\, t_i^3;$$
$$W_2 = 1{,}042 \cdot 10^{-3}\, B_i - 3{,}3913 \cdot 10^{-8}\, B_i^2 + 3{,}3 \cdot 10^{-13}\, B_i^3;$$
$$W_3 = 4 \cdot 10^{-4} + 2{,}577 \cdot 10^{-5}\, B_i - 2{,}492 \cdot 10^{-9}\, B_i^2;$$
$$W_4 = 1 - 1{,}535 \cdot 10^{-1}\, t_i + 8{,}276 \cdot 10^{-3}\, t_i^2 - 1{,}657 \cdot 10^{-4}\, t_i^3;$$
$$W_5 = 6{,}95 \cdot 10^{-3} - 7{,}6 \cdot 10^{-5}\, t_i;$$
$$W_6 = 35 - S_i;$$
$$B_i = P_i - 10{,}1325.$$

The hydrostatic pressure P_i (in decibars) was defined by the method of three-space approximation employed in the U.S. National Center of Oceanic Data.

The computations of electrical conductivity and its vertical gradient were made for each hydrological station according to the temperature and salinity

data (with regard for pressure) on the standard levels up to depth 4000 m with further averaging of the data of all stations with respect to five-degree trapezia for the mean multiple-year, as well as for the thermal and cold half-years. Besides the mean values of electrical conductivity and its gradient in each five-degree trapezium on the same levels their extremeum values were determined, standard deviation, dispersion, coefficients of variation, asymmetry, excess, error in computation of all the calculated amounts, frequency and rate of occurrence with respect to gradations. From the analysis of the main errors in computation governed by the heterogeneity in the spatial distribution of observational data it follows that on the dominant portion of the water area errors in computation of the mean are several times lower than the natural variability in electrical conductivity (standard deviation) in the corresponding five-degree squares. In the least studied central and near-equatorial regions the water area in the upper 200-meter layer of the ocean they do not exceed (1-2) x 10^{-1} Cm/m, dropping to (0.1-0.5) x 10^{-1} Cm/m at its shores. The computation errors linked to the inaccurate determination of temperature, salinity and pressure on the given level, in terms of the climatological-statistical study with large spatial-temporal scales of averaging are insignificant, and in our estimates, do not exceed 0.05 x 10^{-1} Cm/m.

Analysis of the findings of the computation make it possible to reveal the basic laws governing the formation and reconstruction of the field of specific conductivity in the ocean, and to study its vertical structure in the spatial-temporal variability on the characteristic surfaces (standard levels).

With the help of the electrical conductivity vertical distribution curves the following basic elements of its stratification were successfully isolated: surface uniform (homogeneous) layer of electrical conductivity, layer of extremum gradients located in the seasonal thermocline, and finally, the layer of deep maximum of electrical conductivity lying under the main thermocline of the ocean [4].

As a surface uniform layer of electrical conductivity the layer is adopted in which its vertical gradient with respect to the absolute amount does not exceed 1 x 10^{-3} Cm/m^2. The given criterion was selected by us in accordance with the conditions for isolation in the ocean of surface isothermic and isohaline layers within which the vertical gradients usually do not exceed 1 x 10^{-2}° C/m and 1 x 10^{-3} °/oo/m respectively. The thickness of the surface homogeneous layer of electrical conductivity in the northern Pacific Ocean is not constant. Depending on the physical and geographical conditions that determine the intensity of the wind and density processes of mixing it is altered both with respect to the water area and from season to season. From the most average annual values in the central region of the near-equatorial area (75 m) the uniform layer of electrical conductivity gradually is reduced to the north to 10-15 m above the middle latitudes, and up to 0 at the coasts of the ocean (figure 1a). In the cold half year (figure 1b) it is the maximum and the most developed (up to 100-200 m) at the subarctic front and in the region of the southeast branching of the North Pacific Current. In the summer period (figure 1c) the characteristics of the homogeneous layer are close to the mean annual values (the dimensions of the coastal region where it is lacking are somewhat increased).

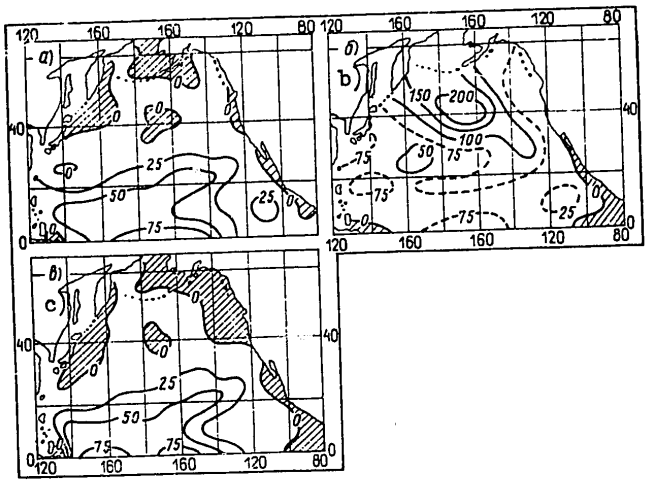

Figure 1. Thickness (in Meters) of Surface Homogeneous Layer of Electrical Conductivity in Northern Pacific Ocean

Key:
a. Average for year b. In cold half year c. In warm half year (hatched sections of water area where homogeneous layer is missing)

The subsurface layer of extremum vertical gradients of electrical conductivity is of certain interest since it is the layer of the jump in electrical conductivity. It is governed by those hydrophysical processes in the ocean which result, in particular in the formation in its surface structural zone of a layer of seasonal jump in water temperature that determines the main laws governing the formation of the electrical conductivity field up to the axis of its deep minimum. The mean annual thickness of the layer of electrical conductivity extremeum gradients, i.e., the layer where its vertical gradients with respect to the absolute amount exceed 5×10^{-3} m/m^2 (which corresponds to the criterion of isolation of the layer of temperature jump with respect to its gradient 5×10^{-2}°C/m) is altered in the northern Pacific Ocean from the north to the south, increasing from 20-30 m in the Bering Sea to 150-200 m in the region of the equator. The average annual depth of occurrence of the nucleus of this layer is greater (150-200 m) in the center of the water area (in region 20°n.l.) and is reduced on the average up to 75-100 m at the equator and up to 20-30 m in the high latitudes (figure 2,a).

The average annual amounts of the gradients in the nucleus of the extremum layer (figure 2b) are $(-6--10) \times 10^{-3}$ Cm/m^2 in the northern to middle latitudes, and in the equatorial-tropical belt reach $(-14--22) \times 10^{-3}$ Cm/m^2.

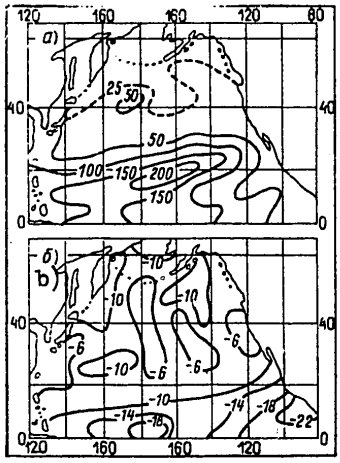

Figure 2. Core of Layer of Maximum Electrical Conductivity Gradients
Key:
a. Topography of core (in meters)
b. Amounts of electrical conductivity gradients (10^{-3} Cm/m^2) in core of maximum layer (northern part of Pacific Ocean, mean values for year)

It is characteristic that in the cold half year above the middle latitudes, due to the fall-winter cooling of the surface waters the layer with gradients over 5×10^{-3} Cm/m^2 is completely washed away, and the deepening of its core on the section of the water area is increased (as compared to the average annual (by 50-100 m).

The most characteristic element in the stratification of the examined field is the layer of deep minimum of electrical conductivity whose formation is linked to the peculiarities in the vertical distribution in the ocean of temperature, salinity and hydrostatic pressure. Under the influence of the first two factors, with respect to the contribution to conductivity of those dominating over pressure within the limits of the surface and intermediate structural zones, electrical conductivity rapidly is reduced with depth, mainly following the course of water temperature in the main thermocline. The partial reduction in electrical conductivity as a consequence of the decrease in salinity with depth is fairly insignificant and according to our data is not more than 10-12% (according to the contribution to electrical conductivity the change in water temperature by 1°C is roughly equivalent to the change in salinity by 1% , however the range of change in the latter in the ocean is almost by an order lower than the temperature).

With a transition to the deep structural zone, under conditions close to the isotherm, and with the practically unchanged salinity, the leading factor that

determines the nature of variability in electrical conductivity with respect to the vertical becomes the hydrostatic pressure that compensates for the effect of temperature and salinity on the axis of minimum electrical conductivity and governs its further growth with depth. In [7] it is demonstrated that the increase in the electrical conductivity as a consequence of an increase in pressure from 0 to 10,000 decibars,(i.e., up to depth roughly 10,000 m) reaches 12%.

In the northern Pacific Ocean the nucleus for the minimum layer occurs at depths 1500-1800 m in the high latitudes, and on the average, at a depth 2500 m in the equatorial-tropical zone. The topography of the minimum layer in the southwest section of the examined water area has a more complicated relief due to the variation with depth in the lower boundary of the thermocline in this region. The values of electrical conductivity in the minimum layer also are altered from north to south, increasing from (29.0-31.0) x 10^{-1} Cm/m in the Bering Sea up to 31.5 x 10^{-1} Cm/m on the equator and in the tropical latitudes. The greatest variability in electrical conductivity in the minimum layer (standard deviation over 0.14 x 10^{-1} Cm/m and the variation coefficient 0.4%) is noted along the western shore of the ocean. This layer is practically not subject to seasonal changes.

In accordance with the thermal pattern of water the maximum average annual values of electrical conductivity are observed on the surface of the ocean (in places at depth 10-20 m)*, where they are zonally altered from 30-31 x 10^{-1} Cm/m at the Bering Strait to (55-57) x 10^{-1} Cm/m in the southwest water area (figure 3a). The farther from the surface the field of electrical conductivity in the ocean is subject to multiple reconstructions, linked to the thermocline factors and water circulation. At depth 200 m (figure 3b) the regions of its extremum values are shifted: the least (30 x 10^{-1} Cm/m) to the Arctic front, the greatest ((45-47) x 10^{-1} Cm/m) to the regions of intensive lowering of warm and highly-saline waters of the subtropics.

In the southeast water area the values of electrical conductivity at these depths become reduced ((37-38) x 10^{-1} Cm/m) as a consequence of the advective effect of the subarctic water and the rise of the deep water along the axis of tropical divergence. With secondary reconstruction of the electrical conductivity field that is traced in the intermediate structural zone of the ocean, roughly from depth 500 m, the features of its zonality begin to be restored (figure 3c), however the reduction in the electrical conductivity at depth 1000 m in the direction of high latitudes is already insignificant (only 1.5-2.0) x 10^{-1} Cm/m). In the deep structural zone the electrical conductivity field is strongly smoothed, being reconstructed in a meridional direction. The mean multiple-year values of electrical conductivity at depth 4000 m are altered from region to region only by a tenth of a unit (from 31.65 to 31.75 x 10^{-1} Cm/m), increasing from the central section of water area to the shores of the ocean (figure 3d).

The absolute and relative variability of electrical conductivity in the northern Pacific Ocean is the maximum in the surface structural zone. The increased average annual values of standard deviation and the variation

*In the winter period the maximum values of electrical conductivity in the high latitudes are noted at depths on the order of 300-500 m and more.

coefficient are confined to regions of dynamic instability of water and are observed in regions of Arctic and subarctic fronts, as well as in California (on the ocean surface) and the region of the tropical cyclonic circulation in the layer 50-100 m (over 3 x 10^{-1} Cm/m and 8% respectively). The extremum values are reached by the standard deviations and the variation coefficients at the shores of Japan, in the region of encounter of warm and cold waters in the Kuroshio and Oyashio currents (respectively over 5 x 10^{-1} Cm/m and 10-14% on the ocean surface (with depth the variability in electrical conductivity, especially in the intermediate structural zone rapidly drops and at depths 4000 m on the average is 0.05 x 10^{-1} Cm/m and 0.1-0.2%).

The intra-annual (seasonal) variability in electrical conductivity governed mainly by thermal factors is most pronounced in the surface structural zone of the ocean. The maximum excess in the summer values of electrical conductivity over the winter are traced on the surface of the Pacific Ocean in the moderate and middle latitudes (positive differences are 6-8 x 10^{-1} CM/m), i.e., there where the seasonal course in the water temperature is most noticeable. In the direction towards the equator the differences are reduced to 0.3-0.7 x 10^{-1} Cm/m. With depth the seasonal differences in electrical conductivity are attenuated and change their nature. The region of the greatest positive differences of electrical conductivity at depth 100 m are shifted to the equator ((1-3) x 10^{-1} Cm/m). The remaining part of the water area at this depth is characterized by an alternation of regions of positive and negative differences in electrical conductivity not exceeding, by the way, the amount 1 x 10^{-1} Cm/m. On the lower boundary of the surface structural ocean zone the seasonal differences are smoothed: the summer values of electrical conductivity noticeably surpass winter only in the southwest section of the water area ((1-2) x 10^{-1} Cm/m).

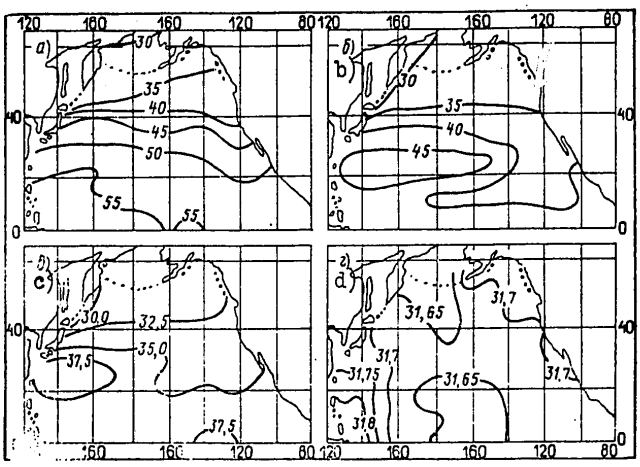

Figure 3. Distribution of Electrical Conductivity of Seawater (10^{-1} Cm/m) on Ocean Surface (a), at Depth 200 m (b), at Depth 500 m (c) and at Depth 4000 m (d) (Northern Part of Pacific Ocean, Mean Values for Year)

The average annual field of vertical gradients of specific conductivity on the studied water area differ in considerable heterogeneity, especially within the surface structural ocean zone. The greatest variability in electrical conductivity along the vertical is characteristic of the layer of water temperature jump. On the average the electrical conductivity gradients from (-1--2) x 10^{-3} Cm/m^2 in the surface 10-meter layer of the ocean increase in absolute amount in the layer 50-75 to (-6--7) x 10^{-3} Cm/m^2 in the western section of the subtropics, and reach the extremum values for the entire water area ((-14--16) x 10^{-3} Cm/m^2) in the region of the tropical cyclonic circulation as a consequence of the sharp thermal contrast produced here by the elevation in cold deep water. The farther from the ocean surface the field of vertical electrical conductivity gradients is smooth, acquiring the features of zonal distribution. In the layer between depths 100 and 500 m in the high latitudes a region is traced of positive gradients with extremum at depth 100-200 m (over 1 x 10^{-3} Cm/m^2) linked to an increase in electrical conductivity below the nucleus of the cold surface layer, characteristic for Arctic type water [2].

The most noticeable attenuation in the vertical gradients with depth is traced roughly up to the axis of intermediate water where it averages (-0.15--0.20) x 10^{-3} Cm/m^2). Below the axis of the deep electrical conductivity minimum the vertical gradients adopt positive values that are constant for the entire ocean (0.03-0.04) x 10^{-3} Cm/m, governed by a rise with depth in the hydrostatic pressure with practically unchanged temperature and water salinity at great depths.

In conclusion one can note that the electrical conductivity of seawater in situ, whose general ideas of spatial-temporal distribution and variability in the example of the northern Pacific Ocean we have attempted to give here, as an integral characteristic of the state of seawater can be employed in solving research problems linked to classification of water masses, isolation of frontal zones, regions of convergence and divergence, zones of upwellings, and so forth, and for applied purposes (electrometry, fishing, marine electric geophysical exploration, underwater communications and so forth). In particular, the knowledge by the developers of probes-electrical salinometers of the basic peculiarities of such an oceanographic field as electrical conductivity of seawater in situ will make it possible to increase quality, effectiveness and accuracy of the created instruments, and this means also the reliability of the observational findings.

BIBLIOGRAPHY

1. Golovanova, L. A. "Description of Set of Programs of Climatological and Statistical Processing of Deep-Water Data on a Computer, as Well as Their Storage in Archives," TRUDY VNIIGMI-MTSD, No 33, 1976.

2. Stepanov, V. N. "Mirovoy okean. Dinamika i svoystva vod" [World Ocean, Dynamics and Properties of Water], Moscow, Znaniye, 1974.

3. Filippov, D. M. "Algorithms of Climatological and Statistical Processing of Deep-Water Data on a Computer," TRUDY VNIIGMI-MTSD, No 33, 1976.

4. Filippov, D. M.; and Oleynikov, S. A. "Layer of Minimum Values of Electrical Conductivity in the World Ocean," DOKLADY AN SSSR, vol 242, No 2, 1978.

5. Khorn, R. "Morskaya khimiya (struktura vody i khimiya gidrosfery)" [Marine Chemistry (Structure of Water and Chemistry of Hydrosphere)], Moscow, Mir, 1972.

6. Aceerboni, E.; and Mosetti, F. "A Physical Relationship Among Salinity, Temperature and Electrical Conductivity of Seawater," BOLL. GEOFIS. TEOR. APPL., vol 9, No 34, 1967.

7. Bradshow, A. L.; and Schleicher, K. E. "The Effect of Pressure on the Electrical Conductance of Seawater," DEEP-SEA RES., vol 12, No 2, 1965.

8. Connors, D. N.; and Kester, D. R. "Effect of Major Ion Variations in the Marine Environment on the Specific Gravity-Conductivity, Chlorinity-Salinity Relationship," MARINE CHEMISTRY, vol 2, No 4, 1974.

9. Cox, R. A.; Culkin, F.; and Riley, J. P. "The Electrical Conductivity/Chlorinity Relationship in Natural Seawater," DEEP-SEA RES., vol 14, No 2, 1967.

10. Ribe, R. L.; and Howe, J. G. "An Empirical Equation Relating Seawater Salinity, Temperature, Pressure and Electrical Conductivity," MAR. TECHNOL. SOC. J., vol 9, No 9, 1975.

11. Thomas, B. D.; Thompson, T. G.; and Utterback, C. L. "The Electrical Conductivity of Seawater," JOURNAL DU CONSEIL PERMAN. INTERNAT. EXPLOR. MER., IX, No 1, 1934.

12. Weyl, P. "On the Change in Electrical Conductance of Seawater with Temperature," LIMNOL. OCEANOGR., vol 9, No 1, 1964.

UDC 551.326.7:626.01

ESTIMATE OF THE CALCULATED THICKNESS OF STRATIFIED ICE

Moscow METEOROLOGIYA I GIDROLOGIYA in Russian No 10, Oct 1979 pp 88-92

[Candidate of Technical Sciences V. P. Afanas'yev, Leningrad Institute of Railroad Transportation Engineers, submitted for publication 12 Feb 1979]

Abstract: It is noted that for structures on open sea areas of temperate latitudes in determining the magnitude of ice pressure one should adopt as the calculated the ice thickness with regard for stratifications. A brief description is given of the process of rafted sea ice formation. A technique is presented for approximate evaluation of the calculated thickness of rafted ice. The technique is designed for use in determining ice pressure on marine hydraulic engineering structures in the absence of systematic observational data.

[Text] In the active norms for determination of ice loads on the hydraulic engineering structures, SNiP II-57-75 [Construction Norms and Regulations] it is recommended that the initial data on the ice situation be adopted on the basis of full-scale observations. However often it is necessary to make computations, especially at the first stage of planning, without having a sufficient volume of materials of these observations. Such cases can occur not only in a short period of observations as compared to the required, but also with planning of structures on water areas where determination of the ice characteristics presents considerable difficulties, for example, on water areas where no ice-navigating ships pass and where the ice drift is the main sign of the dynamic state of the ice cover.

In the absence of full-scale observations to select certain ice characteristics (rate of ice drift, for example) the norms proposed that the recommendations given in them be used. For selection of the ice cover thickness such recommendations are usually missing in the norms. The data given in the hydrological references on the thickness of ice refer to ice thickness of natural (thermal) accumulation. Analogous information is presented by different organizations of the Hydrometeorological Service. Such information, however, in the majority of cases cannot be used for computing the marine hydraulic engineering structures. This is explained by the fact that the ice thickness

of natural accumulation can be adopted as the calculated in planning hydraulic engineering structures only on comparatively closed, limited water areas where the process of ice formation occurs under calm conditions. For structures located on open sections of the sea coast or far from the shores, ice fields must be used as the calculated form of ice formations which consist of stratified ice and hummocked piles. At the same time the thickness of the stratified ice can exceed the thickness of the ice of natural accumulation in the calculated period (as a rule by the end of winter) by almost double.

It should be recalled that the value of ice thickness plays an especial role in computing the magnitude of ice load. This is apparent from the calculated formula of SNiP II-57-75

$$P = mR_p bh, \qquad (1)$$

where P--load from moving ice field on structure with vertical anterior edge;
m--coefficient of support shape;
$R_p = kR_c$, where $k = f(b/h)$ is altered from 0.5 to 2.5;
b,h--width of structure and thickness of ice.

In fact, h affects the value of ice load not only directly, but also through the amount R_p. Thus, for example, with an increase in h 1.7-fold the value of P can rise (for the real width of single supports) already more than 2.0-fold. This is also shown by the graph in figure 1. It is evident that the magnitude of ice load on the structure depends to a considerable degree on the correct selection of the calculated value of ice thickness. And since the ice load is, as a rule, the greatest horizontal*, and consequently, determines the reliability and efficiency of the structure, an estimate of the calculated ice thickness is one of the most important questions of engineering ice technology.

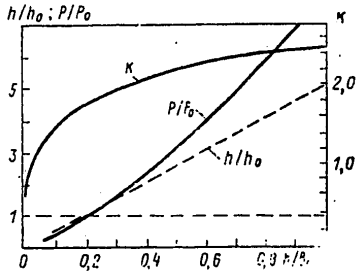

Figure 1. Dependence of Ice Load on Support on Change in Ice Thickness
Key:
P_0--pressure with h/b=0.2, h_0--thickness of ice equal to 0.2b

*As compared to others.

As is known, to estimate ice thickness of thermal origin a number of formulas have been proposed in which the ice thickness is defined mainly depending on the sum of cold with a more or less complete consideration for the hydrometeorological characteristics of the ice formation conditions, for certain regions correlation curves linking ice thickness with the sum of negative temperatures have also been proposed. As an example we will cite the known empirical formula of N. N. Zubov

$$h^2+50\,h=8\Sigma\Theta, \qquad (2)$$

where $\Sigma\Theta$--sum of degree-days of frost.

In order to determine the thickness of the stratified ice, initially formed mechanically from the shape of young ice, until recently there were no calculated relationships. This article examines a technique of approximate estimate of the thickness of this form of ice cover.

The observational data demonstrate that in the open sea one can rarely encounter an ice cover of natural accumulation in a pure form. Usually ice fields dominate that to a certain measure are subject to raftings and pilings [1, 3, 6]. The processes of stratifications during compression of ice prove from the very beginning of ice formation, and are especially pronounced for fields of young ice of thickness up to 10 cm, sometimes with considerable salinity and high temperature, also for ice with great thickness. With thickness over 15-20 cm the solid ice during compression begins to break up, fractionate and form piles. A general idea about the rafted ice formed during compression (shift) of ice in the open sea is given in table 1, compiled from data of full-scale observations taken from different sources and including from the author. It is apparent from table 1 that the number of layers in the stratified ice can reach 10 and with a thickness of the young ice 7-20 cm (thermal accumulation) sections can be formed of ice fields with general ice thickness of the order 70-80 cm, and even about 1 meter. After stratification the ice rapidly freezes together. Although interstratifications between the layers are less strong than the ice of the actual layers, nevertheless such a stratified ice is destroyed as the observations show as one integral without stratification.

One should evidently view the overall thickness of stratified ice as the thickness of ice that has been stratified in the beginning of the summer season plus the increase in ice as a result of further freezing. Based on this conclusion and using for the computation of thermal accumulation of ice the formula of N. N. Zubov given above in order to estimate the thickness of stratified ice in the calculated period one can suggest the following relationship [4]:

$$h_н^2+50h_н=8(\Sigma\Theta_0+\Sigma\Theta_н), \qquad (3)$$

where $h_н$--thickness of stratified ice cover at the end of the calculated period, cm;

$\Sigma\theta_0$--sum of degree-days of frost for the remaining time after stratification;
$\Sigma\theta_h$--sum of degree-days of frost corresponding to the accumulation of ice of thickness equal to the thickness of the initially stratified ice (it is a conditional amount)

TABLE 1

Sea, region	Year and Month of Observations	h--Thickness of Ice of Natural Accumulation, cm	$h_н$--Thickness of Ice of Stratification, cm	Quantity of Layers / Thickness, cm	Author
Gulf of Finland 24-27°e.l.	1898, IV	40-50	90	Several layers	S. O. Makarov [6]
Gulf of Finland	1923-1932 II-IV				
I region		30	82	The same	V. I. Arnol'd-Alyab'yev [1]
II region		50	90		"
III-IV regions		10	60		"
II region	1927, II		55-62	6-8 / 8-6	"
II region	1923, II	20	60	"	"
Gulf of Finland, middle and western sections			70-100	up to 10 / 7-15	V. I. Arnol'd-Alyab'yev [1]
The same, fairway	1962, III-IV	15-20	50-60	"	V. V. Betin [3]
Caspian Sea, northern section	1960, II	26	62	Several layers	L. V. Luk'yanova [5]
Gulf of Finland	1965, IV	30	75	4-5 / 15-17	V. P. Afanas'yev [2]
III region					
"	1966, III	15-20	60	4-5 / 12-15	"

Note: I region 29-23°e.l.; II region 23-26°e.l.; III-IV regions to the west of 26°e.l.

Figure 2 presents a graph that clearly demonstrates the proposed technique for determining the calculated thickness of stratified ice depending on the sum of degree-days of frost and the initial thickness of the rafted ice $h_н^0$. The moment of formation $h_н^0$ is assumed here at thickness of monolayer ice h=15-20 cm, which corresponds to the period with sum of frost $\Sigma\theta_1$, equal to 125-175 degree-days. Curves 1 and 2 are constructed according to formula (3) respectively for $h_н^0$=70 cm (corresponds to $\Sigma\theta_н$, approximately equal to 1110 degree-days) and $h_н^0$=90 cm ($\Sigma\theta_н$ corresponds to 1500 degree-days).* For comparison of the processes of growth in two different types of ice cover the graph gives curve 3 that is constructed according to formula (1) for thickness of an ice cover of natural accumulation (without consideration of the factor of an increase in ice thickness as a consequence of rafting). On the graph ice thickness values are plotted that are taken from table 1. The placement of the data on the graph was made with regard for the sum of degree-days of frost that meet the corresponding ice periods and the region of the sea. The values of ice thickness and natural formation are placed on curve 3, the maximum values of thickness of the stratified ice corresponding to them are placed more or less precisely on curve 1. With respect to the probable period of rafted ice formation we find on the continuation of curve 1 the initial thickness of the stratified ice cover. This amount equals 0.67-0.77 m. The remaining tabular values of stratified ice thickness lie on curve 4. They, in all probability, are not extremum for the given region of the sea and cannot serve as calculated amounts.

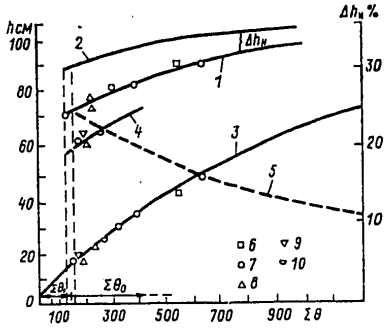

Figure 2. Graph of Growth in Sea Ice Thickness

Key:

1,2,4 Stratified ice

3. Ice of thermal accumulation (according to N. N. Zubov and V. V. Betin)

5. Curve of reduction in h

Observational data:

6. S. O. Makarov
7. V. I. Arnol'd-Alyab'yev
8. V. P. Afanas'yev
9. V. V. Betin
10. L. V. Luk'yanova

$\Sigma\theta$--sum of degree-days of frost from moment of ice formation

*On the x-axis only the actual sum of degree-days is plotted $\Sigma\theta=\Sigma\theta_1+\Sigma\theta_0$.

By examining the graph one can ascertain a satisfactory coincidence of the experimental points with theoretical curves. This indicates the applicability of the proposed method for estimating the thickness of stratified ice. Further, it is apparent from the graph that with an increase in the winter period the difference $\Delta h_н$ between curves 1 and 2 is gradually reduced. In the percentage expression (right y axis) this is demonstrated by curve 5. Thus, whereas in the initial period the difference reaches 25%, already within $\Sigma\theta_0$=900-1000 degree-days it is reduced to 10% (such a period of accumulation in the ice cover thickness corresponds to the hydrometeorological conditions of a number of seas in the Soviet Union). Consequently, the possible error obtained in assigning the initial thickness of the stratified layer $h_н^0$ in the beginning of the winter season gradually during winter towards the calculated period is also reduced. In order to increase the reliability of the planned structure, in our opinion, one should however, adopt for the computation the value $h_н$ on curve 2. As is apparent on curve 5, such an increase in the calculated thickness of ice corresponds to a degree of accuracy of determining other ice magnitudes and the requirements of SNiP II-57-75.

One should add that close results to those obtained in formula (3) can be obtained if instead of formula (2) for compilation of the calculated relationship in evaluating the stratified ice thickness one uses other empirical formulas, for example the Stefan formula

$$h = 3\sqrt{\Sigma\theta}. \qquad (4)$$

In this case the calculated formula will look as follows:

$$h_н = 3\sqrt{\Sigma\theta_0 + \Sigma\theta_н}, \qquad (5)$$

where $\Sigma\theta_0$ and $\Sigma\theta_н$ designate the same as in formula (3), however the numerical value $\Sigma\theta_н$ is assumed to be equal to 700 degree-days. Here the difference in the value of the stratified ice thickness in the calculated period as compared to that computed according to formula (3) is obtained in the limits of one-tenth of a centimeter.

One should also note that the use for the examined calculated formulas of more complex relationships to determine the thickness of the accumulated ice with regard for additional hydrometeorological factors is hardly expedient, since the initial data for them have fairly approximate values.

Thus, the thickness of stratified ice is one of the most important calculated characteristics in determining ice pressure on structures for regions of the open sea, for the formation of the ice cover is closely linked to dynamic processes. An estimate of the thickness of such ice can be made according to one of the empirical formulas for defining the thickness of accumulating ice depending on the sum of degree-days of frost with an increase in this sum by a number corresponding to the thickness of the initially stratified ice cover, approximately equal to 80-90 cm.

In order to pinpoint the values of the stratified ice thickness adopted in the computation in planning hydraulic engineering structures it is desirable

to continue observations by the organizations of the Hydrometeorological Service of formation and development of stratified ice with measurement of its thickness on a broader scale on different seas, not limited to regions of traditional observations.

BIBLIOGRAPHY

1. Arnol'd-Alyab'yev, V. I. "L'dy finskogo zaliva po dannym issledovaniy s sovetskikh ledokolov za period 1922-1932 gg" [Ice of the Gulf of Finland According to Research Data from Soviet Ice Breakers for the Period 1922-1932], Leningrad, 1933.

2. Afanas'yev, V. P. "Ledovyye nagruzki na vertikal'nyye opory morskikh sooruzheniy" [Ice Loads on Vertical Supports of Marine Structures], author's abstract of dissertation for defense of scientific degree candidate of technical sciences, Moscow, 1973.

3. Betin, V. V. "Computation of Main Components of Ice Cover of Baltic Sea," "Leningradskoy GMO" [Leningrad Hydrometeorological Observatory], No 2, Leningrad, 1963.

4. Zubov, N. N. "Morskiye vody i l'dy" [Seawater and Ice], Moscow-Leningrad, Gidrometeoizdat, 1938.

5. Luk'yanova, L. V. "L'dy Kaspiyskogo mory i ikh fiziko-mekhanicheskiye svoystva" [Ice of Caspian Sea and its Physical and Mechanical Properties], author's abstract of dissertation for defense of scientific degree of candidate of geographical sciences, Baku, 1964.

6. Makarov, S. O. "'Yermak' vo l'dakh" ["Yermak" in Ice], St. Petersburg, 1901.

UDC 556.535.6(571.6)

CERTAIN CHARACTERISTICS OF ICE COVER STRENGTH DURING ITS BREAK-UP ON RIVERS OF THE BAYKAL-AMUR TRUNK LINE ZONE

Moscow METEOROLOGIYA I GIDROLOGIYA in Russian No 10, Oct 1979 pp 93-101

[Article by Ye. F. Zabelina, USSR Hydrometeorological Scientific Research Center, submitted for publication 26 February 1979]

Abstract: Using S. N. Bulatov's calculation method probability characteristics are obtained for the thickness and strength of the ice cover by the time of break-up on rivers.

An analysis is made of calculated characteristics recommended by the Construction Norms and Regulations to estimate the dynamic loads on structures during the ice drift period.

The possibility is shown of simplified computation of strength characteristics of the ice cover, including for sections of the Baykal-Amur trunk line river zones not covered by hydrometeorological observations.

[Text] The active development of natural resources in the zone of construction of the Baykal-Amur railroad trunk line (BAM), refinement of the projects for BAM construction, planning of the industrial, general and other structures associated with it, organization of construction work, transportation operations, operation of the hydraulic engineering structures and so forth advance a number of problems in studying the ice cover of rivers, one of which is determination of the thickness and strength of ice.

In all the ice engineering computations, including in the computation of ice loads on hydraulic engineering structures, the most complex, to a considerable measure conventional, is the selection of the magnitude of ice strength limits, especially in relation to the rapid change in mechanical properties of the ice cover in the melting period. Of greatest importance are the strength characteristics of the spring ice in the period of shift and ice drift, i.e., in that period when dynamic effect of the ice on the structures occurs.

By now fairly extensive material has been accumulated on the strength of spring ice under full-scale conditions. However there are no published data of experimental determinations of ice strength on rivers in the BAM zone, with the exception of results of tests on the Amur River at Komsomol'ska-Na-Amur made by V. M. Timchenko [10].

It is necessary to note that field tests of ice cover strength in the majority of cases end several days before they start to shift, which results in an exaggeration of the strength values for the ice drift periods, and consequently, a surplus increase in the supplies of strength of the structures and construction outlays.

The SNIP II-57-75 [Construction Norms and Regulations] that has been active since 1 January 1976 recommends the use of the tensile strength of ice for compression depending on the mean air temperature during the previous ice drift of 3-6 days and ice salinity (see table 27 SNIP).

N. K. Korzhavin [6], considering that the data of table 27 of SNIP do not take into consideration in a proper manner the entire set of factors, and primarily, the length of the preparatory period before break-up, proposes for rivers in the zone of BAM development to adopt for the initial stages of ice drift (first shifts) an increased tensile strength of ice for compression, equal to 75 T/m^2, which corresponds to the mean air temperature (according to table 27 of SNIP) equal to -3°C, and for the highest levels of ice drift--45 T/m^2. The tensile strength for bending $R_и$ is assumed to be equal to 3/4 of the magnitude of tensile strength for compression R_c.

The current state of research makes it possible to make an indirect estimate of the strength characteristics of the ice cover according to the factors that determine them in the period of melting. The method developed in the USSR Hydrometeorological Center by S. N. Bulatov [1, 2] makes it possible to compute the thickness and strength of melting ice for each day, starting from the date of removal of snow from it to the moment of complete loss of strength. The calculated formula here looks like

$$\varphi = (1 - \sqrt{S/S_0})^2, \qquad (1)$$

where φ--relative breaking point of melting ice for bending;
S--quantity of solar radiation absorbed by ice, determining the content in ice of its liquid phase;
S_0--quantity of solar radiation during whose absorption the ice completely loses strength. The quantity S_0 depends on the ice structure. In the calculations S_0 is assumed to be constant, equal to 44 cal/cm^3. Determination of the S values is made by computing according to meteorological elements for the period of melting the fractions of solar radiation absorbed by the ice cover layers and the averaging of these fractions with respect to ice thickness. The ice thickness is computed in parallel with computation of the amount S. The accuracy of the computation is fairly high [11]. In particular, this was confirmed for the examined region by 78 tests made on the Amur River of ice overhangs for bending [10, 11].

Since the S. N. Bulatov method in mass calculation becomes very awkward, a program was developed and checked-out on the Fortran language for the

computer BESM-6. The initial information here is the data on temperature and air humidity, wind velocity and the relative cloud cover according to observations on the closest meteorological station to the assigned section of the river, the thickness of the ice cover and the height of the snow cover on the ice before the start of melting, as well as the latitude of the locality. The strength characteristics φ and thickness of ice h were computed for the period from 1950 to 1975 for certain sections of the river located both in the eastern and in the western part of the BAM route. The selection of these sections was defined, first, by the presence of a meteorological station near the water-measuring post, second, we strived so that these stations would reflect the conditions of different rivers in the zone. Thus, for example, the areas of the basins of the examined rivers changes from 2410 km^2 (Byssa River) to 1.720 million km^2 (Amur River). The maximum ice thickness for winter fluctuates in limits from 0.87 m (Byssa-River--Byssa point) to 1.82 m (Olekma River--Ust'-Nyukzha point).

Figure 1 presents the course of change in the mean values of ice strength and its thickness (in relative units) for the period of melting. It is apparent on the figure that after the removal of snow the ice thickness is reduced slowly, while its strength under the influence of the absorbed solar radiation drops quickly. Thus, in the first 10-12 days after removal of snow the ice cover above and below almost did not melt, but in its mass intensive formation of liquid phase occurs, which governs a decrease in the relative ice strength to 0.3-0.5 of the initial amount.

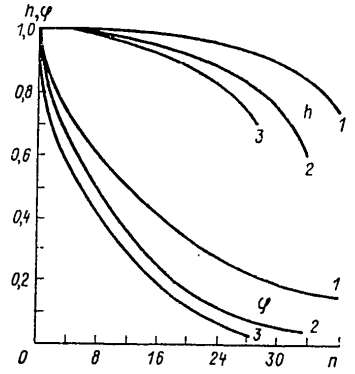

Figure 1. Course of Reduction in Averaged Computed Values of Thickness h and Strength of Ice Cover φ for Period of Melting in Relative Units; (n--days of ice melting after removal of snow).

Key:
1. Olekma River--Ust'-Nyukzha point
2. Selemdzha River--Stoyba station
3. Byssa River--Byssa point

Publications [6, 9] examine the strength characteristics of spring ice depending on the duration of the preparatory period by which is understood the

difference in the dates of break-up of the river and transition of the mean air temperature through 0°C in the given point. Such an approach to an estimate of ice cover strength is someqhat conditional and for the examined region is not indicative. The main decisive reason for reducing the ice strength during melting is absorption by the ice of solar radiation. On the examined rivers the intensity of solar radiation influx in the summer period is great, while the low snow cover is destroyed long before the transition of the mean diurnal air temperature through 0°C. The melting period of the ice cover is 1.5-2-fold greater than the duration of the preparatory period, determined according to the transition of temperature through 0°C, consequently, the degree of reduction in spring ice strength is considerably greater.

In the formula (1) given above $\varphi=R/R_0$, then

$$R = R_0(1 - \sqrt{S/S_0})^2, \qquad (2)$$

where R--ultimate strength of melting ice during bending, i.e., one of the parameters recommended by SNIP for computations of the load of the ice effect on hydraulic engineering structures;

R_0--ultimate strength for bending for ice not subject to the effect of solar radiation and having temperature of 0°C.

V. A. Koren'kov [5] from data of his own observations, as well as the observations of I. P. Butyagin, V. M. Sokol'nikov et al. gives the value of ultimate strength of ice for bending in the pre-ice drift period as $R_0=55$ T/m^2. S. N. Bulatov [1], considering that these data are exaggerated by 5-10% as a consequence of the lack of consideration for the scale effect suggests that the mean value of ice ultimate strength be adopted as 50 T/m^2. V. M. Timchenko [10] as a result of the experimental studies of physical and mechanical properties of melting ice cover on the Amur River at Komsomol'ska-na-Maur obtained $R_0=70$ T/m^2.

To analyze the calculated characteristics recommended by SNIP in estimating the dynamic load on structures in the ice drift period a computation was made of the ultimate strength of ice for bending and the thickness of the ice cover by the moment of drift of rivers intercepted by the BAM route. The strength during shift was viewed as the greatest in break-up. The computation was made in each case for nine points. A total of 220 cases were computed.

Guarantee of the current level of planning requires information of the probability characteristics of the ice cover strength. SNIP does not contain any information about the frequency of the proposed calculated values of ice strength.

In order to obtain the probability characteristics for ice ultimate strength for bending the moment of shift curves of frequency were constructed whose coordinates are given in table 1. In the numerator values are shown of the ice ultimate strength determined with $R_0=50$ T/m^2, and in the denominator--with $R_0=70$ T/m^2. The data of table 1 indicate that the computed values of ice strength not only are average, but also with probability of excess 1%,

in other words, with frequency one in 100 years are considerably lower than those that are recommended by the active SNIP to estimate the loads and effect of ice on structures at the moment of break-up. Thus, for example, the ultimate strength of ice for bending $R_{и}$, according to SNIP must be assumed to be equal to 33 T/m^2. K. N. Korzhavin [6] for rivers intersected by the BAM route suggests for the starting states of ice drift the value $R_{и}=56$ T/m^2. According to the data of our computation on the studied rivers the ice of such strength cannot be encountered once in 100 years.

TABLE 1 - PROBABILITY CHARACTERISTIC OF ULTIMATE STRENGTH OF ICE (T/m^2) AT MOMENT OF SHIFT

(1) Река	(2) Пункт	(3) Предел прочности льда в момент подвижки обеспеченностью (%)									
		1	2	10	25	50	75	90	95	98	99
(4) Киренга (12)	Казачинское	9,2 / 12,0	8,0 / 10,0	4.4 / 5,6	2,8 / 3,6	1,6 / 2,4	0,8 / 1,2	0,2 / 0,4	—	—	—
(5) Олекма (13)	Усть-Нюкжа	14,8 / 20,4	14,0 / 19,6	12,0 / 16,8	10,2 / 14,4	8,0 / 11,6	5,6 / 8,4	3,6 / 5,2	2,2 / 2,8	1,0 / 1,2	0,8 / 0,9
(6) Зея (14)	Бомнак *	10,5 / 14,7	9,0 / 12,6	7,3 / 10,2	4,0 / 5,6	2,6 / 3,6	1,4 / 2,0	0,8 / 1,1	0,7 / 1,0	0,6 / 0,8	0,5 / 0,7
(7) Нора (15)	Устье Эльги	12,8 / 17,6	11,2 / 16,0	7,4 / 11,2	4,8 / 7,6	3,2 / 4,8	2,0 / 2,8	1,0 / 1,4	0,8 / 0,4	0,3 / 0,4	0,3 / 0,4
(8) Селемджа	Стойба (16)	18,6 / 23,6	16,4 / 21,6	12,0 / 15,6	8,0 / 11,0	4,4 / 6,0	2,3 / 3,2	0,9 / 1,6	0,4 / 1.0	0,3 / 0,5	0,3 / 0,4
(9) Быcса	Быcса (17)	12,2 / 15,4	10,8 / 14,0	6,8 / 10,0	4,0 / 7,0	1,8 / 2,4	0,4 / 0,7	0,1 / 0,2	—	--	—
(10) Амгунь	Ирумка (18)	12,0 / 16,8	11,2 / 15,4	8,7 / 12,0	6,6 / 9,2	4,4 / 6,0	2,2 / 3,0	1,0 / 1,4	0,4 / 0,8	0,2 / 0,5	0,2 / 0,4
(11) Амгунь	Дуки * (19)	9,5 / 12,6	8,2 / 11,5	5,6 / 7,8	3,6 / 5,0	1,8 / 2,5	0,8 / 1,1	0,3 / 0,4	0,1 / 0,2	—	—

Key:
1. River
2. Point
3. Ultimate strength of ice at moment of shift with frequency (%)
4. Kirenga
5. Olekma
6. Zeya
7. Nora
8. Selemdzha
9. Byssa
10. Amgun'
11. Amgun'
12. Kazachinskoye
13. Ust'-Nyukzha
14. Bomnak
15. Ust'ye El'gi
16. Stoyba
17. Byssa
18. Irumka
19. Duki

*The values of ultimate strength of ice bending were determined according to the data of computation of relative ice cover strength given in publication [9].

The reason for the exaggeration in the calculated strength of ice is the fact that table 27 of SNIP does not take into consideration change in the ultimate strength of ice under the influence of positive air temperatures and the radiation influx of heat. As was shown above, on the examined sections of the rivers break-up was preceded by a period with air temperature above 0°C and a lengthy period of decrease in ice strength under the influence of solar radiation.

In order to estimate the dynamic loads from the effect of ice on structures it is necessary to have information not only about the strength of the ice cover, but also its thickness by the moment of break-up. SNIP recommends assuming the calculated ice thickness to be equal to 0.8 of the maximum ice thickness for the winter period, with frequency of 1%. In order to verify the correctness of these recommendations in the examined region curves of frequency were constructed for ice thickness at the moment of shift. The data of table 2 indicate that the obtained amounts, with probability of excess 1%, correspond to the calculated values of ice thickness determined according to SNIP.

TABLE 2 - PROBABILITY CHARACTERISTICS OF ICE COVER THICKNESS (m) AT MOMENT OF SHIFT

(1) Река	(2) Пункт	(3) Число лет наблюдений	(4) Максимальная толщина льда обеспеченностью 1%	(5) Толщина ледяного покрова в момент подвижки обеспеченностью (%)									
				1	2	10	25	50	75	90	95	98	99
(6) Киренга	12 Казачинское	18	0,96	0,72	0,69	0,60	0,50	0,25	0,19	0,08	0,04	—	—
(7) Олекма	13 Усть-Нюкжа	26	3,20	2,60	2,48	2,12	1,80	1,52	1,24	1,00	0,84	0,66	0,56
(8) Нора	14 Устье Эльги	25	1,64	1,36	1,30	1,08	0,98	0,80	0,62	0,50	0,44	0,36	0,32
(9) Селемджа	Стойба 15	26	2,55	2,08	1,92	1,42	1,12	0,88	0,66	0,44	0,34	0,24	0,20
(10) Быссa	Быссa 16	26	1,60	1,24	1,12	0,90	0,72	0,56	0,42	0,29	0,23	0,19	0,18
(11) Амгунь	Ирумка 17	25	1,88	1,46	1,40	1,23	1,10	0,92	0,68	0,45	0,32	0,16	—

Key:
1. River
2. Point
3. Number of years of observations
4. Maximum thickness of ice with frequency 1%
5. Thickness of ice cover at moment of shift with frequency (%)
6. Kirenga
7. Olekma
8. Nora
9. Selemdzha
10. Byssa
11. Angun'
12. Kazachinskoye
13. Ust'-Nyukzha
14. Ust'ye El'gi
15. Stoyba
16. Byssa
17. Irumka

It is necessary to note that currently probability characteristics have been obtained for the maximum ice thickness for rivers in the development zone of the BAM route [4], consequently, determination of the calculated characteristics of ice cover thickness by the moment of break-up do not produce any difficulties in solving a different type of planning task.

The calculated relationships recommended by SNIP for estimating the load and effect of ice on structures includes complex characteristics of strength that are a product of the ultimate strength of ice and its thickness to certain degrees. In order to obtain the probability characteristics for the date of shift for each year the amounts of the complexes of strength of the type $R_ч h^2$, $R_c^{1/2} h$, $R_c h$ were computed. To guarantee the necessary margin of safety we started from the greatest measured value for the initial ice strength, assuming $R_0 = 70 T/m^2$. According to these data curves of frequency were constructed whose coordinates are given in table 3. Analysis of the findings demonstrates that the amounts for the complexes of strength determined according to the SNIP recommendations are two times and more greater than the computed values of the complexes, with probability of excess 1%.

The approximate extrapolation of curves for frequency 0.33% (frequency of once in 300 years) demonstrates that in the given case the obtained amounts for the complexes of strength are 1.5-fold and more lower than the complexes determined according to SNIP. Therefore it is expedient in planning to take into consideration the amounts of the ultimate strength computed with regard for its spring reduction for frequency once in 100 years (frequency 1%). The adoption here for all rivers in the BAM zone of any one constant amount is not rational, since $R_ч$ with frequency 1% changes from point to point to considerable limits (see table 1).

At the same time fulfillment of such computations for ice strength with the help of a computer under real conditions of planning is difficult due to the excessive labor intensity of collecting such meteorological data for a fairly long series of years. In addition often the need arises for computing the ice cover strength of sections of river that are generally not covered by hydrometeorological observations. In such circumstances another approach can be recommended: direct computation of the parameters for the curves of frequency of ice strength by the moment of break-up, and precisely--the mean amount of strength of ice $\overline{R}_ч$, its mean quadratic deviation from the norm σ and coefficient of asymmetry C_s.

We will begin with computation of the ice strength norm.

The main factors that determine ice cover strength by the moment of break-up are the maximum ice thickness and intensity of the influx of solar radiation in the spring period. Since the BAM route is extended along a latitude in limits 51-57°n.l. one can consider that the difference in the average multiple-year influx of solar radiation is not great, and the effect of this factor over the territory is equivalent.

Analysis of the maximum ice thickness on the rivers of the BAM zone demonstrated that on a majority of rivers it is in the average multiple-year

TABLE 3 - PROBABILITY CHARACTERISTICS OF COMPLEXES OF STRENGTH AT MOMENT OF SHIFT

(1) Река	(2) Пункт	(3) Число лет наблюдений	(4) Комплексы прочности	(5) Величины комплексов прочности, определенных по СНИП	(6) Комплексы прочности		
					1	2	10
(7) Киренга	Казачинское (13)	18	$R_c h$	34,6	9,8	8,9	5,6
			$R_ж h^2$	19,9	4,0	3,4	2,0
			$\frac{1}{R_c^2} h$	5,2	1,0	0,9	0,6
(8) Олекма	Усть-Нюкжа (14)	26	$R_c h$	115,2	65,3	57,8	42,0
			$R_ж h^2$	220,8	120,0	108,0	68,0
			$\frac{1}{R_c^2} h$	17,2	4,5	4,1	3,0
(9) Нора	Устье Эльги (15)	25	$R_c h$	58,9	26,1	23,1	14,9
			$R_ж h^2$	57,8	21,0	18,2	11,2
			$\frac{1}{R_c^2} h$	8,8	1,9	1,7	1,2
(10) Селемджа	Стойба (16)	26	$R_c h$	91,8	59,7	50,9	28,9
			$R_ж h^2$	140,2	80,0	68,0	34,0
			$\frac{1}{R_c^2} h$	13,5	2,6	2,4	1,8
(11) Быcса	Быcса (17)	26	$R_c h$	57,6	21,5	18,7	9,7
			$R_ж h^2$	55,2	16,0	13,0	6,4
			$\frac{1}{R_c^2} h$	8,6	1,8	1,6	1,0
(12) Амгунь	Ирумка (18)	25	$R_c h$	67,5	28,0	24,6	17,1
			$R_ж h^2$	75,8	29,0	25,0	15,0
			$\frac{1}{R_c^2} h$	10,0	2,0	1,8	1,4

Key:
1. River
2. Point
3. Number of years of observations
4. Complexes of strength
5. Amounts of complexes of strength determined according to SNIP
6. Complexes of strength at moment of shift with frequency (%)
7. Kirenga
8. Olekma
9. Nora
10. Selemdzha
11. Byssa
12. Amgun'
13. Kazachinskoye
14. Ust'-Nyukzha
15. Ust'ye El'gi
16. Stoyba
17. Byssa
18. Irumka

[Continuation of table 3]

в момент подвижки обеспеченностью (%) (6--continuation)						
25	50	75	90	95	98	99
3,3 1,2	1,1 0,3	0,4 0,05	0,09 0,04	0,05 0,03	— —	— —
0,3	0,1	0,04	0,02	0,01	—	—
32,6 46,0	23,3 28,0	14,9 15,0	7,6 7,0	3,2 2,5	0,7 0,5	0,4 0,4
2,4	1,8	1,2	0,7	0,4	0,2	0,08
8,9 7,2	4,8 3,6	2,2 1,2	1,1 0,5	0,7 0,4	0,3 0,3	0,2 0,2
0,9	0,6	0,4	0,2	0,1	0,08	0,04
16,8 14,0	7,5 5,0	2,8 2,0	0,9 0,8	0,7 0,6	0,6 0,5	0,5 0,4
1,2	0,8	0,4	0,2	0,1	0,08	0,07
6,8 3,0	2,0 1,0	0,4 0,4	0,1 0,1	— —	— —	— —
0,6	0,2	0,06	0,02	—	—	—
14,0 11,0	8,6 6,5	2,9 2,0	0,9 0,8	0,6 0,4	0,5 0,3	0,4 0,2
1,2	0,8	0,4	0,2	0,08	0,04	0,03

period 1.2-1.4 m, and on certain sections of the rivers in the basins Olekma and Aldan 1.6-1.9 m. A greater ice thickness occurs only on the small freezing rivers at area of the basin up to 600 km^2, however on such rivers, as a rule, with start of water run-off the ice travels upwards, gradually washing the channel, and the ice effects on the structures are insignificant.

The dependence of the ice cover strength norm at the moment of start of shifts ($\overline{R_н}$) on the norm of maximum ice thickness ($\overline{h}$) is expressed by the equation

$$\overline{R_н} = 6.57\overline{h} - 3.94$$

Two other parameters of distribution of ice strength as the calculations showed are altered on the rivers of the BAM zone in comparatively small limits. Therefore one can adopt the amount of the mean quadratic deviation from the norm σ=2.8 T/m^2, and the coefficients of asymmetry C_s=1.20.

The obtained parameters make it possible to compute the amount of ice ultimate strength of bending by the moment of break-up of any frequency, by using the tables of normed amounts of ordinates for the assigned frequency (Foster-Rybkin tables). The ordinates taken from the tables for the adopted C_s and frequency P are multiplied by the assumed amount σ. The obtained deviation from the norm is added to the mean strength of ice $R_н$ computed according to equation (3).

The errors in constructing the frequency curve of ice cover strength are determined for the amounts that exceed the norm (table 4).

TABLE 4 - PROBABILITY ERRORS DETERMINED FOR $R_н$ WITH DIFFERENT FREQUENCY

	(a) Обеспеченность, %				
	1	3	5	10	25
δ T/м^2	1,6	1,3	1,2	1,2	0,7
$\delta_{отн}$	0,05	0,04	0,04	0,04	0,02

Key:
a. Frequency, %

The overall accuracy of the computations is characterized by a probable error 1.1 T/m^2.

Table 4 traces the increase in error with a reduction in frequency. Therefore an analysis was attempted which revealed the link between the deviations in ice strength from the calculated amount with the norm of the maximum height of snow. This is explained by the following reasons. The first, the greater the amount of snow-supplies in the basin, the higher the rise in the level in the period of break-up and the more considerable the mechanical strength of the effect of the flow on the ice cover. From here, with a high snow cover one can expect a higher strength of the broken ice. Second, the greater height of snow on the ice corresponds to the greater height of snow on the basin. Therefore with a great height of snow the period of effect on ice of solar radiation will be lower, and consequently, the strength of the spring ice by the moment of break-up is greater.

The effect of snow on the strength of the ice cover, naturally, is more significant in the extremum years, and therefore is traced for cases of 1% frequency. For consideration of this effect the empirical formula is suggested

$$\Delta R_н = 25\bar{h}_c - 10, \qquad (4)$$

where $\Delta R_{и}$--error for effect of snow,
$\bar{h}_c$--norm of maximum snow height.

With regard for the correction the accuracy of computation $R_{и1\%}$ is increased and is characterized by the probable error 1.1 T/m^2. The formula is constructed with such regard that a possible underestimation of the ice cover strength is the minimum.

For the most simplified evaluation of ice strength by the moment of break-up the empirical formula can be used

$$R_{и\,1\%} = 12\bar{h}_л + 35\bar{h}_c - 16{,}4, \qquad (5)$$

where $R_{и1\%}$--ultimate strength of ice for bending with frequency 1%,
$\bar{h}_л$ --norm of maximum ice thickness,
$\bar{h}_c$ --norm of maximum snow height.

The accuracy of computations according to the given formula is characterized by probable error 1.5 T/m^2. If one even assumes an error with frequency 1% and computes the ice cover strength by the moment of break-up for the greatest norm of maximum ice thickness in the BAM zone 1.9 m, we obtain $R_{и1\%}$=23 T/m^2. As is apparent, even this amount is significantly lower than that recommended by SNIP.

In fulfilling computation in the case of the absence of observations the norm of maximum ice thickness $\bar{h}_л$ and the norm of maximum snow height $\bar{h}_c$ can be determined according to charts [4, 7].

The aforementioned makes it possible to draw the following conclusions:
1. A reduction in the strength of the ice cover before break-up on the examined rivers is very significant. This is characteristic for rivers of the given region and is linked to the insignificant height of the snow cover on the ice and the intensive influx of solar radiation in the spring period.

2. The computation of complexes characterizing the ice strength during break-up demonstrates that in all cases, even with frequency of once in 100 years and once in 300 years adopted in the calculations as the limit, these complexes are 1.5-2-fold lower than those adopted in the active SNIP.

3. The calculations made permit obtaining of probability characteristics for the ice cover strength by the moment of break-up, including for sections of rivers not covered by hydrometeorological observations.

BIBLIOGRAPHY

1. Bulatov, S. N. "Computation of strength of Melting Ice Cover and Start of Wind Drift of Ice," TRUDY GIDROMETSENTRA SSSR, No 74, 1970.

2. Bulatov, S. N. "Metodyka rascheta tolshchiny i prochnosti tayushchego ledyanogo pokrova dlya tseley rascheta i prognoza srokov vskrypiya rek i vokhranilishch: Metodicheskiye ukazaniya" [Technique for Computing

Thickness and Strength of Melting Ice Cover for Purposes of Calculating and Predicting the Periods of Break-up of Rivers and Reservoirs: Method Instructions], Moscow, Gidrometteentr, USSR, 1974.

3. Butyagin, I. P. "Prochnost' l'da i ledyanogo pokrova" [Strength of Ice and Ice Cover], Novosibirsk, Nauka, 1966.

4. Ginzburg, B. M. et al. "Osnovnyye kharakteristiki ledovogo rezhima rek rayona Baykalo-Amurskoy magistrali" [Basic Characteristics of Ice Pattern of Rivers in the Baykal-Amur Trunk Line Region], Moscow, Gidrometteentr USSR, 1976.

5. Koren'kov, V. A. "Reduction in Ice Strength in Spring Period," "Sbornik dokladov po gidrotekhnike" [Collection of Reports on Hydraulic Engineering], No 8, 1967, Leningrad, Energiya.

6. Korzhavin, K. N. "Effect of Ice on Bridge Supports on BAM Route," TRUDY NIIZHT, No 181, 1977.

7. Pupkov, V. N. "Formation, Distribution and Variability in Snow Cover on Asian Territory of USSR," METEOROLOGIYA I GIDROLOGIYA, No 8, 1964.

8. SNIP II-57-75. "Nagruzki i vozdeystviya na gidrotekhnicheskiye sooruzheniya (volnovyye, ledovyye i ot sudov)" [Construction Norms and Regulations II-57-75. Loads and Effects on Hydraulic Engineering Structures (Wave, Ice and From Ships)], Moscow, Stroyizdat, 1976.

9. Samochkin, V. M. "Zoning of Major Siberian Rivers According to Nature of Spring Ice Drift," TRUDY NIIZHT, No 94, 1969.

10. Timchenko, V. M.; and Shilina, L. I. "Properties of Ice Cover on Rivers of Eastern BAM Zone in Spring Period," TRUDY DVNIGMI, No 69, 1977.

11. Timchenko, V. M. "Experimental Studies of Melting of Ice Cover of Amur River," TRUDY DVNIGMI, No 52, 1975.

UDC 551.509:631.811.1

USE OF METEOROLOGICAL FORECASTS IN DIFFERENTIATING NITROGEN SUPPLEMENTS

Moscow METEOROLOGIYA I GIDROLOGIYA in Russian No 10, Oct 1979 pp 102-110

[Article by Candidate of Technical Sciences Ye. Ye. Zhukovskiy, and Professor A. P. Fedoseyev, Agrophysical Institute, All-union Scientific Research Institute of Agricultural Meteorology, submitted for publication 3 Apr 1979]

Abstract: The question is examined of agrometeorological substantiation for economically optimal periods of conducting nitrogen supplementary feedings. A technique is described that makes it possible to formulate requirements for the justifiability of the seasonal forecast of precipitation used for the annual differentiation of agricultural engineering decisions in accordance with the expected agrometeorological conditions. With the help of the proposed technique for a number of regions of the Nonchernozem zone the effectiveness of different economic strategies is evaluated.

[Text] The accumulated experimental data and available production experience indicate that in the general complex of agricultural-engineering measures directed towards obtaining high yields of grain crops, an important place is occupied by a scientifically substantiated system of fertilizing that takes into consideration both the soil-climate conditions of the examined region of farming, and the specific agrometeorological peculiarities of each specific year [6, 9-12]. In this sense not only the main fertilizings, but also the nitrogen supplementary feedings made in different periods have serious importance.

From an organizational viewpoint the fall supplementary feedings of winter crops with nitrogen have indisputable advantages, since they facilitate mechanization, permit significant reduction in the intensity of the spring field work, and so forth. In addition, in conducting supplementary feedings in fall their action is manifest from the very early spring, immediately after the beginning of vegetation, as a consequence of which the danger of lodging of the plantings is reduced. However the nitrogen fertilizers, in falling in late fall on the surface of the soil or on the snow cover, under certain

conditions of weather can be removed by the melting-snow water or blown away by the wind together with the loose snow. Therefore in individual unfavorable years effectiveness of fall supplementary feeding is significantly lower than the effectiveness of spring introduction of fertilizers. As shown by analysis here a decisive role is played by precipitation that falls in the winter period. With a relatively small quantity of it the effectiveness of the fall supplementary feeding is increased, and with a large quantity--on the contrary, is reduced. Thus, one should attempt to switch to the use of differentiated agricultural engineering and guarantee a change in the periods of conducting supplementary feedings depending on the peculiarities of each specific year [12].

It is evident that to solve the set task, in the first place, long-term (seasonal) forecast of precipitation is required. However, as has been indicated in a more general term many times, this one condition is insufficient: it is necessary in addition, for the success of forecasts to exceed a certain minimum permissible level [2, 4, 8]. Otherwise instead of differentiation of the economic solutions according to the expected (predictable) weather conditions it is more advantageous to adhere to the so-called climatologically optimal strategy [3, 4]. The latter in the given case will consist of conducting supplementary feedings either always in spring, or always in fall (depending on the specific condition of a certain region of farming).

Taking the aforementioned into account, we will describe a certain technique that makes it possible to formulate requirements for the success of the corresponding seasonal predictions, and by using it we will make a number of numerical estimates that indicate where and in what cases the transition to differentiation of supplementary feeding is actually expedient, and where it is not. The calculated scheme stated in the work of Ye. Ye. Zhukovskiy [5] was placed as the basis of this technique.

Model for Making Optimal Solutions With the Use of Alternative Forecasts

We will designate by θ_{ij} expressed in monetary or natural units of measurement the profit from supplementary feeding d_j ($j=1,2$) under conditions where winter refers to type Fi($i=1,2$). For definiteness we will stipulate further that F1 be considered winter with normal or insufficient quantity of precipitation (according to the terminology adopted below "dry" winter), while F_2--winter with excess quantity of precipitation ("moist" winter), d_1 fall supplementary feeding, and d_2--spring supplementary feeding. In accordance with such designation the amounts θ_{11} and θ_{12} will characterize the profit from fall and spring supplementary feeding in the year with dry winter, while θ_{21} and θ_{22}--the profit from the same supplementary feedings in moist years. The matrix of utility that responds to the examined alternative model for decision making can be described in the form of a square (2 x 2) in table 1.

It is evident that the amounts θ_{ij} will depend on increases in the harvest which are obtained as a consequence of introducing fertilizers, the outlay for conducting supplementary feeding and the cost of one centner of finished product. In the first approximation they can be computed according to the formulas

$$\left.\begin{aligned}\theta_{11}&=gy_{11}-a+b,\quad \theta_{12}=gy_{12}-a,\\ \theta_{21}&=gy_{21}-a+b,\quad \theta_{22}=gy_{22}-a\end{aligned}\right\}. \qquad (1)$$

Here y_{ij} $(i,j=1,2)$--increase in harvest from introduction of supplementary feeding d_j under conditions of winter F_i;
g--cost of one centner of increase in grain with subtraction of additional outlays for its harvesting, transport and drying;
a--outlays for spring supplementary feeding;
b--"organizational"economic effect obtained as a result of transition from spring supplementary feeding to fall.

TABLE 1 - OVERALL VIEW OF MATRIX OF UTILITY 2 x 2

F	d	
	d_1	d_2
F_1	θ_{11}	θ_{12}
F_2	θ_{21}	θ_{22}

TABLE 2 - MATRIX OF CONTINGENCY FOR ALTERNATIVE FORECASTS

F	Π		Σ
	Π_1	Π_2	
F_1	p_{11}	p_{12}	p_{10}
F_2	p_{21}	p_{22}	p_{20}
Σ	p_{01}	p_{02}	1

Further we will examine only the case where between elements θ_{ij} the following correlations occur

$$\theta_{11} > \theta_{12},\ \theta_{22} > \theta_{21}, \qquad (2)$$

i.e., in the years with dry winter fall supplementary feedings economically more advantageous, and in the years with moist winter--spring.

We will further assume that the consumer has at his disposal a categoric alternative forecast of precipitation which is characterized by a matrix of contingency $\|p_{ij}\|$, assigned in the form of table 2. The elements included in it $p_{ij}(i,j=1,2)$ are combined probabilities of the forecasted (Π_j) and the actually realized (F_i) weather conditions; p_{10} and p_{20}--climatological probabilities of dry and moist winters; p_{01} and p_{02}--probabilities of corresponding formulations of forecast. It is natural to consider that the examined forecast in a method relationship is substantiated, and consequently, the inequalities occur

$$\left.\begin{aligned} p_{1|1} = p_{11}/p_{01} > p_{10}, \\ p_{2|2} = p_{22}/p_{02} > p_{20} \end{aligned}\right\}. \qquad (3)$$

Here $p_1/_1$ and $p_2/_2$--probabilities of realization of those weather conditions which were expected from the meteorological forecast (probabilities of correct predictions).*

Further adhering to the Bayes' approach we will consider that the optimum are such economic solutions which result in the obtaining of the maximum average gain [1, 4]. From this viewpoint, with assumptions (3) three strategies are important:

F_1--constant (regardless of the forecasting recommendations) conducting of nitrogen supplementary feedings in the fall;

S_2--constant conducting of supplementary feedings in the spring;

S_f--differentiated agricultural engineering that provides for the establishment of different periods for introducing fertilizers depending on the predictable winter conditions, and precisely: with expected dry winter fall supplementary feeding is conducted, and with moist--spring. There is no sense in examining the strategy of action that goes against the forecast consisting of conducting spring supplementary feeding with an expected dry winter and fall supplementary feeding with a moist winter, since in the fulfillment of conditions (3) this strategy will be inevitably worse than S_1 or S_2.

The following amounts of the mean gain G meet the listed variants for making economic decisions:

$$G_1=\Theta_{11}p_{10}+\Theta_{21}p_{20}, \tag{4}$$

$$G_2=\Theta_{12}p_{10}+\Theta_{22}p_{20}, \tag{5}$$

$$G_f=\sum_{i=1}^{2}\sum_{j=1}^{2}\Theta_{ij}p_{ij}. \tag{6}$$

By comparing these expressions with each other it is easy to show that the differentiated strategy S_f provides better (from the viewpoint of the mean gain) economic results than the nondifferentiated (climatological) strategies S_1 and S_2 if the two-sided inequality is fulfilled

$$x_2<\beta<x_1. \tag{7}$$

Here

$$\left.\begin{aligned}\beta&=\frac{\Theta_{22}-\Theta_{21}}{\Theta_{11}-\Theta_{12}},\\ x_1&=\frac{p_{11}}{p_{21}}=\frac{p_{1|1}}{1-p_{1|1}},\\ x_2&=\frac{p_{12}}{p_{22}}=\frac{1-p_{2|2}}{p_{2|2}}\end{aligned}\right\}. \tag{8}$$

*It is easy to show that conditions (3) are interrelated and fulfillment of one of them mandatorily results in the fulfillment of the other.

For any method-substantiated forecast due to conditions (3) the amount $\varkappa_2$ is less than $\varkappa_1$, and consequently, such β is always found for which correlation (7) actually occurs. With $\beta<\varkappa_2$ the best of the three comparable strategies will be strategy S_1 (fall supplementary feedings), and with $\beta>\varkappa_1$ strategy S_2 (spring supplementary feedings). Thus, the selection of the optimal economic strategy in each specific case defined by three indices β, $\varkappa_1$ and $\varkappa_2$, the first of which is determined by its peculiarities of economics, and the two others depend on the success of the forecast. It is advantageous to use the forecasts only when β is not too large and not too small, falling within the interval $[\varkappa_2, \varkappa_1]$.

In order to estimate the effectiveness of the "meteorological" differentiation of economic decisions it is sufficient to compute the amount

$$\lambda = \frac{G_f - \max(G_1, G_2)}{\max(G_1, G_2)}, \qquad (9)$$

indicating, by how many percents the profit is increased, or, on the contrary, decreased from supplementary feedings with a variation in the periods of their conducting as compared to the profit which could be y elded by the best of the nondifferentiated strategies (S_1, S_2). The relationship $\lambda=\lambda(\beta)$ is depicted in figure 1. From the cited graph it is well evident that the greatest effect from using forecasts will be obtained by the so-called "ideal consumers" [7] for which $\beta=p_{10}/p_{20}$. The amount λ in this case is the maximum and can be defined according to the formula

$$\lambda = \lambda_{max} = \frac{(\theta_{11} - \theta_{12})(\theta_{22} - \theta_{21})}{\theta_{11}\theta_{22} - \theta_{12}\theta_{21}} Q, \qquad (10)$$

where

$$Q = \frac{p_{11}}{p_{10}} + \frac{p_{22}}{p_{20}} - 1. \qquad (11)$$

--Obukhov's criterion of success.

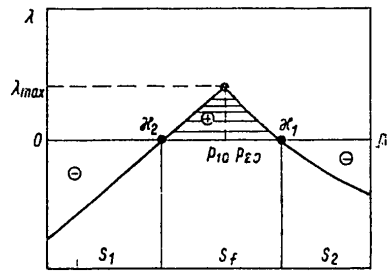

Figure 1. Overall View of Relationship $\lambda=\lambda(\beta)$

Negative λ meet the values $\beta<\chi_2$ and $\beta>\chi_1$ as should be expected, which indicates the inexpediency of using the examined forecasts by all the consumers for thich the corresponding β are characteristic.

In addition to the examined statement of the question, when the characteristics of success of the forecast are assigned and it is established for which consumers this forecast is economically useful, the discussed technique and formulas (7)-(8) can be used to solve the opposite problem that consists of a clarification of the requirements that an alternative forecast might satisfy in order for a certain specific consumer to orient himself on it [5].

By transforming the inequality (7) with regard for correlations (8) it is easy to show that the forecast will be economically effective if the probabilities of the correct forecast $p_{1/1}$ and $p_{2/2}$ exceed the corresponding levels

$$p_{1|1}^{\min} = \frac{\beta}{1+\beta}. \qquad (12)$$

and

$$p_{2|2}^{\min} = \frac{1}{1+\beta}. \qquad (13)$$

We will show that for the method-substantiated forecast one of the inequalities

$$\left.\begin{aligned} p_{1|1} &> p_{1|1}^{\min}, \\ p_{2|2} &> p_{2|2}^{\min} \end{aligned}\right\} \qquad (14)$$

occurs mandatorily. In fact, according to the correlations (12)-(13) the nonfulfillment of both inequalities (14) will designate that the sum $\mu=p_{1/1}+p_{2/2}$ is less than a unit. However according to condition (3) for any successful forecast the amount μ must be bigger than a unit. Therefore the assumption on the simultaneous nonobservance of both inequalities (14) contradicts the previously made assumption on the method of substantiation of the employed forecasting technique. Consequently, only one of the probabilities must satisfy certain requirements that make a successful forecast also economically useful--depending on the conditions either $p_{1/1}$, or $p_{2/2}$.

In particular, if

$$\beta > p_{10}/p_{20} \qquad (15)$$

then the requirements are made for the amount $p_{1/1}$, and vice versa, with

$$\beta < p_{10}/p_{20} \qquad (16)$$

The amount $p_{2/2}$ is important.*

From a qualitative aspect the latter conclusion has a very clear explanation. As follows from a joint examination of formulas (4)-(5), in the absence of forecasts with $\beta > p_{10}/p_{20}$ the preference is given to strategy S_2, i.e., spring supplementary feedings are constantly made. In order in this case for it to be advantageous to switch to an annual differentiation in the periods of introducing fertilizer, it is necessary to guarantee a fairly reliable forecast of the onset of dry winter, i.e., to satisfy the first of the inequalities (14). On the contrary, with $\beta < p_{10}/p_{20}$ the climatologically optimal strategy is a constant conducting of fall supplementary feedings, and consequently, for differentiation of solutions according to the expected weather conditions it is necessary to be able to predict fairly well the onset of a moist winter, i.e., to guarantee a fairly high value of probability $p_{2/2}$.

Certain Numerical Estimates

As shown by the analysis of the available experimental data, in the forest-steppe and steppe regions of the European territory of the country that are distinguished by comparatively small quantity of winter precipitation the late-fall supplementary feedings have a persistent advantage. Therefore the question of differentiation in the periods of introducing fertilizer mainly is urgent for the Nonchernozem zone where the effectiveness of fall and spring supplementary feedings is not constant from year to year and significantly depends on the soil and weather conditions.

In particular in the central region of the Nonchernozem zone on medium and heavy-loamy soils in 28% of the cases fall supplementary feedings yield a greater increase in the harvest, in 43% of the cases--spring, and roughly with 30% of probability both types of supplementary feedings are of equal value. Under the same climate conditions, but on other soils (light loams and sandy loams) the success of spring supplementary feedings rises to 62%, which is explained by the increased probability of nitrogen washing out from the light soil by the snow-melt spring waters. The same effect is noted in the regions of the Baltic area and Belorussia, where the fall supplementary feedings yield greater increases in the harvest than the spring, only in 10% of the cases, in 20% of the years both types of supplementary feedings are of equal value, and in 70% of the cases the

*What has been stated, of course, in no way should be understood in that sense that the "not important" probability has no value at all. It is in fact not important only from the viewpoint of a qualitative solution to the question, in which case the forecast will be economically useful. As for the degree of this utility, then it always will be higher the greater both probabilities--$p_{1/1}$ and $p_{2/2}$.

spring introduction of fertilizer is more effective. Of especial interest is the Volga-Vyatskiy region where a considerable (up to 43%) increase in the success of fall supplementary feeding is observed and a 29 frequency of cases when the fall and spring supplementary feedings yield the same results. The high effectiveness of the spring supplementary feedings is governed here by considerable frequency of winters with a small quantity of precipitation.

Table 3 gives the mean increases in harvest corresponding to the conducting of fall and spring supplementary feedings in different soil-climate zones in years with moist and dry winters. In dividing all our available cases into the two indicated categories consideration was made for the summary quantity of precipitation W_{XI-III} falling from November through March, whereby winter refers to the type "moist" if the amount W_{XI-III} exceeded a certain level of W_0, and to the "dry" type if W_{XI-III} was smaller than W_0. For the medium and heavy-loamy soils the value W_0 was established as equal to 200 mm, and for light-loamy and sandy loam soils--160 mm. Based on the mean increases in the harvest obtained thus, and taking into consideration that the cost of one centner of increase in grain (with deduction for additional outlays for harvesting, transport and drying) in the Nonchernozem zone it is 11.86 R, outlays for conducting spring supplementary feeding, including the cost of fertilizer equal 7.92 R, and the "organizational" effect from replacement of spring supplementary feedings with fall is estimated at an amount of 2.80 R, according to formulas (1) it is easy to compute the profits θ_{ij} corresponding to the different cases. Results of these computations are given in table 4. We will dwell on them in more detail.

TABLE 3 - AVERAGE INCREASES IN HARVEST (CENTNER/) FROM INTRODUCING FALL AND SPRING SUPPLEMENTARY FEEDINGS UNDER DIFFERENT WEATHER CONDITIONS

(1) Район	(2) Почва	(3) Влажная зима		(4) Сухая зима	
		(5) осенняя подкормка	(6) весенняя подкормка	(5) осенняя подкормка	(6) весенняя подкормка
(7) Центральный (8) Нечерноземный (9) То же	(12) Средние и тяжелые суглинки	6,0	8,1	6,8	4,8
	(13) Легкие суглинки и супеси	1,7	2,8	4,2	4,3
(10) Прибалтика и Белоруссия	(13) Легкие суглинки и супеси	4,3	7,3	3,7	4,0
Волго-Вятский (11)	(14) Суглинистые почвы	3,9	3,5	4,8	3,4

Key:
1. Region
2. Soil
3. Moist winter
4. Dry winter
5. Fall supplementary feeding
6. Spring supplementary feeding
7. Central
8. Nonchernozem
9. The same
10. Baltic and Belorussia
11. Volga-Vyatskiy
12. Medium and heavy loams

[Key continued on next page]

13. Light loams and sandy loams
14. Loamy soils

TABLE 4 - PROFITS θ_{ij} (R/ha) FROM INTRODUCING FALL (d_1) AND SPRING (d_2) NITROGEN SUPPLEMENTARY FEEDINGS UNDER DIFFERENT CONDITIONS OF NONCHERNOZEM ZONE

(1) Район	(2) Почва	W	d_1	d_2
(3) Центральный (4) Нечерноземный	(7) Средние и тяжелые суглинки	<200	75,5	49,0
		>200	66,0	88,1
	(8) Легкие суглинки и супеси	<160	44,7	43,1
		>160	15,0	25,3
(5) Прибалтика и Белоруссия	(8) Легкие суглинки и супеси	<160	38,5	39,5
		>160	45,9	78,7
(6) Волго-Вятский	(9) Суглинистые почвы	<200	51,8	32,4
		>200	41,1	33,6

Key:
1. Region
2. Soil
3. Central
4. Nonchernozem
5. Baltic and Belorussia
6. Volga-Vyatskiy
7. Medium and heavy loams
8. Light loams and sandy loam
9. Loamy soils

As for the regions of the Baltic and Belorussia, as well as the Volga-Vyatskiy region, then these cases can immediately be excluded from further examination since regardless of the conditions formed in the first of them the economic advantage always remains for the spring supplementary feeding ($\theta_{11}<\theta_{12}$, $\theta_{21}<\theta_{22}$), and in the second case--for the fall ($\theta_{11}>\theta_{12}$, $\theta_{21}>\theta_{22}$). Thus only the variants are important for the central region for which a different effectiveness of various periods of spring fertilizings is characteristic--in dry years here late-fall supplementary feedings are economically more advantageous, and in moist years--spring. Consequently, for these two cases it makes sense to solve the question of differentiation of agricultural engineering depending on the expected conditions of the fall-winter period.

According to table 4 for the mean-and heavy-loamy soils of the central Nonchernozem region the parameter

$$\beta = \frac{88,1-66,0}{75,5-49,0} = 0,83.$$

The frequency of winter conditions that foster in an economic sense fall supplementary feeding for this zone can be assumed to be equal to 57%. From here

$$\frac{p_{10}}{p_{20}} = \frac{0,57}{0,43} = 1,33.$$

Comparison of the computed values of parameter β and the ratio p_{10}/p_{20} shows that in the given case in absence of forecasts it is more advantageous to conduct fall supplementary feedings ($\beta < p_{10}/p_{20}$) and for the transition to differentiated economic strategy it is necessary to guarantee a fairly reliable forecast of the onset of moist winter. According to the formula (13) the probability $p_{2/2}$ here must exceed the level

$$p_{2|2}^{\min} = \frac{1}{1+0,83} = 0,55\ (55\%).$$

The use of forecasts that from the viewpoint of correctness of the prediction of moist winters have a lower successfulness results in the fact that the economic effect for the use of differentiated supplementary feeding will be lower than with a constant application of fertilizers in the fall.

In a certain sense the opposite situation is formed on the light loamy and sandy loam soils. In this case the amount

$$\beta = \frac{25,3-15,0}{44,7-43,1} = 6,44.$$

The frequency of dry winters under the given conditions is about 38%, and consequently,

$$\frac{p_{10}}{p_{20}} = \frac{0,38}{0,62} = 0,61.$$

Thus, the ratio p_{10}/p_{20} is lower than β, and in the absence of forecasts the spring supplementary feedings will be more advantageous. For differentiation in the periods of field operations in accordance with formula (12) it is necessary to have forecasts which guarantee correct prediction of dry winters with probability $p_{1/1}$, greater than

$$p_{1|1}^{\min} = \frac{6,44}{1+6,44} = 0,87\ (87\%)$$

If one takes into consideration that the natural frequency of dry winters in the examined region is about 38%, then it is necessary to conclude the requirements for the forecasting technique in the given case are very high and currently, apparently, difficult to attain. At least, it seems that the transition to differentiation of periods of spring supplementary feeding on the sandy-loam and light-loamy soils of the central region of the Nonchernozem zone is significantly more problematic than on the heavy and medium loams, where for such a transition it is sufficient to bring the probability of direct forecasting of moist winters to level 0.55-0.60 with natural frequency of the predictable conditions p_{20}=0.43.

In conclusion we would like to note that an absolute value should not be assigned to the conducted analysis and the conclusions made on its basis, as other particular recommendations of such type. The adoption of a final agricultural engineering solution is always to linked to consideration for a very large number of influencing factors, while the developed recommendations reflect only individual agrometeorological aspects of the examined problem. The value of the obtained results, first of all, consists of the fact that with their help an objective estimate is guaranteed of economic consequences of differentiating the periods for conducting nitrogen supplementary feeding and the possibility appears of formulating substantiated requirements for the quality of the forecasting information necessary for the practical realization of the corresponding differentiated agricultural engineering.

BIBLIOGRAPHY

1. Bagrov, N. A. "Economic Utility of Forecasts," METEOROLOGIYA I GIDROLOGIYA, No 2, 1966.

2. Gandin, L. S.; and Zhukovskiy, Ye. Ye. "Rational Use of Forecasting and Climatological Information in Making Economic Decisions," METEOROLOGIYA I GIDROLOGIYA, No 2, 1973.

3. Zhukovskiy, Ye. Ye. "Making Optimal Decisions as Method of Increasing Effectiveness of Agrometeorological Forecasts," METEOROLOGIYA I GIDROLOGIYA, No 2, 1974.

4. Zhukovskiy, Ye. Ye.; and Chudnovskiy, A. F. "Metody optimal'nogo is pol'zovaniya meteorologicheskoy informatsii pri prinyatii resheniy" [Methods of Optimal Use of Meteorological Information in Making Decisions], Leningrad, Gidrometeoizdat, 1978.

5. Zhukovskiy, Ye. Ye. "Alternative Weather Forecasts: Economic Effectiveness and Requirements for Success," BYULLETEN' NTI PO AGRONOMICHESKOY FIZIKE, No 36, 1978.

6. Pannikov, V. D.; and Mineyev, V. G. "Pochva, klimat, udobreniye i urozhay" [Soil, Climate, Fertilizer and Harvest], Moscow, Kolos, 1977.

7. Obukhov, A. M. "Question of Evaluating the Successfulness of Alternative Forecasts," IZV AN SSSR. SER. GEOFIZ., No 4, 1955.

8. Omshanskiy, M. A. "Consideration for the Accuracy of Forecasts and Their Use," ZHURNAL GEOFIZIKI, vol 3, No 4, 1933.

9. Fedoseyev, A. P. "Effectiveness of Fertilizers in Relation to Agricultural and Climate Conditions," AGROKHIMIYA, No 8, 1973.

10. Fedoseyev, A. P. "Agrometeorological Aspects of Chemization of Farming," METEOROLOGIYA I GIDROLOGIYA, No 9, 1976.

11. Fedoseyev, A. P. "Agrometeorologicheskoye obespecheniye khimizatsii zemledeliya" [Agrometeorological Provision for Farming Chemization], Moscow, Gidrometeoizdat, 1977.

12. Fedoseyev, A. P. "Effektivnost' mineral'nykh udobreniy i klimat" [Effectiveness of Mineral Fertilizers and Climate], Moscow, Znaniye, 1978.

UDC 631.432

CERTAIN METHOD QUESTIONS OF USING TENSIOMETERS IN STUDIES OF SOIL WATER PATTERN

Moscow METEOROLOGIYA I GIDROLOGIYA in Russian No 10, Oct 1979 pp 111-117

[Article by Candidate of Biological Sciences N. A. Muromtsev, Soil Institute, submitted for publication 11 Mar 1979]

Abstract: The possibility is shown of using tensiometers to determine soil moisture content and supplies of soil moisture.

A detailed description is made of the methods for installing tensiometers under field and laboratory conditions, and in particular, installation of tensiometers into soil wells, open pits and soil trench-shelters.

In a number of examples the difference is shown between values of capillary potential of soil moisture determined for the same soil under conditions of steady-state and unsteady equilibrium.

[Text] In the area of moisture that is optimal for plant growth, i.e., in the interval from the least specific retention (LR) to moisture corresponding to MRC (moisture of rupture in capillary bond) the peculiarities of the behavior of soil moisture and its accessibility for plants are governed to a considerable degree by capillary forces which can be characterized by the capillary potential of soil moisture [6, 7, 9, 12]. The capillary potential of soil moisture P_k is measured by tensiometers and capillary meters, tensiometric and capillary-metric units [2, 5].

Despite the available considerable experience of using tensiometers in many countries, nevertheless many method questions of tensiometry are still far from final resolution. In particular, a technique has not been definitively developed for determining the moisture content of the soil, and the optimal method for installing tensiometers in the soil has not been

revealed, especially on irrigated field; a reliable evaluation of the reliability of tensiometric information is lacking, and the requirements for the "performance capacity" of tensiometers during their manufacture and operation have not been systematized.

This work covers certain method questions of tensiometry, partially indicated above.

Design of tensiometers. Currently tensiometers are used in different systems and designs, and the difference between them is reduced to a difference in the design of the manometers. Without classifying the tensiometric instruments we will attempt to conventionally systematize them.

Many variants of the design of tensiometers are known: tensiometers with mercury, alcohol and water manometers [4, 9], tensiometric units primarily with mercury manometers [10], tensiometers of the membrane type with spring or contact vacuum gages [3], tensiometers of the membrane type with pressure sensors [3], tensiometers with manometers of the bellows type [3, 13], and tensiometers tensioscopes [13].

Almost all the listed tensiometers (with the exception of the tensiometer of the Hydrometeorological Service AM-20-11--instrument of membrane type with spring measurer) are manufactured for the most part by the researchers themselves that are designed mainly for research purposes. Therefore the tensiometers made according to the same type but in different laboratories can differ among themselves in their design execution.

The experience of manufacturing and operating tensiometric instruments has demonstrated that the following can be isolated as primary measures that guarantee their reliable operation:

--guarantee of the vacuum-stability with vacuums up to 0.85 atm. This condition or requirement is fulfilled by the use of ceramic sensor-filters of the type F-7 and F-9 with pore sizes in the limits 0.9-1.3 μm, that prevent penetration of air into the tensiometer with high vacuums in it. This includes a thorough connection of the instrument assemblies with vacuum-stable rubber in the form of vacuum hoses.

--mandatory presence in the tensiometer of a device or attachment for removal of air adsorbed in water and penetrating into the tensiometer through the pores of the ceramic sensor with high vacuums.

--reduction to a minimum of the effect of the temperature of air and soil on the readings of the tensiometers, which is achieved to a considerable degree by the use of materials with low heat conductivity and placement of the latter in especially equipped soil trench-shelters where the diurnal fluctuation in air temperature is considerably lower.

--increase in the sensitivity of the manometer. For the mercury manometer this is achieved by the use of glass pipe-capillaries with inner diameter

of 1 mm and increase in the accuracy of the graduation of the manometer scale.

--achievement of a reliable contact between the ceramic sensor of the tensiometer and the soil. This requirement can be completely satisfied with the installation of the tensiometers in the wall of the soil open pit.

--correspondence of the soil core samples and bulk samples used in callibrating the tensiometers, in water-physical and chemical properties to the field mass of soils for which the obtained callibrated dependence of the capillary potential of moisture on soil moisture content is further used.

Methods of installing tensiometers in soil. Under field conditions tensiometers should be installed on a special platform that is representative for the entire soil mass or an individual section of it. The dimensions of the platform are selected with regard for the placement on it of the drilling wells for control determinations of soil moisture content, phenological observations, and observations of the harvest structure. One can recommend a platform 5 by 5 m in size. The tensiometers are installed in the center of the platform at different depths of the soil profile with 2-3-fold frequency with the use of one of three methods.

First method is installation of the instruments in one of the walls of the soil open pit. In the wall of the soil open pit a vertical narrow slit is dug out to the necessary depth, the tensiometer is installed vertically into it and it is covered with soil that was dug out in making the open pit with strict observation of the order of the soil layers.

The second approach consists of installing tensiometers into wells drilled by a drill whose diameter of the cutting part exceeds the diameter of the instrument by 1-2 mm. If tensiometers are used with ceramic filter of small diameter (about 1.8 cm),then in this case one can use a metal pipe 1.9-2.0 cm in diameter.

The experience of installing tensiometers according to the second variant demonstrates that it is fairly difficult to install instruments to depths of soil exceeding 60-70 cm from the surface, especially tensiometers with thick ceramic filter (for example the tensiometers AM-20-11). The difficulty is produced, primarily, by the friction of the upper surface of the tensiometer on the wall of the soil well.

The third approach is installation of the tensiometers in special soil trench-shelters reinforced (walls, ceiling and floor) with thin planks, concrete, bricks or other material. The body of the tensiometer is mounted on one of the walls of such a shelter, while the ceramic center can be installed parallel to the daytime surface (or the surface of the floor), but most conveniently--at an angle of 10-15° that guarantees the greatest convenience in filling (refueling) the tensiometers with water. The third variant for installing tensiometers in our opinion, is the most expedient

since the range of oscillations in the diurnal temperature is lower in the shelter.

Figure 1 presents a plan for the placement of tensiometers and other hydrophysical equipment in a reinforced soil trench-shelter that we used on the irrigation system "Gorki-2." The depth of the trench exceeds 4 m and uncovers the level of subsoil water (LSW), and the tensiometers are installed at a distance of 25 cm from each other. In accordance with the scheme the soil profile 1 is uncovered to the LSW 2 , the vertical trench-shelter 3 is reinforced with thin planks 4, on one of the walls of the latter tensiometers 5 are placed and thermometers 6, the entrance to the trench is made from above on a stair (not designated on the plan) through hatched 7 covered by roofs 8 and 9. In the bottom of the trench a ground well 10 is made, and at a certain distance from the bottom, on one of the lateral walls of the trench piezometer 11 is placed equipped with spigots 12. Besides the openings in the walls of the trench designed for installation of tensiometers and thermometers, there are a number of spare openings 13 covered with asphalted stoppers and designed for additional tensiometers or other soil moisture content sensors. At a certain distance from the trench (about 2 m) casing 14 is installed that is designed to control the level of subsoil water.

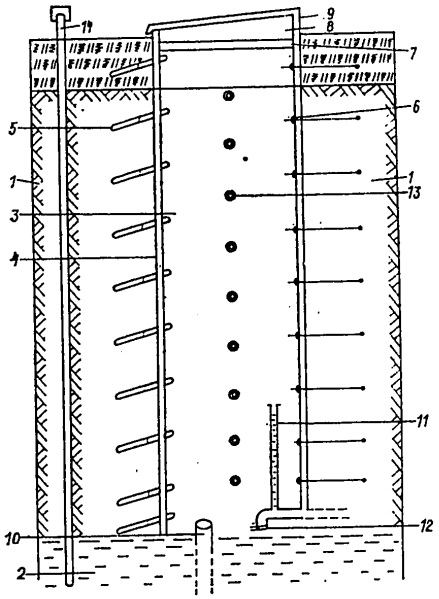

Figure 1. Soil Trench-Shelter for Installation of Tensiometers

During installation of tensiometers under field conditions, especially in drilling wells, it is very important to guarantee the close contact of its ceramic sensor with the soil. With a poor quality contact around the sensor sometimes cavities are observed which considerably affect the readings of the tensiometers. The cavities can be formed, in particular, in soils of heavy granulometric composition as a consequence of the swelling and shrinking caused by alternation (exchange) of abundant moisture of the soil during irrigation, and its drying up during the inter-irrigation period. Here on the soil surface fairly wide and extended cracks are formed that sometimes reach over 10 cm in the cross section. Under these condtions the tensiometers installed in the surface 20-centimeter layer of soil are often in the "nonworking" state. Since the surface layer is the layer of intensive moisture exchange of soil with the atmosphere and installation of tensiometers is very desirable in it, one can recommend tensiometers with ceramic sensor of the type truncated cone, in which only the plane of the base is porous. The tensiometers with such filters are the most stable in the surface layer, and the probability of appearance of an air space from below, even with formed cracks, is considerably lower than for tensiometers with cylindrical sensors.

Under laboratory conditions the installation of tensiometers in soil is considerably simpler. With the use of bulk soil samples the instruments are installed simultaneously with filling of the material into the working vessel, and in core samples the latter can be installed in openings made by a metal pipe of corresponding diameter.

Methods of calibrating the tensiometers. In calibrating the tensiometers under field conditions one can recommend a plan according to which the tensiometers are installed in all the genetic levels of soil at distance 15-20 cm from each other in the form of an isosceles triangle. The distance between the tensiometers installed at different depths of soil is 30-40 cm. Around the instruments in the form of a rectangle at a distance 15-20 from each other drilling wells are placed, marking them with numbered pegs. It is necessary to take the readings of the tensiometers daily, at the same time of day, and the soil moisture content should be determined with three-fold frequency as the P_k drops, but no less than once in 5 days. The data of simultaneous determinations of P_k and soil moisture content are used to construct calibration relationships P_k (w).

The shortcomings of the field method of calibration include: labor intensity and length (due to the thermostat-weight method of determining soil moisture contents) and the narrow interval of changes in moisture content of the soil P_k. The latter is governed by the fact that even under conditions of an insufficient moistening of the soil (moisture content deficit) the supplies of moisture in deep layers of the soil, especially under irrigation conditions, rarely are lower than 50-60% of the least specific retention.

Under laboratory conditions the tensiometers can be calibrated on samples of soil of intact structure and in a pattern of dessication (desorbtion branch of hysteresis) which brings the obtained data the maximum closest to the field conditions. To conduct work it is expedient to use metal, glass, plastic, textolite and other cylinders whose dimensions must be in a certain correspondence with the dimensions of the ceramic sensor of the tensiometer. With length of the latter about 11 cm, diameter about 2 cm it is desirable to use cylinders of such dimensions: height 15 cm, length and width can be the same and are 8-10 cm. Only one tensiometer should be placed in one cylinder.

After moistening the soil samples to LR P_K is determined. For this purpose the cylinders are closely covered with caps and placed in a chamber with high relative air humidity where evaporation from the soil surface practically is lacking. With the passage of 2-3 days of keeping the samples in the chamber the latter are taken from it and the tensiometer readings are recorded, and the cylinders are weighed. Then the soil samples with the tensiometers are placed under conditions of intensive evaporation, for example in a chamber with a stream of dry heated air. After loss by the soil of a large portion of the water which is established according to the difference in the weighings of the cylinders, the latter again are placed in the chamber with high air humidity for 1-2 days. This is necessary in order for the moisture after partial evaporation to be uniformally distributed over the entire soil volume. The described procedure is repeated until the readings of the tensiometer reach the limit values (0.85 atm).

The main shortcoming of the laboratory method for calibration is the difficulty in creating uniform distribution of moisture over the entire mass of the soil sample, especially with considerable volumes of the latter and high intensity of evaporation from the soil surface. Here the volume of the sample and uniformity of distribution of moisture in it are in a certain contradiction, since the larger the volume of soil, the more reliable the findings. On the other hand, the larger the sample of soil, the longer the process of uniform distribution of moisture in it and the achievement of equilibrium in the system soil-tensiometer.

Besides the described methods the tensiometers can be calibrated in vegetation vessels with plants. After the plants have been developed to the phase of bushing out or to the phase of "emergence into tubule," parallel measurements of P_K and soil moisture content are started, which is computed according to the difference in the weights in the current and previous weighings. The powerful root system of the plants completely assimilates the soil of the vegetation vessel, thanks to which the consumption of moisture by the plant roots is implemented uniformally and simultaneously from the entire volume of soil.

Determination of soil moisture content according to tensiometer readings. The main hydrophysical relationship P_K (W) can be used to determine the soil moisture content according to tensiometer readings. Such relationships

need to be determined for all the soil-genetic levels that significantly differ among themselves in their granulometric composition and other water-physical properties. Usually tensiometers are callibrated according to the soil moisture content, therefore in those cases where information is required about the moisture supplies it is necessary to make additional computations linked to the translation of moisture content values into moisture supplies. To avoid additional computations of the number of cases it is expedient to callibrate the tensiometers according to moisture supplies. Figure 2 presents such callibration relationships that we obtained under field conditions for the Ciscaucasian medium-loamy chernozem--variant a (dependence of the moisture potential on soil moisture content) of the Rostovskaya oblast, and for the light-chestnut medium-loamy soil of the Saratovskaya oblast--variant b (dependence of P_k on moisture supplies in the soil). The studies used AM-20-11 tensiometers installed in layers of soil 10-20, 40-50 and 90-100 cm (variant a) and in layers 10-20, 40-50 and 70-80 cm (variant b). The second variant used evaporators GGI-500-100 in each of which one tensiometer was installed.

Analysis of the relationships shows that in variant a they practically do not differ among themselves, i.e., the dependences of P_k on soil moisture content for its different layers coincide among themselves. The correlation coefficient between the values of the capillary moisture potential is 0.86, which indicates the high closeness of the link between the obtained relationships. Analogous relationships for the variant b significantly differ among themselves. This is explained by the fact that in the first case (variant a) P_k and the soil moisture content were determined in the same layers (10-20, 40-50 and 90-100 cm), and in the second (variant b) P_k was determined in the 10-centimeter layers of soil as in variant a, while the supplies of soil moisture were computed by the increasing result for the layer 0-80 cm. The correlation coefficient between P_k and moisture supplies in the layer 0-80 cm differs, the closest link is observed in those cases when for construction of the relationship the values P_k are used for the layers 40-50 (relationship 2) and 70-80 cm (relationship 3), for which the correlation coefficient is respectively 0.86 and 0.91 (for the layer 10-20 cm its value is reduced to 0.80).

An even greater discrepancy between relationships P_k (supplies of soil moisture) is constructed for different soil layers is observed for the Ciscaucasian medium-loamy chernozem on a field under corn and potatoes (figure 3, variants a and b respectively). In this experiment in the same way as in the variant with evaporaters, P_k is determined in the 10-centimeter layers of soil (10-20, 40-50 and 90-100 cm) while the supplies of soil moisture are computed by the increasing result for the entire meter layer. The closeness of the link between the values P_k and the supplies of soil moisture almost in all variants is high; the correlation coefficient fluctuates in limits 0.97-0.84 with the exception of the layer 90-100 cm (variant b, relationship 3) for which the correlation coefficient is only 0.23. The reason for the low closeness of the link here is apparently, the poor contact of the tensiometers installed in this layer with the soil.

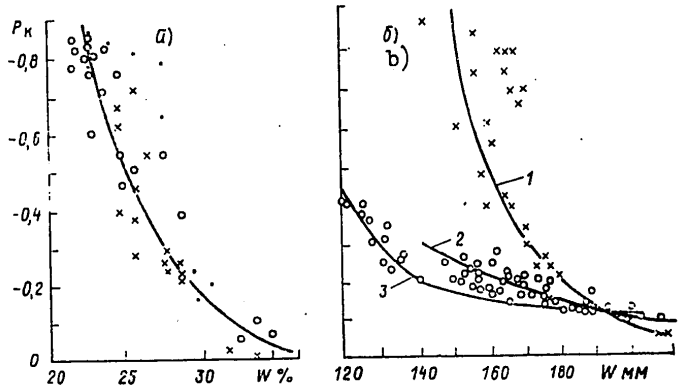

Figure 2. Dependence of Capillary Potential of Soil Moisture (P_k atm) on Moisture Content (W%) for Ciscaucasian Medium-Loamy Chernozem of the Rostovskaya Oblast (a) and on Moisture Supply (W mm) for Light Chestnut Medium-Loamy Soil of the Sartovskaya Oblast (b).

Key:

1. P_k is determined in layer 10-20 cm, moisture supplies computed for layer 0-80 cm
2. P_k is determined in layer 40-50 cm, supplies computed for layer 0-80 cm
3. P_k is determined in layer 70-80 cm, moisture supplies computed for layer 0-80 cm

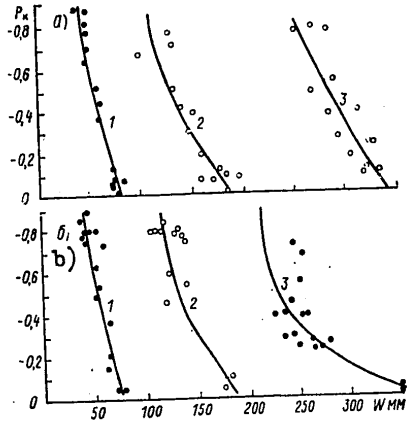

Figure 3. Dependence of Capillary Potential of Soil Moisture (P_k atm) on Moisture Supply in Ciscaucasian Medium-Loamy Chernozem of the Rostovskaya Oblast Under Corn (a) and Under Potatoes (b)

[Key on next page]

Key:

1. P_k determined in layer 10-20 cm, moisture supplies computed in layers 0-100 cm
2. P_k determined in layer 40-50 cm, moisture supplies computed for layers 0-100 cm
3. P_k determined in layer 90-100 cm, moisture supplies computed for layers 0-100 cm

Thus, the cited data indicate that the dependence of P_k on supplies of soil moisture obtained for a soil layer limited in thickness cannot be used to determine the moisture supplies in other, layers of soil that are thicker with respect to depth, even in that case where the granulometric composition differs insignificantly in the limits of the soil profile. At the same time, the presence of a high correlation between P_k and supplies of soil moisture (in the case where both parameters were determined in a soil layer that was the same in thickness) confirms the widespread opinion on the expediency of using tensiometers as soil moisture gages. However, due to the limited nature of the intervals P_k measured by the tensiometers the latter will be most effectively employed in irrigated farms and in regions with excess atmospheric moistening.

Limits and reliability of measuring soil moisture content according to readings of tensiometers. The limits of soil moisture content measured according to the readings of tensiometers are limited to the interval of P_k (0--0.85 atm). With complete specific retention of nonsalinized soils P_k is an amount close to zero. The lower boundary of soil moisture content which can be characterized from the tensiometer readings, in each specific case depends on the granulometric composition and water-physical properties of the soils. On the whole, apparently, one can state that the lower limit of application of tensiometers for determining the moisture content is characterized by an amount that corresponds to 60-70% LR, which in turn corresponds to the MRC [8].

The reliability of the soil moisture content values determined from the tensiometer readings is determined by a number of factors, some of which have been examined above: quality of contact of ceramic sensor with soil, method of installing tensiometers in soil, and accuracy of the calibration relationship. Below we will examine the effect of drift and length of establishing equilibrium in the system soil-tensiometer on the tensiometer reading and the soil moisture content values.

Drift depends on the rate of decrease in the vacuum in the tensiometer during irrigation and considerable precipitation. An unambiguous estimate of the drift of tensiometers is not possible since it is directly determined by many factors, among which one should note the pore size of the ceramic sensor and the correlation of it with the porosity of the soil,

water-physical properties of the soil, especially the coefficient of filtering, depth of installation of the instruments, and quantity of irrigation or rain water entering the soil. On the whole the practice of using tensiometers in irrigated farming shows that with abundant irrigation on the soils with satisfactory filtering properties the drift is insignificant. The increase in the readings of the tensiometers from -0.85 to -0.05 atm with the entrance of a sufficient quantity of water into the layer in which the tensiometers are installed occurs in the space of 20-30 minutes.

However the rapid drop in low values of the potential (high readings of the tensiometers) does not mean that in the system soil-tensiometer equilibrium has occurred. The conditions of equilibrium are also affected by many factors, and primarily the moisture content in the layer of location of the ceramic sensor, the rate of its flow in the system soil-tensiometer, the presence of trapped and free air in the tensiometer, and certain others.

Klute and Gardner [15] have proposed an equation according to which one can determine the length of leveling of the tensiometer. With such soil moisture content when its moisture conductivity is above the moisture conductivity of the walls of the ceramic sensor, the advance of moisture between the tensiometer and the soil is described by the equation

$$\frac{dg}{dt} = K(P_n - P_T), \qquad (1)$$

where dg--quantity of moisture that has passed during time dt, i.e., the flow density;

K--moisture conductivity of filter walls;

P_n and P_t--moisture potentials respectively in soil adjacent to wall of tensiometer, and water in tensiometer.

With low soil moisture content, when its water conductivity becomes considerably lower than the water conductivity of the walls of the ceramic sensor one can use the following equation from [15]:

$$\frac{P_T - P_n}{P_i - P_n} = \frac{1}{4\pi K_n S L t}, \qquad (2)$$

where P_t--moisture potential in tensiometer by beginning of experiment;

P_i--moisture potential in tensiometer by beginning of process of leveling;

K_n--coefficient of moisture conductivity of soil (considered constant in given interval of moisture content);

L --length of tensiometer;

t --time of leveling;

S --sensitivity of manometer.

Calculations according to the given formulas indicated that for leveling of the moisture potential in the soil-tensiometer system from several hours (with high soil moisture content) to several days (with low moisture content of soil--in limits P_k=0.8--0.85 atm) are required.

The length of leveling of potentials in the soil-tensiometer system is the most important condition that determines the reliability of soil moisture content and analysis according to tensiometer readings. If recording of the tensiometer reading occurs before the onset of equilibrium, then this results in significant errors in the values of the latter. Thus, the vegetation experiments of Hack [14] indicate that delay in the tensiometer readings in relation to the soil moisture content changes (we have in mind the nonequilibrium conditions) results in errors in determining the latter up to 25%. Smiles and others studied the dependence of P_k on moisture content in a horizontal column for static and dynamic conditions with absorption and draining of water [16]. The findings demonstrate that under nonstationary conditions the relationship P_k (W) refers to different rates of change in the moisture content and moisture potential, depending on what distance from the source of water the measurements are made. It has also been established that the dynamic curves for the processes of absorption coincide with the curves obtained under equilibrium conditions, while the dynamic curves for conditions of draining differ from the equilibrium. Here the soil moisture content that corresponds to the determined values P_k is higher the higher the rate of change in moisture content.

Since between the soil moisture content and P_k an inverse relationship exists, then it is evident that with the given amount of soil moisture content P_k under dynamic conditions will be higher the greater the rate of moisture flow. Confirmation of this is found in the work of Berezkin [1]. In accordance with the data it contains the dynamic relationships P_k (W) do not coincide with the static relationships for quartz sand, whereby the differences between them increase as the rate of moisture flow increases. Thus, P_k under static conditions with moisture content 0.2 g/g was 22.5 cm Hg, and under dynamic conditions--20, 14.5, 13, 9.5 and 5 mm Hg respectively for rates of flow 0.4 x 10^{-5}, 0.64 x 10^{-5}, 0.976 x 10^{-5}, 1.2 x 10^{-5} and 1.34 x 10^{-5} g/(cm3 x s).

Thus, the examined materials make it possible to draw the following conclusions:

1. According to the tensiometer readings one can analyze not only the soil moisture content, but also its supplies. The correlation coefficient of the dependence of P_k on moisture supplies characterizes a fairly high closeness of the link between these parameters and is in the limits 0.91-0.80. The dependence of P_k on soil moisture content, and especially on the moisture supplies needs to be determined for each soil-genetic layer.

2. When installing tensiometers under field conditions it is expedient to use specially equipped soil trench-shelters in which the effect of temperature on the instrument readings is less significant than on the soil surface.

3. It is expedient to calibrate the tensiometers on soil core samples under laboratory conditions, here the most precise relationship P_k (W) is obtained with the use of the so-called "vegetation" method.

4. The drift in the majority of tensiometers (at least with mercury manometers) is insignificant, and it does not have an important effect on the tensiometer readings.

5. The time for establishment of equilibrium of potentials in the soil-tensiometer system can be considerable and depends on the soil moisture content and its moisture conductivity and the conductivity of walls of the ceramic sensor of the tensiometer, as well as on the water-physical properties of the soil and other conditions that affect the water pattern of the soil. Removal of nonequilibrium readings of the tensiometers significantly decreases the reliability of the obtained information.

BIBLIOGRAPHY

1. Berezkin, V. V. "Issledozaniye zavisimosti kapillyarnogo davleniya ot vlagosoderzhaniya pri isparenii vlagi iz kapillyarno-poristykh tel" [Study of the Dependence of Capillary Pressure on Moisture Content During Evaporation of Moisture from Capillary-Porous Bodies], author's abstract of dissertation for defense of scientific degree of candidate of sciences, Leningrad, 1974.

2. Vadyunina, A. F.; and Kochagina, Z. A. "Metody issledovaniya fizicheskikh svoystv pochv i gruntov" [Methods of Studying Physical Properties of Soils and Ground], Moscow, Vysshaya shkola, 1974.

3. Globus, A. N. "Eksperimental'naya gidrofizika pochv" [Experimental Hydrophysics of Soils], Leningrad, Gidrometeoizdat, 1969.

4. Korchunov, S. S. "Determination of Moisture Coefficients in Peat," TRUDY VNIITP, No 13, 1956.

5. Muromtsev, N. A. "Diagnosing Irrigation of Plants According to Tensiometers," POCHVOVEDENIYE, No 1, 1974.

6. Muromtsev, N. A. "Use of Thermodynamic Potential on Soil Moisture in Studies on Hydrophysics of Soils and Plants," POCHVOVEDENIYE, No 3, 1976.

7. Muromtsev, N. A.; and Sudnitsyn, I. I. "Use of Tensiometers in Characteristics of Moisture Supply of Plants," VESTNIK MGU. BIOLOGIYA I POCHVOVEDENIYE, No 4, 1972.

8. Rode, A. A. "Osnovy ucheniya o pochvennoy vlage" [Fundamentals of Science on Soil Moisture], vol 1, Leningrad, Gidrometeoizdat, 1965.

9. Sudnitsyn, I. I. "Question of the Use of Tensiometric and Electrometric Sensors for Measuring Soil Moisture Content," POCHVOVEDENIYE, No 12, 1959.

10. Sudnitsyn, I. I.; Muromtsev, N. A.; and Shein, Ye. V. "Use of Sensing Method for Determining Coefficient of the Soil Moisture Conductivity," DOKLADY VYSSHEY SHKOLY. BIOL. NAUKI, No 1, 1973.

11. Sudnitsyn, I. I.; and Muromtsev, N. A. "Sposob laboratornoy tarirovki datchikov vlazhnosti pochv" [Method of Laboratory Callibration of Soil Moisture Content Sensors], A. S. 381 989, class G 01 N 33/24 (USSR).

12. "Tolkovyy slovar' po pochvovedeniyu" [Explanatory Dictionary on Soil Science], Moscow, Nauka, 1975.

13. Shishkov, K. N. "Soil Moisture Gage and Application in Land Reclamation," GIDROTEKHNIKA I MELIORATSIYA, No 3, 1950.

14. Hack, H. R. B. "Soil Moisture Tensiometers. Some Limitations and Applications to Growth Studies: Advances Horticult. Sci. and Their Applications," Oxford-London-New York-Paris, Pergamon Press, vol 1, 1961.

15. Klute, A.; and Gardner, W. K. "Tensiometer Response Time," SOIL SCI., vol 93, No 3, 1962.

16. Smiles, D. E.; Vachaud, G.; and Vanclin, M. "A Test of the Uniqueness of the Soil Moisture Characteristic During Transient Nonhysteretic Flow of Water in a Rigid Soil," SOIL SCI. SOC. AMER. PROC., vol 35, No 4, 1971.

NEW PAPERS ON THE WATER BALANCE OF THE DANUBE RIVER

Moscow METEOROLOGIYA I GIDROLOGIYA in Russian No 10, Oct 1979 pp 118-119

[Article by Doctor of Geographical Sciences K. P. Voskresnenskiy, and Candidate of Geographical Sciences V. I. Babkin]

[Text] The working group on scientific hydrology of the Danube River basin in the Danube commission published the results of works on computing the water balance of the Danube: "Sbornik rabot III--Vodnyy balans rek basseyna Dunaya" [Collection of Works III. Water Balance of Rivers in the Danube Basin], Bratislava, 1977, 84 pages, 4 maps.

The examined work is one of the examples of integrated efforts of the socialist countries in the area of studying hydrology, in particular, evaluation of water resources of the Danube used in the interests of all the countries near the Danube.

In the modern period planning of the efficient use of water is based on a study of water balance. Therefore to solve specific water management tasks in individual countries the necessary water-balance studies are being carried out.

One of the latest works on water balance is the study made by the indicated working group.

In amount of water resources after the Volga the Danube is the second river of Europe. The water-balance study on individual parts of the Danube basin or on the basins of its tributaries flowing over the territories of individual countries have been made before. The results of the indicated studies were published by D. Dukich, R. Keller, M. I. L'vovich, K. P. Voskresenskiy and other authors. However, due to the differences in the technique of determining the balance elements and the completeness of the employed data the results of these computations are incomparable to a great extent.

The studies published by the working group on scientific hydrology of the Danube River basin were made according to a unified program with the use

of the most complete hydrometeorological information available in individual countries near the Danube. In this respect they undoubtedly have a great advantage over other previously conducted work.

The work was carried out by the common efforts of specialists of People's Republic Of Bulgaria, Hungarian People's Republic, USSR and CSSR.

The publication gives a technique agreed upon by the participating countries for computing water resources and balance, as well as the research results in the form of multiple-year annual and monthly amounts of the water balance components for the calculated sections on the Danube and its tributaries flowing in the limits of the indicated countries.

The study was made in accordance with the method instructions and programs approved by the working group on scientific hydrology of the Danube basin of the Danube commission.

In order to compute the average multiple-year water balance of river catchment areas in the Danube basin for individual time intervals a four-term equation of water balance was used in its classic form. The calculated sections, of which the total number is 66, were selected on large tributaries before their entrance into the Danube, on the Danube River or its tributaries in the boundary section, and at points isolated at the suggestion of individual states.

The estimate of the water balance for a multiple-year period was made according to data for 1941-1970. For the USSR territory multiple-year balances are also given for individual months and for years characteristic in water content.

The average multiple-year amounts of precipitation in the limits of individual river basins and the entire examined territory were computed according to observational data of precipitation-measuring points. The total number of precipitation-measuring points is 1,722, including 197 in the limits of the People's Republic of Bulgaria, 736 in the Hungarian People's Republic, 262 in the USSR and 477 in the CSSR. In necessary cases, in the absence of large series of observations or in the presence of omissions in them caused, in particular, by military actions on the territory of individual countries, the precipitation was reduced to a multiple-year period (1941-1970) by the method of graphic correlation of data for precipitation of points with short series of observations (with the presence of omissions) with reference point-analogs.

In computing the mean amount of precipitation in the basins of the mountain rivers their distribution with respect to altitude zones was considered. However in those cases where meteorological stations are located primarily on flat territory, for example, in the Hungarian People's Republic, the effect on precipitation of altitude of the locality was not considered.

In the mountain regions within the USSR and CSSR, besides the data of precipitation-measuring points, results were also used of observations of precipitation from summary rain gages. The readings of these rain gages are reduced to the calculated multiple-year period for station-analogs.

According to the decision of the experts of individual countries the instrument corrections for measured precipitation on the effect of wind, wetting of the rain gage vessel and evaporation from it were not introduced. Based on the findings for precipitation in the observation points, with regard for the high-altitude region a chart was compiled of the average annual quantity of precipitation in the Danube basin on the territories of the People's Republic of Bulgaria, Hungarian People's Republic, USSR and CSSR. The average precipitation for individual water basins was defined either by the method of average arithmetical, or was established from the precipitation chart. In order to determine the annual and monthly river run-off that was the average for the multiple-year period observational materials were used from 1941 through 1970. Short series were reduced to the calculated for the reference point-analogs.

Errors in determining the average run-off in the basins of the main river-analogs is about 5%. On the whole for the entire territory in the majority of cases the error of determining run-off does not exceed 10%.

In order to estimate the water resources if possible data were used from points with natural run-off, not distorted by the effect of economic activity. The effect of agricultural-forest land reclamation measures on the river run-off was not considered, since these measures are little used in the limits of the examined part of the Danube basin territory.

In estimating the water resources of river basins and territories of the socialist countries that participated in the given work volumes of water of local run-off, influx of river waters from adjacent countries and outflow beyond the limits of the given territory were determined. In addition, the correlation of surface and underwater run-off was defined.

Calculation of the total evaporation from the surface of river basins in the limits of individual countries was made by different methods in accordance with the presence of the initial data. For the basins of rivers of the Hungarian People's Republic and CSSR it was determined by the method of water balance--according to the difference in precipitation and run-off. For the territory of the Danube basin located in the limits of the USSR the total evaporation was evaluated by the complex method of M. I. Budyko.

As a result of determining the elements of water balance according to individual countries generalized indices were compiled for water balance and water resources of the territories of the People's Republic of Bulgaria, Hungarian People's Republic, USSR and CSSR located in the limits of the Danube basin. These data are important for water management organizations

involved in the development of efficient plans for the complex use and protection of water resources of the Danube basin. The tables and charts given in the appendices to the indicated publication are especially valuable for this purpose.

In the tabular appendices characteristic data are given for the water-measurement points in the Danube basin with indication of the high-altitude marks above sea level, mean extremum level and expenditures of water and the daily expenditures of water of different duration.

In addition, the tables give information about the water resources of 57 rivers in the Danube basin with indication of the influx of river water into the country, run-off, formed directly on its territory, and outflow beyond the limits of the country. The characteristics of the water resources are given in the form of average modules and volumes of run-off. Consumptions of water of different frequency are also given. For the territory of the USSR included in the limits of the Danube River basin the mean monthly and annual consumption of water of different frequency are given. A special table shows the results of computing the multiple-year average water balances in the Danube basin. Four maps on the scale 1:1,000,000 are added to the work: hydrographic network, mean multiple-year precipitation, run-off and evaporation.

The examined work made by the joint efforts of four socialist countries is an example of the fruitful cooperation of the European countries in the area of research on hydrology. The given work, essentially for the first time succeeded in widely using observational materials of the components of balance in individual points of river basins of the People's Republic of Bulgaria, Hungarian People's Republic, USSR and CSSR for a more reliable estimate of the balance components both for the indicated countries, and for the entire studied section of the Danube basin as a whole.

REVIEW OF BOOK BY N. A. ZAYTSEVA AND V. I. SHLYAKHOV: AEROLOGIYA (AEROLOGY), LENINGRAD, GIDROMETEOIZDAT, 1978, 289 pages

Moscow METEOROLOGIYA I GIDROLOGIYA in Russian No 10, Oct 1979 pp 120-121

[Article by Candidate of Technical Sciences N. F. Pavlov]

[Text] In 1978 the hydrometeorological publishing house published the book of N. A. Zaytseva and V. I. Shlyakhov [2] designed as a textbook for hydrometeorological technical schools, having thus filled a significant gap in the supply of educational literature for the students of technical schools. Over 15 years had passed since the publication of the previous textbook [1]. During this time new methods of research of the free atmosphere and the technical resources for implementing them had appeared. The nomenclature of the specialties that are taught in the hydrometeorological technical schools have changed: instead of engineer-aerologists currently the technical schools graduate radio engineer-aerologists, at the same time having brought the graduated specialists closer to the task of operating the modern systems of radio sensing and meteorological radar stations.

The indicated circumstances are also the main prerequisite for those requirements that the modern textbook on aerology must satisfy. The textbook prepared by N. A. Zaytseva and V. I. Shlyakhov, in our opinion, to a considerable degree satisfy such requirements.

The textbook consists of 11 chapters, one of which is the introduction. It gives a definition of aerology as a science, substantiates the structure of the educational discipline and formulates its tasks. Here it is appropriate to note that the definition of aerology given in the chapter as a science, "whose subject of study is physical phenomena and processes occurring in the free atmosphere, and methods of study of these phenomena," does not precisely correspond to the definition given in "Meteorologicheskiy slovar'" [Meteorological Dictionary], of S. P. Khromov and L. I. Mamontova [4], according to which aerology is currently called "the science on methods of study of the free atmosphere." It should be indicated that despite the difference in definitions the textbook covers precisely an examination of the research methods.

The second chapter that is considerable in size is given to a description of wind, in the first place pilot-balloon measurements. It seems to us that this section of the textbook contains information of a practical nature (design of hydrogen balloons, balloon gas generator) which without damage to the textbook could be omitted. This important program information, in our opinion, must be studied in practical studies and in the process of passing the educational practice for which special textbook-method manuals must be developed.

The material stated in the third chapter, to a certain degree covers the material stated in the course "Meteorologicheskiye pribory i izmereniya" [Meteorological Instrument Measurements] whose second edition was just published by the Hydrometeorological Publishing House [3]. It seems to us that this chapter could have been limited only to a statement of the peculiarities of corresponding primary measuring transformers linked to their use in aerological instruments that are already known to the students, as well as the examination of specific errors inherent to them, methods for reducing them, and consideration during processing of measurement results.

The fourth, fifth and sixth chapters of the textbook cover an examination of the basic modern method for obtaining aerological information--the method of radiosondes, description of systems of radio sensing, radiosondes and structure of the aerological network. In this section primary attention is focused on systems of radio sensing and radiosondes, including radiosondes of special sensing. A positive moment here is the examination of the future development of atmospheric sensing systems which will permit the future specialists to successfully master in practical work new systems of atmospheric sensing.

This part of the material, in our opinion, is in successful correspondence with the materials on the principle of action and design of radar meteorological stations of the radio sensing systems studied in another discipline.

A considerable place in the textbook has been given to an examination of aerostat, airplane and rocket methods of atmospheric study (seventh, eighth, and ninth chapters). This part of the textbook completely reflects the current state of the fields indicated above and has been written, in our opinion, successfully.

The tenth chapter presents materials on remote sensing of the atmosphere: meteorological radar, meteorological laser location and methods of obtaining information with the help of meteorological satellites. In our opinion, this part of the textbook, especially questions of radar meteorological which currently has been introduced into the practice of the operational weather service could have been more completely reflected. A similar remark could be made also for the material of the 11th chapter that refers to modification of clouds and fog. It is known that currently the service of active modification of atmospheric processes is being intensively developed, in the first place, the anti hail service that protects enormous areas of agricultural crops in the southern and southeast regions of the country.

The future radio engineering-aerologists, undoubtedly, will work in this service, and therefore questions of active modification should be more completely reflected in a modern textbook on aerology.

In evaluating the textbook as a whole, one should indicate that it is a result of great labor of the authors. It collects, generalizes and systematizes all the modern methods for studying the free atmosphere. As for the remarks made above, they primarily, refer to the program of educational discipline in accordance with which the textbook has been prepared.

The book has been written in simple language, the material is presented in sequence and purposefully. It is a high-quality textbook and will promote an increase in the level of training of specialists of the hydrometeorological service. Evidently it will be widely used also in the higher educational institutions that are preparing personnel of a meteorological profile.

BIBLIOGRAPHY

1. Belinskiy, V. A.; and Pobiyakho, V. A. "Aerologiya," [Aerology], Leningrad, Gidrometeoizdat, 1962.

2. Zaytseva, N. A.; and Shlyakhov, V. I. "Aerologiya," [Aerology], Leningrad, Gidrometeoizdat, 1978.

3. Sternzat, N. S. "Meteorologicheskiye pribory i izmereniya" [Meteorological Instruments and Measurements], Leningrad, Gidrometeoizdat, 1978.

4. Khromov, S. P.; and Mamontova, L. A. "Meteorologicheskiy, slovar'" [Meteorological Dictionary], Leningrad, Gidrometeoizdat, 1974.

SIXTIETH BIRTHDAY OF MARK YEVSEYEVICH BERYLAND

Moscow METEOROLOGIYA I GIDROLOGIYA in Russian No 10, Oct 1979 p 122

[Article by the editorial staff of METEOROLOGIYA I GIDROLOGIYA]

[Text] Twenty-eight October 1979 was the 60th birthday of the prominent scientist in the area of theoretical and applied meteorology, study, control and protection of the environment, author of numerous monographs, well-known in our country and abroad, member of the editorial staff of the journal

METEOROLOGIYA I GIDROLOGIYA, winner of the Voyeykov prize, head of the coordination center of CEMA on meteorological aspects of atmospheric pollution, doctor of physical and mathematical sciences, professor Mark Yevseyevich Beryland.

The editorial staff of the journal warmly congratulates him on this remarkable date and wishes him good health, long years of life and further success in his multifaceted activity.

SEVENTIETH BIRTHDAY OF OLEG ALEKSEYEVICH DROZDOV

Moscow METEOROLOGIYA I GIDROLOGIYA in Russian No 10, Oct 1979 pp 123-124

[Article by N. I. Budyko, V. V. Kupriyanov, A. A. Sokolov, and I. A. Shiklomanov]

[Text] Eighteen October marked the 70th birthday and the 50th anniversary of scientific activity of one of the most prominent scientists in the area of climatology, Oleg Alekseyevich Drozdov. In 1930 he graduated from Kazan' University, and in 1931 his first scientific work was published that covered climate oscillation. In 1938 he was awarded a scientific degree of candidate of technical and mathematical sciences, and in 1948--doctor of geographical sciences.

In the system of the Hydrometeorological Service Oleg Alekseyevich worked from 1931, from 1934 through 1975--in the Main Geophysical Observatory where he headed the section of climatology for many years, from 1975--in the State Hydrological Institute. During his entire labor activity he successfully combined scientific research work with pedagogical, and since 1954 has headed the department of meteorology and climatology of the Leningrad State University.

O. A. Drozdov is the author of seven monographs and textbooks, and has published over 250 works. Part of them have been translated into four languages and published abroad. Many works of O. A. Drozdov are reference books of climatologists.

The circle of scientific interests of Oleg Alekseyevich is broad, however his primary scientific activity covers the problems of climatology. His studies are characterized by a combination of deep physical analysis of complex natural processes and the use of statistical methods for verifying the reliability of the findings.

Oleg Alekseyevich is the author of studies that reveal the physical essence of many questions of climate formation and indicate their manifestation in a geographical aspect. He has made a great contribution to the study of laws governing the distribution of precipitation on the territory of the USSR, and has focused especial attention on the effect on the precipitation

pattern of the relief and atmospheric circulation. These works are being successfully continued and developed by his students.

A special place in the work of O. A. Drozdov belongs to studies on the problem of moisture circulation in the atmosphere and its possible changes under the influence of economic activity.

Oleg Alekseyevich returned to studies of changes in climate many times. Especially, however, one should note the works of the 1960's-1970's on studying oscillations in moistening. In a number of original works he studies the natural oscillation in climate, taking into consideration the mutual relationship of processes in the atmosphere and hydrosphere. The links established by O. A. Drozdov in the temperature pattern of the Arctic with precipitation of the Northern Hemisphere are very important for solving the question of climate changes.

In studying the oscillations in moistening Oleg Alekseyevich focuses a lot of attention on the question of establishing the temporal structure of drought and the detection of the dependence of harvest of agricultural crops on climate factors.

O. A. Drozdov is one of the founders of the Soviet school of methods of climatological processing of observational data. He created the fundamentals for the theory of the structure of meteorological fields. The ideas and methods of Drozdov have been used in creating a reference on climate of the

USSR that is of great importance for providing climatological information to the national economy and scientific studies. Part of this reference on variability and climate characteristics was carried out under the direct supervision of O. A. Drozdov.

Deep knowledge of mathematical statistics and climatology permitted O. A. Drozdov to give a scientific substantiation for the methods of rationalization of the meteorological network which were the basis for planning the system of hydrometeorological observations on a national scale.

Oleg Alekseyevich has been successfully working on questions of mountain climatology and glaciology. The numerous series of climate maps compiled and edited by O. A. Drozdov are a major contribution to the climatography of the Soviet Union and the entire world.

O. A. Drozdov is a participant and leader of a number of scientific expeditions. He has trained over 30 candidates of sciences, some of whom have become prominent scientists and doctors of sciences.

Oleg Alekseyevich effectively participates in social activity: for many years he has been a chairman of the meteorological commission of the All-union Geographical Society, and has participated in the commissions of GKNT [State Committee for Science and Technology], is the member of two method councils of the MViSSO [Ministry of Higher and Special Secondary Education], several editorial staffs and publishing councils, method council and chairman of the philosophical seminar in the geographic department of the Leningrad State University. O. A. Drozdov has published articles on philosophical problems of natural science.

The name of O. A. Drozdov is widely known and deserves authority among the hydrometeorologists in our country and abroad. His scientific work has been noted by government prizes: the Order of the Red Banner of Labor, two orders "sign of honor" and medals, he has been awarded two A. I. Voyeykov prizes, two prizes of Leningrad State University, a number of certificates, diplomas and medals of VDNKh [Exhibition of Achievements of the USSR National Economy].

Oleg Alekseyevich meets his anniversary in the bloom of his creative forces. He is full of plans for the future, and there is no doubt that we will be witnesses of his new and remarkable scientific achievements.

We wish him good health and great creative successes in his versatile scientific activity.

SIXTIETH BIRTHDAY OF LARISA RAKIPOVNA RAKIPOVA

Moscow METEOROLOGIYA I GIDROLOGIYA in Russian No 10, Oct 1979 p 124

[Article by a group of comrades]

[Text] Twenty six June 1979 marked the 60th birthday of the head of the laboratory of the Main Geophysical Observatory, Doctor of Physical and Mathematical Sciences, Professor Larisa Rakipovna Rakipova.

After graduating from Leningrad University in 1943 her labor activity began in the system of the State Committee for Hydrometeorology and Environmental Control, in the Main Geophysical Observatory at first as an engineer, and after finishing post graduate work and defense of her candidate dissertation in 1947--senior scientist. From 1962 she has headed the laboratory of atmospheric thermodynamics and heliogeophysics.

During the period of continuous 37-year scientific work in the Main Geophysical Observatory L. R. Rakipov became a major specialist in the field of dynamic meteorology. In 1958 she defended her dissertation for defense of scientific degree of doctor of physical and mathematical sciences. In 1975 Larisa Rakipovna was given the scientific title of professor for pedagogical activity.

She has published about 90 scientific works, including 2 monographs: "Teplovoy rezhim atmosfery" [Thermal Pattern of the Atmosphere] and "Dinamika verkhney atmosfery" [Dynamics of the Upper Atmosphere]. Her works on the theory of thermal pattern of the atmosphere, anthropogenic and natural changes in climate, on questions of studying the mechanism in the link between solar activity and the dynamics of different layers of the atmosphere, thermal and circulating patterns of the stratosphere and mesosphere, and stratospheric warmings are widely known both in the USSR and abroad. The theoretical conclusions of the scientific developments of Larisa Rakipovna are successfully confirmed in experimental studies of the atmosphere. Thus the mechanism that she proposed back in the 1950's for the dynamic link between different layers of the atmosphere, as well as the ozone mechanism for influence of solar activity on the climate developed in 1972 are confirmed in the theoretical and statistical studies of foreign and Soviet

authors; her theoretical conclusions on the nature of the dependence of mesospheric dynamics on solar activity have been confirmed in the analysis of long series of radio-meteor observations made in the USSR and abroad in recent years.

Larisa Rakipovna is carrying out extensive scientific-method and coordination work, being an active member of three sections of the interdepartmental scientific councils and the geophysical committee for problems of solar-atmospheric bonds in forecasts of weather, ionosphere and aeronomy, and the biosphere. She is a member of the scientific councils of the main geophysical observatory and editor of TRUDY GGO.

Persistence and initiative in setting up and solving scientific problems, high principles and performance capacity are inherent to Larisa Rakipovna. Now she is in the bloom of her creative forces.

On the day of her 60th birthday we wish her strong health, new creative findings, and success in her production activity.

SIXTIETH BIRTHDAY OF SERGEY DMITRIYEVICH KOSHINSKIY

Moscow METEOROLOGIYA I GIDROLOGIYA in Russian No 10, Oct 1979 p 125

[Article by group of colleagues of West Siberian Regional Scientific Research Hydrometeorological Institute]

[Text] Eight October 1979 marked the 60th birthday of Sergey Dmitriyevich Koshinskiy, a leading specialist in the field of synoptic meteorology and climatology, doctor of geographic sciences, and head of the department of meteorology and climate of the West Siberian Regional Scientific Research Hydrometeorological Institute [RNIGMI].

Sergey Dmitriyevich began his scientific-production activity in the Baku weather bureau after graduating in 1949 from Azerbaijan University. The results of the initial stage in scientific activity were development of a

regional method for short-term forecast of strong and storm winds, and construction of a series of maps of the typical wind fields of the Caspian Sea. Their introduction at the end of the 1950's into the operational practice of the merchant marine in the Caspian Sea had great national economic importance.

All the subsequent work of Sergey Dmitriyevich was linked with Novosibirisk, where he moved in 1961. Working in the Novosibirisk branch of NIIAK [Scientific Research Institute of Aeroclimatology], the Novosibirisk branch of the USSR Hydrometeorological Center, and since 1971 in the West Siberian RNIGMI, where he has been actively engaged in the theme of studies on Siberian hydrometeorology. The extent of his scientific interests and knowledge permit S. D. Koshinskiy to be engaged in very broad circle of questions of synoptic and marine meteorology, aerology, climatology, and methods of processing pattern information. His direct participation in the creation and introduction of a system of mechanized processing of climate characteristics on punched card computers and electronic computers promoted the preparation and publication in 1962-1969 of the multiple volume "Spravochnika po klimatu SSSR" [Reference on USSR Climate]. A considerable contribution to the study of the continental shelf of the USSR seas has been his research that has been generalized in several volumes of the monograph "Rezhimnyye kharakteristiki sil'mykh vetrov na moryakh Sovetskogo Soyuza" [Pattern Characteristics of Strong Winds on Seas of the Soviet Union]. Other works published by him have great practical directivity; there are over 90 of them.

Sergey Dmitriyevich focuses a lot of attention on the scientific-organizational, publishing, pedagogical and social work. For many years he has been chairman of the meteorological seminar, editor of TRUDY ZAP.-SIB. RNIGMI, and the scientific leader of post-graduate students and competitors. Communist S. D. Koshinskiy is a propagandist, and a continuous leader of a philosophical seminar.

For his services to the motherland during the years of the war and for brilliant work Sergey Dmitriyevich has been awarded the Order of Great Patriotic War and many medals, and has been given the badge "outstanding worker of the USSR hydrometeorological service".

In congratulating him we wish him strong health, long years of life and further creative successes.

AT THE USSR STATE COMMITTEE FOR SCIENCE AND TECHNOLOGY

Moscow METEOROLOGIYA I GIDROLOGIYA in Russian No 10, Oct 1979 pp 125-126

[Article by V. Zakharov]

[Text] A new staff has been approved for the section of service and underground water resources and water balance of the scientific council "Complex Use and Protection of Water Resources" of the USSR State Committee of Science and Technology.

The director of the GGI [State Hydrological Institute], Doctor of Geographical Sciences A. A. Sokolov has been approved as chairman, cochairman--Doctor of Geological-Mineral Sciences G. V. Kulikov, deputy chairman--deputy director of the GGI, Doctor of Geographical Sciences A. I. Shiklomanov and head of the department of the Institute of Water Problems of the USSR Academy of Sciences, Doctor of Geological-Mineral Sciences I. S. Zektser, and scientific secretary--candidate of technical sciences V. S. Vuglinskiy (GGI) and candidate of geological-mineral sciences N. P. Akhnet'yeva (Institute of Water Problems of the USSR Academy of Sciences).

G. A. Alekseyev (GGI), L. V. Brazhnikova (GKhI) [State Scientific and Technical Publishing House of Chemical Literature], E. V. Buryak (State Committee for Hydrometeorology and Environmental Control), B. M. Dobroumov (GGI), A. S. Dubov (GGO) [A. I. Voyeykov Main Geophysical Observatory], I. A. Zheleznyak (UkrNIGMI) [Ukrainian Scientific Research Hydrometeorological Institute], Yu. N. Ivanov (SARNIGNI) [Saratov Scientific Research Hydrometeorological Institute], I. F. Karasev (GGI), V. D. Komarov (USSR Hydrometeorological Center), V. V. Kupriyanov (GGI), R. A. Nizhekhovskiy (GGI), Ye. G. Popov (USSR Hydrometeorological Center), O. V. Popov (GGI), V. A. Rumyantsev (GGI), G. G. Svanidze (ZakNIGMI) [Transcaucasian Scientific Research Hydrometeorological Institute], V. G. Fedorey (DVNIGMI) [Far East Scientific Research Hydrometeorological Institute], and S. I. Kharchenko (GGI) entered the staff of the section from the State Committee for Hydrometeorology and Environmental Control.

NOTES FROM ABROAD

Moscow METEOROLOGIYA I GIDROLOGIYA in Russian No 10, Oct 1979 pp 126-127

[Article by B. I. Silkin]

[Text] As reported in SCIENCE NEWS, vol 114, No 12, 1978, p 200, among the specialists there is no unity on the question of how great is the mass of solid products entering the earth's atmosphere as a result of volcanic activity. Estimates of different scientists are in extremely broad limits between 4 and 150 trillion grams per year.

For the purposes of pinpointing this amount a group of colleagues of the University of Washington (Seattle, Washington) headed by Dzh. L. Stit flew over six active volcanoes on a laboratory airplane in the states of Alaska and Washington (extreme northwest of the United States).

During the flights volumes of clouds of volcanic origin were measured and the quantity of gases SO_2 and H_2S, water vapor and solid particles, contained in them was determined, as well as the dimensions of particles of discharge during different phases of eruption.

As should be expected the more active stages of eruption, especially those referring to the explosive type yield a greater quantity of solid particles than those occurring "calmly." Thus the St. Augustine volcano in Alaska during active eruption discharges into the atmosphere about 4×10^5 kg/s of solid particles, and during less intensive activity--only 3×10^2 kg/s. Then during a decrease in intensity of volcanic activity this amount dropped to 4×10^1 kg/s.

However an unexpected observation was made, that is especially important to meteorology and climatology. It was found that the discharges which follow directly after the active eruption, as well as the emission of gases that is uniformally emerging that is inherent to more moderate, stable phases of eruption are the most important sources of smaller solid particles and gases, which essentially, mainly effect the weather-forming factors.

Based on their measurements the researchers drew the conclusion that the St. Augustine volcano during eruption between 1976 and 1977 discharged into the atmosphere about 2.5×10^{11} g of particles that remained for a long time in the air space.

The leader of the expedition Dzh. L. Stit compared the St. Augustine volcano in volume of sulfur products discharged by it with the "average dimensions of a metallurgical plant." In addition, the volcanoes were an important source for the influx of hydrogen sulfide into the atmosphere. All the active volcanoes of the earth, taken together, evidently erupt into the air shell roughly 1 billion grams of this gas per year.

***

As reported in EOS, vol 59, No 9, 1978, p 849 the American artificial earth satellite "Geos-3" was equipped with on-board equipment that permitted it in any weather to record important meteorological and oceanographic information in relation to the central and northern regions of the Atlantic. In particular, it records data on the state of the sea surface (altitude, wave direction), wind velocity, site of location of the Gulf Stream Channel and rate of movement of water masses in it.

It was established that the eastern "edge" of the Gulf Stream lies 1 m higher than the western which is located 100 km from it. This gradient, that is distinguished by the precise apparatus of the satellite (radar altimeter) permits determination of the current boundaries.

All of these data are being transmitted to earth and enter the space center on Wollops Island that belongs to National Aeronautics and Space Administration of the United States. This is served by the system of information on ocean dynamics set up by NASA which records in computer memory the time that the observation was made, and the geographical coordinates of the points to which it refers.

***

As reported in NEW SCIENTIST, vol 80, No 1131, 1978, p 670 the environmental protection administration of Great Britain has published official report on the state of the environment and its change in the last 5 years. This document contains statistical data according to which the discharge of sulfur dioxide by industrial enterprises and residential facilities of the country has been reduced by 20% as compared to 1970. It is especially stressed that at the same time the complaints of the Scandinavian countries are being satisfied to a certain measure that sulfur dioxide transported by the prevailing winds from the British Isles, falling with the precipitation, increases the acidity of the lakes of Sweden and Norway to a degree that is harmful for commercial fishing.

A reduction in the quantity of sulfur dioxide entering the atmosphere of the British Isles was started 8 years ago and is directly linked to two factors. First, from this moment oil and gas extracted on the shelf in the

North Sea and replacing the coal that in combustion produces sulfur dioxide began to play an ever greater role in power engineering of England. Second, in the same period new rules were introduced that significantly reduce the limits of permissible discharges.

The report also states that between 1973 and 1976 the quantity of lead entering in the form of particles into the air space of the British Isles from the metallurgical enterprises of England and Wales was roughly halved. However the degree of total atmospheric pollution with lead was not reduced, since the discharge of this element by automobile engines sharply increased. In the period between 1970 and 1976 automobile transport operating on gasoline increased the discharge of carbon monoxide, lead, hydrocarbons and nitric oxides almost by 20%, and diesel automobiles--roughly by 10%.

The official document also contains data about the degree of pollution of river water, pollution with oil of seacoasts, lead content in drinking water, radioactivity of milk and "noise pollution" among the aviation on the entire territory of Great Britain.

***

As reported in SCIENCE NEWS, vol 114, No 16, 1978, p 264 a lengthy series of observations made on the territory of St. Louis (United States) indicated that "a warm island", section of atmosphere above a major industrial center has a significant effect on the weather and climate of the surrounding space. It is clearly felt even at a distance of 40 km, on the opposite shore of the Mississippi River, in the adjacent section of the state of Illinois. Among the most noticeable results of such an effect is the increase in the quantity of precipitation, frequency and duration of thunder storms.

In order to verify the applicability of such conclusions to conditions of other cities the same group of specialists that studied the weather of St. Louis headed by Stanley M. Shannon (hydrological administration of the state of Illinois) set up analogous experiments in the environs of Chicago. At the same time the study was made of the effect on meteorological conditions of a large fresh water basin such as Lake Michigan on whose shores Chicago stands.

The observations (including radar) demonstrated that the average quantity of precipitation falling during thunder storms emerging to the northwest of Chicago increases as they advance over the city of Chicago and further, over the territory of the northern section of the neighboring state of Indiana. The effect of such an increase in precipitation was traced up to the city of La Port (Indiana) that is located roughly 80 km from Chicago. It is assumed that the factor that promotes this phenomenon is the existence of a large region almost deprived of vegetation.

At the same time it was established that the effect of Lake Michigan on the climate and weather of Chicago is not so great. Although it results in a

certain decrease in the mean temperatures, the lake cannot significantly alter the effect of the urban "warm island."

The observations in the region of Chicago for further accumulation of data will be conducted for another 2 years.

OBITUARY OF FEOFAN FARNEYEVICH DAVITAYA (1911-1979)

Moscow METEOROLOGIYA I GIDROLOGIYA in Russian No 10, Oct 1979 pp 127-128

[Article by staff of USSR State Committee for Hydrometeorology and Environmental Control]

[Text] Soviet science has borne a heavy loss. In the bloom of his creative forces at 68 years old on 29 June 1979 the most prominent scientist in the area of agroclimatology, the honored scientist of the Georgian SSR, academician of the Georgian SSR Academy of Sciences, director of the Institute of Geography of the Georgian SSR, and president of the geographical society of Georgia Feofan Farneyevich Davitaya died.

Davitaya gave about 50 years to fruitful service of science. After graduating in 1932 from the All-union Institute of Subtropical Cultures he entered post-graduate studies at the Main Geophysical Observatory. In those years Feofan Farneyevich gave a scientific substantiation to the climate zones of grapes in the USSR, and in 1936 successfully defended his candidate dissertation. In 1938 his monograph "Klimaticheskiye zony vinograda v SSSR" [Climate Zones of Grapes in the USSR] was published which became a reference book for agrometeorologists, viticulturists, and viniculturists. In this work for the first time a number of important method questions were solved on an agricultural evaluation of climate, agroclimate zoning and specialization of production, which had a significant effect on the formation of scientific thinking of many agrometeorologists and climatologists. In 1950 Feofan Farneyevich became a doctor of agricultural sciences. His dissertation was based on the theory and technique of agroclimate zoning of agriculture in the example of development of a more specific problem, arrangement of viniculture and specialization of wine making, as well as their advance into the more northern regions. Possessing great erudition and a broad range of scientific interests he took up the solution of both general-theoretical problems and applied tasks. Under his leadership and editing in the first years of development of virgin land in 1955 a monograph was published "Agroklimaticheskiye i vodnyye resursy raynov osvoyeniya tselinnykh i zalezhnykh zemel'" [Agroclimate and Water Resources of Regions of Development of Virgin and Unused Land]. The method that he created for predicting

the provision of heat in the vegetation period made it possible to give forecasts with high frequency (80-90%).

F. F. Davitaya was the chief editor of "Klimaticheskogo atlasa SSSR" [USSR Climate Atlas] that was published in two volumes in 1960. He published a unique work "Klimaticheskiye resursy Kuby" [Climate Resources of Cuba] and another more than 300 scientific works.

In 1960 F. F. Davitaya was elected an active member of the Georgian SSR Academy of Sciences, he was director of the Institute of Geography of the Georgian SSR where he headed a new trend in climatology, study of mountain climatology.

The entire conscious life of Feofan Farneyevich Davitaya was a selfless service to science. Being a professor of Leningrad, Moscow and Tbilisi Universities, as well as an important worker in major scientific centers, Feofan Farneyevich Davitaya always remained principled and demanding in his affairs, a sensitive and sympathetic man with a highly developed sense of citizenship and a high duty to the motherland.

His services were highly evaluated by the party and government: he was awarded five orders, 11 USSR medals, the gold medal of the Cuban Academy of Sciences, the large gold medal of the geographical society of the USSR, and he was the winner of state prizes of the USSR and Georgian SSR.

The bright memory of F.F. Davitaya as a talented scientist, excellent and sympathetic man will be preserved in the hearts of his numerous students, companions, followers and all those who are lucky to meet this man.

[2-9035]

9035
CSO: 1864

-END-